International
Progress Report

IPR-00-02

Äspö Hard Rock Laboratory

High-permeability features (HPF)

Ingvar Rhén, Torbjörn Forsmark

VBB VIAK

January 2000

Svensk Kärnbränslehantering AB
Swedish Nuclear Fuel
and Waste Management Co
Box 5864
SE-102 40 Stockholm Sweden
Tel +46 8 459 84 00
Fax +46 8 661 57 19

Äspö Hard Rock
Laboratory

Report no.
IPR-00-02
No.

Author
Rhén, Forsmark
Date
2000-01-24
Checked by
Peter Wikberg
Date
2000-02-09
Approved
Olle Olsson
Date
2000-02-09

Äspö Hard Rock Laboratory

High-permeability features (HPF)

Ingvar Rhén, Torbjörn Forsmark

VBB VIAK

January 2000

Keywords: Äspö Hard Rock Laboratory, hydrogeological investigations, high-permeability features, transmissivity, statistics

Abstract

The results from the construction phase of the Äspö Hard Rock Laboratory (HRL) showed a relatively high number of events with a high inflow rate during drilling. These features (with high flow rates) were in several cases not a part of the deterministically defined major discontinuities.

A study was made to compile and analyse data that can be related to High Permeability Features (HPF) at southern Äspö. With HPF in this report is understood a fracture, system of fractures or fracture zone with an inflow rate (observed during drilling or flow logging) which exceeds 100 l/min or alternatively show a transmissivity $T \geq 10^{-5}$ m^2/s.

The main conclusions are:

- Somewhat less than half of the HPF:s can be explained by what was classified during the mapping as crush zones of the cores and the rest of the HPF:s by one or a few natural joints. It clearly shows that high permeability features in the sparsely fractured rock mass exist.
- About 50 % of the HPF:s can be connected to the deterministically defined fracture zones with a large extent, which existence, extension and properties were based on evaluation of geological, geophysical hydrogeological and hydrochemistry data.
- HPF:s are found in all rock types but are most frequent in fine-grained granite.
- The arithmetic mean distance between HPF:s, defined as features having a transmissivity $T \geq 10^{-5}$ m^2/s, is ≈ 75-105 m.

Sammanfattning

Resultaten från konstruktionsfasen av Äspölaboratoriet visade på ett relativt stort antal händelser med höga inflöden under borrning från tunneln och att dessa i flera fall ej kunde kopplas till större deterministiskt definierade zoner.

En studie har genomförts för att sammanställa och analysera data som kan sättas i samband med Hög Permeabla Flödande strukturer (HPF) på södra Äspö. Med HPF i denna rapport avses en spricka, sprick system eller sprick zon med ett inflöde (observerat under borrning eller flödesloggning) vilket överskrider 100 l/min eller att transmissiviten T $\geq 10^{-5}$ m^2/s.

Huvudslutsatser är:

- Något färre än hälften av HPF kan kopplas till vad som klassificerades som krosszon vid kärnkarteringen och resterande del med en eller några få naturliga sprickor. Resultaten visar klart att HPF existerar i den glest uppspruckna bergmassan.
- Omkring 50 % av HPF:s kan kopplas till deterministiskt definierade större sprickzoner med stor utsträckning, vilkas existens, utsträckning och egenskaper var baserat på utvärdering av geologiska, geofysiska, hydrogeologiska och hydrokemiska data.
- HPF:s är mest frekvent i finkornig granit, om man tar hänsyn till volymsandelsen av de olika bergarterna vid Äspölaboratoriet.
- Det aritmetiska medel avståndet mellan HPF med en transmissivitet T $\geq 10^{-5}$ m^2/s, är $\approx$ 75-105 m.

Executive summary

The results from the construction phase of the Äspö HRL showed a relatively high number of events with a high inflow rate during drilling. Features with a high transmissivity were drilled through at a number of times and these features were in several cases not a part of the deterministically defined major discontinuities. This has also been seen in bore holes made in the operation phase of the Äspö HRL.

During the 4th IJC/TEF meeting at Västervik in mid May 1997 it was identified important to assess the possibility to predict fractures or features with high transmissvities at Äspö from data collected during the pre-investigation phase.

With the term High Permeability Feature (HPF) in this report is understood a fracture, system of fractures or fracture zone with an inflow rate (observed during drilling or flow logging) which exceeds 100 l/min or alternatively show a transmissivity $T \geq 10^{-5}$ m^2/s.

The objective with the current study is to:

- compile information that can be coupled to High Permeability Features at southern Äspö.
- analyse these data statistically and to investigate possible correlation between HPF and other observed features.

In *Table 1* the results of the expected distances between HPF:s, based on three different data sets, are summarised. The results presented may to some extent be biased due to a few reasons. First the water conducting fractures have been found to be sub-vertical and therefore one could expect to find larger mean distances in the sub-vertical bore holes compared to sub-horizontal ones. This cannot be seen in *Table 1*. Secondly the major fracture zones, which were deterministically defined, are all sub-vertical and then drilling sub-vertical bore holes through them may give a long intersection length which possibly can result in a few more HPF:s compared if the bore hole had been horizontal. As several of the sub-vertical bore holes drilled from the surface were targeting these major zones this may be the explanation why there is no clear difference between sub-horizontal and sub-vertical bore holes. Despite the difficulties mentioned above, the statistics for the three data sets representing different bore hole groups are surprisingly similar.

If features having a transmissivity $T \geq 10^{-6}$ m^2/s are studied one can see the expected difference between sub-vertical and sub-horizontal bore holes. The reason is that the calculated distances are based on a larger data set that is less affected of the major fracture zones and probably gives better statistical estimates of the rock mass. However, this study has mainly been focusing on features having a transmissivity $T \geq 10^{-5}$ m^2/s.

Table 1. The statistics of the distance between hydraulic conductors with a transmissivity (T) greater than a specified value of the transmissivity (T_j). Method A, B and C are different ways of estimating the distances.

Bore holes drilled at surface **T_j (m^2/s)**	**Arithmetic mean distance** **D_a (m)**	**Geometric mean distance D_g (m)**	**Standard deviation of $Log_{10}D$**
$T \geq 10^{-5}$ (Method A)	45	11	0.70
$T \geq 10^{-5}$ (Method B)	60 - 80	16 - 18	0.75 - 0.81
$T \geq 10^{-5}$ (Method B) (bottom of KAS08 excluded)	75 - 100	24 -27	0.75 - 0.81
$T \geq 10^{-5}$ (Method C)	85	-	-
$T \geq 10^{-5}$ (Method C) (bottom of KAS08 excluded)	106	-	-
Core holes in the tunnel **T_j (m^2/s)**			
$T \geq 10^{-5}$ (Method A)	27	9	0.73
$T \geq 10^{-5}$ (3 m section data) (Method A)	36	21	0.47
$T \geq 10^{-5}$ (3 m section data) (Method B)	80 - 100	30 - 34	0.65 - 0.71
$T \geq 10^{-5}$ (3 m section data) (Method C)	106	-	-
Probe holes in the tunnel **T_j (m^2/s)**			
$T \geq 10^{-5}$ (Method B)	73 - 78	27 - 31	0.66 - 0.71

It is of interest to make a first attempt at setting the occurrence of HPF:s in a structural geological context. Of special interest in this study is shown if HPF:s occurs in the vicinity of :

- any special rock type
- any special rock contact
- rock veins

- crush zones/natural joints
- areas where RQD is high/low

  Rockveins: Part of core mapped as rockvein if length of mapped rock type along the core < 1m.

  Crush zones: Part of core mapped as crush zone if the core could not be reconstructed due to gravel–like material and/or core loss. Width of crush zones are generally a few centimetres or larger.

  Natural joints: The mapped fractures that are considered open for water flow.

  RQD: Rock Quality Designation. Based on core mapping and represents the total length of whole (full-diameter) bits of core, 10 cm or longer, in competent rock, calculated as a percentage of the theoretical length of considered (at least 1 m), including any loss of core. The calculation is based on natural joints.

The evaluation of HPF:s for the surface bore holes is based on the injection tests with a packer spacing of 3 metres and accordingly the geological data for the same packer interval.

The evaluation of HPF:s in the tunnel core holes is based on positions of flows into the bore holes. If these are based on drilling records it is judged that there exist an uncertainty of +/- 1-meter from the given position. If flow logging is the base of position it is judged as more certain. However, in this evaluation +/- 1 meter from the observed HPF has been the base for the bore hole section to be used for the evaluation.

In the bore holes mentioned above the total number of HPF:s, based on $T \geq 10^{-5}$ m^2/s are 79, and the correlation study is based on those data.

The results of the correlation study are presented in *Figure 1.* A total of 79 HPF:s were identified in the bore holes studied. In those cases where a HPF occurs there must be a crush zone or a natural joint. Of these 79 cases, 34 were related to a crush zone while in 45 cases there was one or several natural joints in the section defined for the HPF.

There are normally just one rock type (not taking into account the veins) within the interval for the HPF:s. Rock veins are found in 27 sections and rock contacts are found in 15 sections, and among these, rock veins and rock contacts are both found in 7 sections. If sections having veins or rock contacts are excluded, still 44 sections of 79 have just one rock type, see *Figure 1.* In 15 of these 44 sections, the rock type is fine-grained granite. In 37 of the 79 sections, fine-grained granite is present, if sections with veins of fine-grained granite are also included.

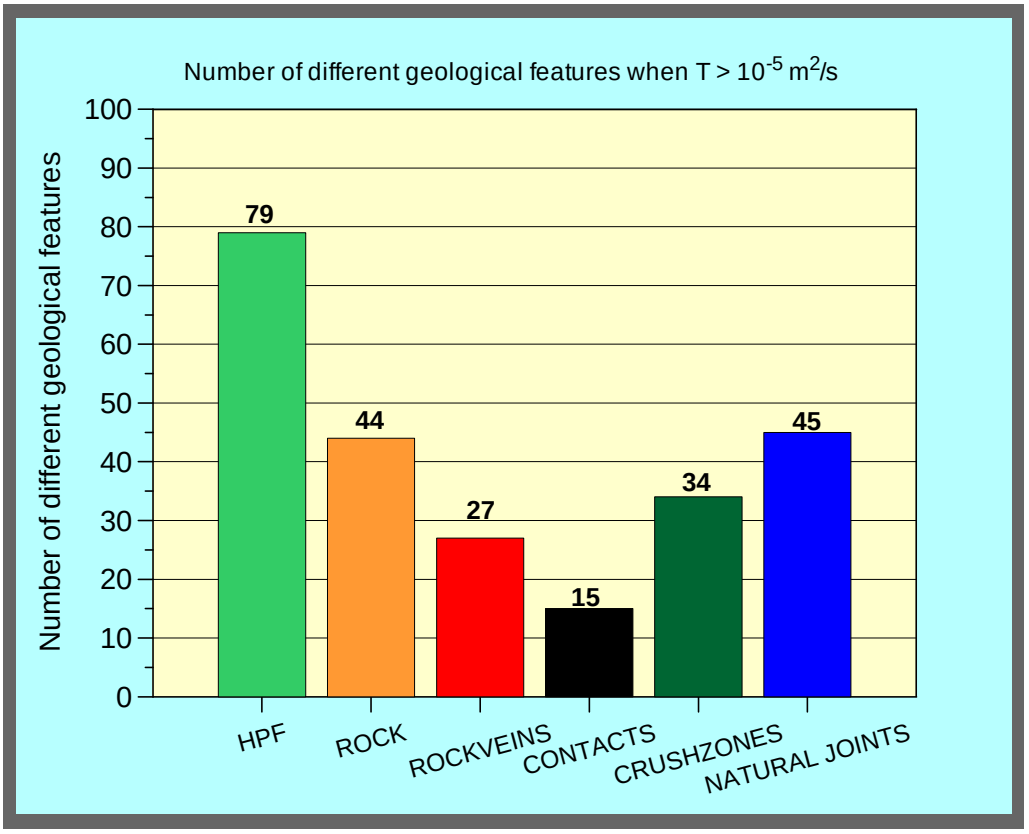

CRITERIA :

TUNNEL BOREHOLES - HPF POSITION +/- 1 meter
SURFACE BOREHOLES - WITHIN PACKER INTERVAL (3 m)

Figure 1. *The total number of HPF:s and the number of different geological features within an interval associated to the HPF.*

The definition of the HPF:s (High-Permeability Features) as having a transmissivity $T \geq 10^{-5}$ m^2/s or a flow rate $Q \geq 100$ l/min into a bore hole with pressure close to atmospheric was more or less arbitrarily chosen for this study. However, it was known from the previous studies at Äspö HRL that features, with properties around these values mentioned above, were not uncommon and not all of them could be explained by fracture zones with large extent defined deterministically using geological, geophysical, hydrogeological and hydrochemistry data. This study has shown this in a more clear way and the main conclusions are presented below.

HPF:s and large deterministically defined fracture zones:

- About 50 % of the HPF:s can be connected to the deterministically defined fracture zones with a large extent, which were based on evaluation of geological, geophysical hydrogeological and hydrochemistry data. The rest of the HPF should be modelled as fairly large features in-between the deterministic zones. The radius of these features may be around 30-100m.

- The implication of the size of the HPF:s is that there should be a correlation model for the assigning of the hydraulic properties to the hydraulic rock domains taking the size into account. The present SKB model over Äspö from 1997 does not consider this. The hydraulic conductor domains in the present model are not affected of the results.

Distances between HPF:s:

- The distances between HPF:s have a lognormal distribution.

- The arithmetic mean distance between HPF:s, defined as features having a transmissivity $T \geq 10^{-5}$ m^2/s, is for the sub-vertical bore holes drilled from surface 75–106 m. The arithmetic mean distance between HPF:s, is for the sub-horizontal bore holes drilled from the tunnel spiral 73-106 m. The corresponding geometric mean values are 24-27 m and 27 - 34 m respectively. Possibly, the distances estimated from the sub-vertical bore holes should be somewhat larger than the figures given above.

- The statistics of the distances is dependent of the scale of observations. It is possibly better to use larger interval than 3 m to describe the spatial distribution of distances between HPF:s on a scale of several hundred meters, at least if simple measures as arithmetic mean is used as a measure for HPF:s between the large deterministic zones.

The coupling between HPF and lithology and fracturing:

- Somewhat less than half of the HPF:s can be explained by what was classified as crush zones during the mapping of the cores and the rest by one or a few natural joints. It clearly shows that high permeability features exist in the sparsely fractured rock mass. The evaluation of the RQD for the intervals having a HPF shows the same thing, both very low and very high RQD value are found in the bore hole intervals having a HPF.

- HPF:s are most frequent in fine-grained granite, taking into account the amount of different rock types at Äspö HRL. Äspö diorite and Småland (Ävrö) granite, which are the dominating lithological units, have approximately the same frequency of HPF:s and is about half of the frequency in fine-grained granite. The frequency of HPF:s in greenstone is somewhat greater than in Äspö diorite and Småland (Ävrö) granite. In pegmatite and mylonite-hybridized rock the frequency is about the same as in greenstone, but the conclusion is very uncertain due to the small sample size

- Only about 20 % of the HPF:s are found near rock contacts. Fine-grained granite is the dominating rock type found in these rock contacts.

- About 35 % of the HPF:s are found in intervals containing rock veins. Fine-grained granite, pegmatite and greenstone are the dominating rock types found in intervals having a HPF and rock veins.

- Further can be concluded that rock contacts and veins are not dominating sections with HPF:s. Most sections with a HPF has just one rock type and no rock contacts or veins.

- In the sections with HPF:s and veins and/or rock contacts, the resolution of the data has not permitted to see if HPF:s are located close to a rock contact, within, or close to a vein. It may be the case that for example veins of fine-grained granite increase the probability of getting a HPF. In nearly 50 % of the sections with HPF fine-grained granite was present as the rock type or as a vein.

- Mapping of groutfilled fractures in the tunnel and analyses of the transmissvities from the probe holes drilled along the tunnel has shown that subvertical fractures with strike WNW-NW and around N-S are important hydraulic conductors. If there are any differences of the frequency of the HPF:s in the horizontal plane has not been investigated but is likely, due to the above mentioned investigations.

- Most of the investigated rock volume is between large fracture zones (EW-1 and NE-1). This rock volume may have been sheared, creating the existing hydraulically important subvertical fractures, which seems to be in an en-échelon pattern, with strikes WNW-NW and around N-S. These fracture sets also seems to form larger subvertical hydraulic features striking NNW, which hydraulic interference tests seem to conform. However, in most bore holes it is not possible to examine the direction of individual fractures, as it is not documented in the data base. It is therefor difficult to conform that the HPF:s are a part of the subvertical fractures with strike WNW-NW and around N-S.

- The ductile deformations giving foliation and gneissic zones trending NE-ENE, dipping to the NNW does not seem to have any major impact on the dominant hydraulic features, consisting of subvertical fractures with strike WNW-NW and around N-S.

- Some of the larger bodies of fine-grained granite occur as dikes but it is not very clear because of strong deformation. These bodies, at least near the surface, are elongated in the ENE-NE direction. Considering the hydraulic interference tests, the direction of the fine-grained bodies does not seem to have a large impact of the direction of the larger hydraulic features, as the NNW features. One exception is possible one or several fine-granite body(ies) that is believed to be at a depth of about 300 m within the tunnel spiral .

- The brittle deformation has caused a much denser fracture pattern in the fin-grained granite compared to the other rock types. Fine-grained granite may in an effective way interconnect fracture systems even if the amount of fine-grained granite is fairly small. If fine-grained granite is distributed within the rock mass as a large number of veins, as can be seen in the Äspö tunnel, possibly the fine-grained granite can be parts of larger fracture planes or system of larger fracture planes forming HPF:s. However, in the tunnel there are also many examples of small and winding veins of fine-grained granite that are not fractured.

Contents

1 Background

1.1 Äspö Hard Rock Laboratory

In order to prepare for the siting and licensing of a spent fuel repository SKB has constructed an underground research laboratory.

In the autumn of 1990, SKB began the construction of the Äspö Hard Rock Laboratory (Äspö HRL) near Oskarshamn in the south-eastern part of Sweden, see *Figure 1-1*. A 3.6 km long tunnel was excavated in crystalline rock down to a depth of approximately 460 m.

The laboratory was completed in 1995 and research concerning the disposal of nuclear waste in crystalline rock has since then been carried out.

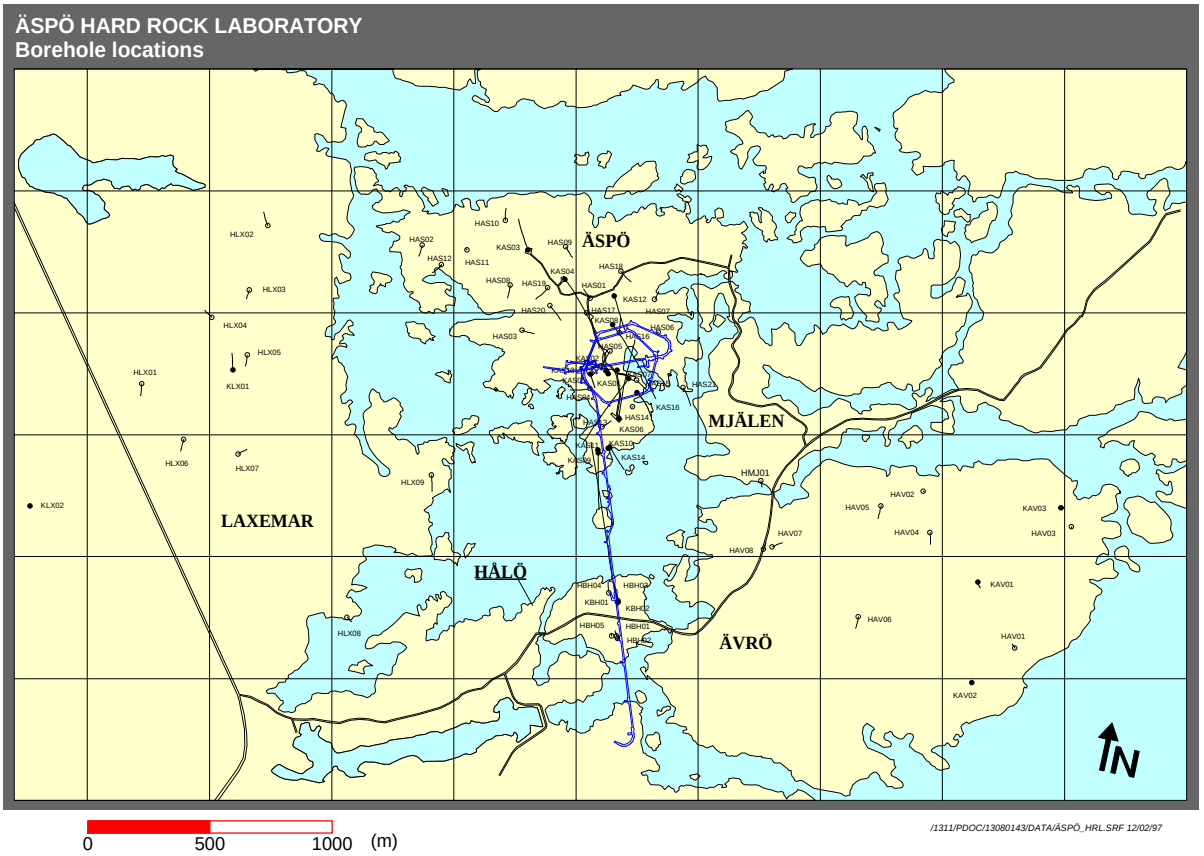

Figure 1-1. *The figure shows the location of the bore holes and the tunnel to the Äspö Hard Rock Laboratory. Magnetic north is indicated by N in the figure.*

1.2 High Permeability Features

In August 1996 a cored bore hole KA2563A was drilled through the rock volume allocated for the TRUE Block Scale Experiment, see Figure 4-6. Geology and permeable zones along the bore hole had been predicted, primarily based on data from the nearby

\

bore hole KA2511A. The inference made indicated that inflows in the order of 20-30 l/min should be expected at given locations in KA2563A.

The outcome of KA2563A showed two major inflows in the range 60-100 l/min and one inflow of approximately 700 l/min. Concerning the results from the construction phase of the Äspö HRL it is not an unexpected event with a high inflow rate during drilling. Features with a high transmissivity were drilled through a number of times and these features were in several cases not a part of the deterministically defined major discontinuities.

During the 4th IJC/TEF meeting at Västervik in mid May 1997 the findings from the characterisation of the TRUE BS were reported. The existence of an unexpected highly permeable feature of the magnitude found in KA2563A caused some concern among the IJC delegates. It was identified as important to assess the possibility to predict fractures or features with high transmissvities at Äspö from data collected during the pre-investigation phase. Specifically it was identified that:

1. A review of all information about (highly) water bearing fractures should be conducted.

2. Statistics of such zones should be compiled.

3. Reporting of results (1 + 2).

With the term High Permeability Feature (HPF) in this report is understood a fracture, system of fractures or fracture zone with an inflow rate (observed during drilling or flow logging) which exceeds 100 l/min or alternatively shows a transmissivity $T \geq 10^{-5}$ m^2/s from performed hydraulic tests.

2 Objective

The objective with the current study is to:

- compile information that can be coupled to High Permeability Features at southern Äspö.
- analyse these data statistically and to investigate possible correlation between HPF and other observed features.

3 Scope

The scope of this study is to:

- produce an overview of HPF:s at Äspö.
- assess some characteristic distances between the HPF:s.
- make a first attempt to correlate the occurrence of a HPF to geological feature.
- produce relevant statistics of hydrogeological parameters of grouting bore holes.

As a base for the calculation of the characteristic distances cumulative density frequency plots of the distance between HPF:s along bore holes where based on three different definitions of the HPF:s: Transmissivity(T) ≥ than a prescribed transmissivity (T_j) or within an prescribed interval: $T_i \geq T \geq T_j$, or inflow to a bore hole section (Q) ≥ 100 l/min. Not all these definitions were used for all data sets.

Data from the Äspö island that were used:

- Core holes drilled from the surface on Äspö.
- Long core holes drilled from the tunnel after tunnel chainage 1400 m.
- Probe holes drilled from the tunnel after tunnel chainage 1400 m.
- Grouting bore holes drilled after tunnel section 1400 m. (These holes were made at the tunnel face during excavation of the tunnel in order to inject grout and thus decrease the water flow into the tunnel.)

4 Overview of Geology, Hydrogeology and HPF

In this Chapter the geology and hydrogeology on southern Äspö and plots of the position of HPF:s in existing bore holes are presented. In *Rhén et al. /1997b/* more details are found about the geological and hydrogeological models.

4.1 Overview of Geology

4.1.1 Lithological model

Four main rock types - Äspö diorite, Småland (Ävrö) granite, green-stone and fine-grained granite make up most of the rock mass in the Äspö tunnel area (see *Figures 4-1* and *4-2*). Äspö diorite and Småland (Ävrö) granite are two varieties of the country rock called ”Småland granite”. Rocks belonging to the Äspö diorite group are by far the most common within the Äspö area, both on the surface and in the tunnel. The rocks are usually grey to reddish grey, medium-grained, and contain more or less scattered, large crystals of potassium feldspar. Grano-diorites and quartz monzonites are most common, but there are also some tonalites, quartz diorites and quartz monzonites included in this group. Age determination gave a well defined age of 1804 ±3 million years for the Äspö diorite.

Macroscopically, the Småland (Ävrö) granite differs from the previous group in its brighter, sometimes distinctly more reddish colour. The amount of potassium feldspar phenocrysts is lower and the crystals are much more irregularly distributed. In many places the Småland (Ävrö) granite can be seen to cut the Äspö diorite, which implies that the former is younger. The age difference between the two groups is probably very small. The Småland (Ävrö) granite - which is exposed on Ävrö south of Äspö and on Äspö over the southern part of the spiral probably extends northwards folded beneath the Äspö diorite.

The greenstones - fine-grained (probably of volcanic origin) and medium to coarse-grained green-stone (diorites to gabbros) are easily distinguished from the granitoid rocks by their very dark, greenish or greyish black colour. As a rule they occur as minor inclusions or irregular, often elongated bodies within the granitoids and dioritoids following the common E-W foliation trend within the area. Except the smallest inclusions, the green-stones are often intensely penetrated by fine-grained, granitic material.

Fine-grained granites occur rather frequently, both on the surface of the island of Äspö and its surroundings, as well as in the tunnel. From the surface mapping it is clear that many of the granites occur as dikes. The dike character is sometimes not very clear because of strong deformation in the fine-grained granites, which has obscured contacts.

The brittle deformation has caused a joint pattern in the fine-grained granites, often characterised by many short joints lying closely together, which divide the rock into small blocks. This is quite different from the pattern in the medium to coarse-grained granitoids where joints are much more widely spaced. No significant difference has been found between the joint patterns on outcrops surface and in the tunnel.

Most of the greenstone has the character of inclusions but dikes are also mapped mostly trending EW to the NE. All the rock mass is veined by fine-grained granite but the number of veins in the Småland (Ävrö) granite in the tunnel is sparse compared with the number of veins and dikes in the Äspö diorite. Most of the dikes of fine-grained granite trending NE confirm the idea that the fine-grained granite is closely related to the Småland (Ävrö) granite, which is obviously younger than the Äspö diorite.

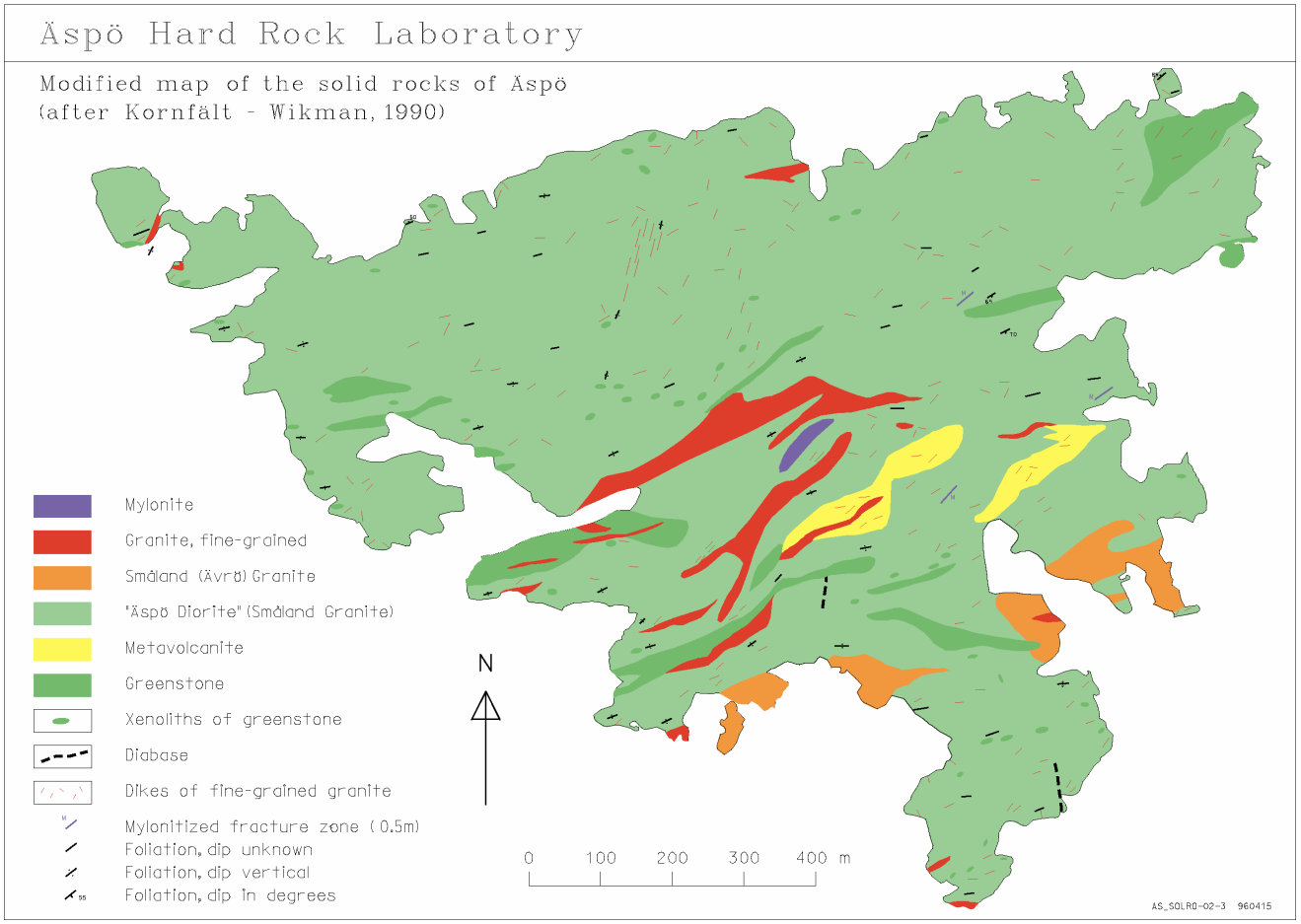

Figure 4-1. *Map of solid rocks on Äspö /Rhén et al. ,1997b/.*

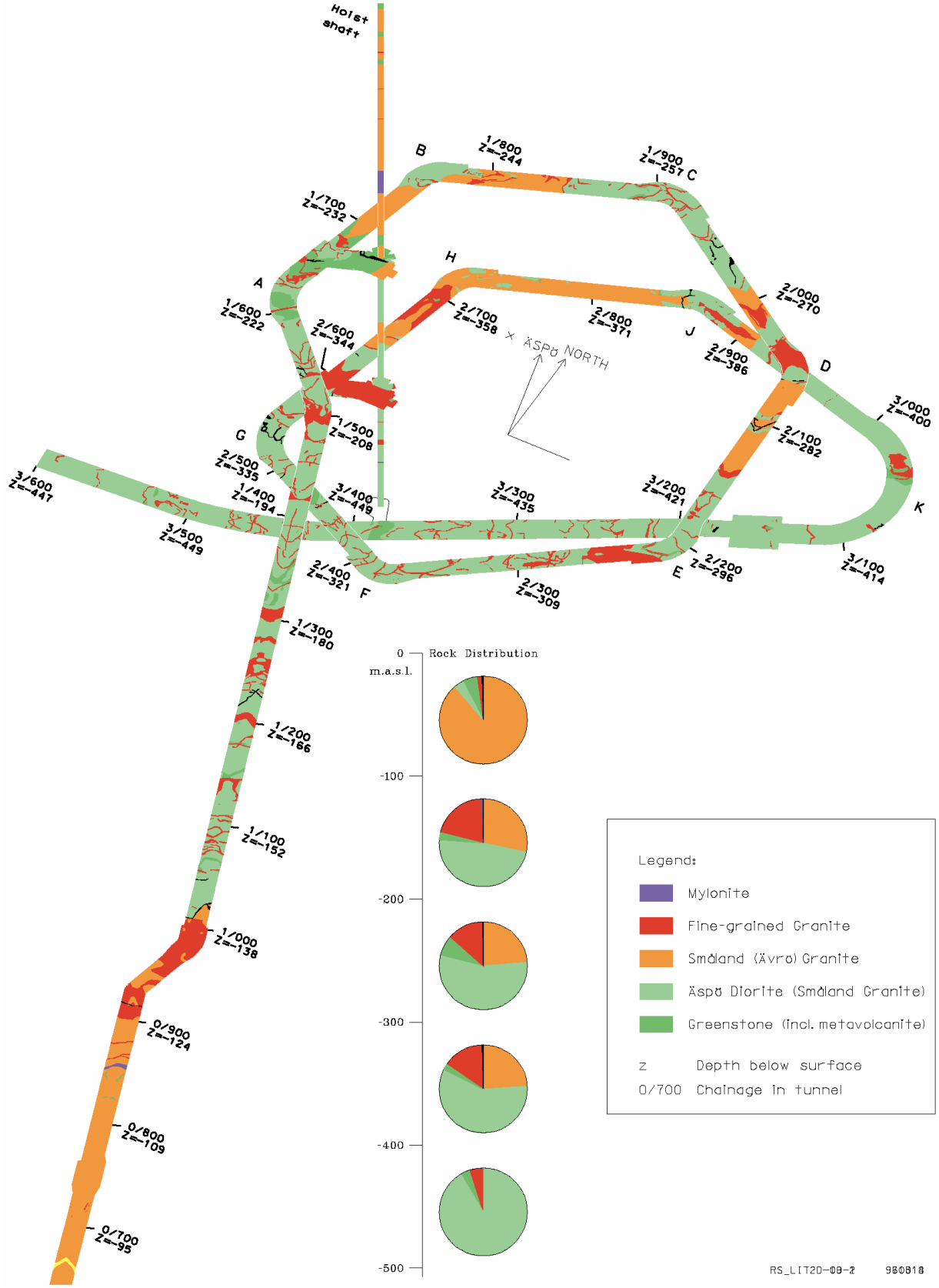

Figure 4-2. *Lithology of the Äspö tunnel. Diagrams illustrate distribution of main rock types at depth /Rhén et al. ,1997b/.*

4.1.2 Structural model

The geological-structural model describes the geometrical distribution and character of discontinuities in a rock volume. Discontinuity is the general term for any mechanical feature in a rock mass having zero or low tensile strength. It is the collective term for most fractures, weak schistosity planes, weakness (fracture) zones and faults. During pre-investigation and tunnel mapping of the Äspö HRL discontinuities were divided into fracture zones (major and minor) and small scale fractures in the rock mass between fracture zones. In *Figure 4-3* the model of the hydraulically significant major features is shown and these features correspond mostly to the major fracture zones but in some cases also to minor fracture zones.

An almost vertical, penetrating foliation trending NE-ENE is the most dominant structural element in the 1700-1800 million year old Äspö granitoids and seems to be the oldest sign of the ductile deformation related to the sub-horizontal NNW-SSE compression. This deformation is also marked by the orientation of mafic sheets often back-veined by two or three generations of fine-grained granites.

Strong foliation and mylonites are common in the Äspö shear zone - where more than 10-metre-long bodies of mylonite occur trending E-W and dipping steeply to the north. Regional evidence suggests that the E-W trending mylonites are older than those trending NE. The first brittle faults probably developed in the region in response to the emplacement of younger granites. These faults and older ductile zones were reactivated several times. Fracture zones on Äspö have a wide range of orientations and styles and most of them reactivate older structures. The style of each fracture zone tends to depend on the nature of any older structure being reactivated, such as EW gneissic zones, mylonites trending NE or E-W and gently dipping alteration zones. Fracture zones trending N, NE or E-W on Äspö normally had ductile precursors whereas those trending NW apparently did not.

Major fracture zones

EW-7 was estimated to trend almost parallel to the main lineament trending ENE-NE and geophysical anomalies in the Hålö-Äspö area. Only one branch of EW-7 was indicated in borehole (KBH02). In the tunnel EW-7 consists of one set of fractures trending NNE - which are the most conductive structures - and one fracture set trending WNW.

NE-4 was indicated during pre-investigations by geophysical methods (ground magnetics and seismic refraction) and borehole data (KBH02) and estimated to consist of three branches trending NE. The dominating rock type in the zone - which is found to consist of two more or less continuous branches - is Småland (Ävrö) granite with inclusions of mylonite and greenstone.

NE-3 was indicated by ground magnetics and seismic refraction and confirmed in borehole KBH02 in the pre-investigation phase. After excavation, NE-3 was found approximately 49 m wide in the tunnel. Fine-grained granite is the dominating rock type with some intersections of Småland (Ävrö) granite and greenstone.

NE-1 was clearly indicated by geophysics and several boreholes in the pre-investigations and was estimated to be composed of three branches. All three branches are connected to a rather complex rock mass with Äspö diorite, fine-grained granite and

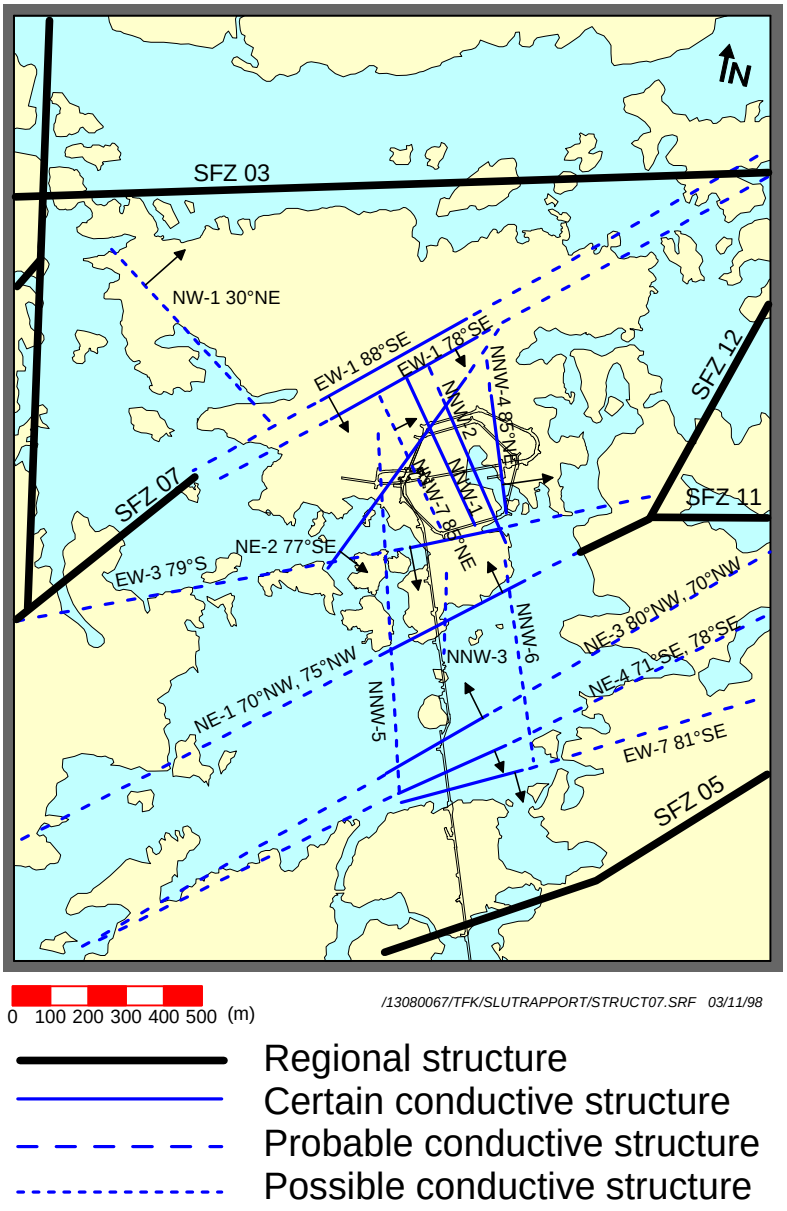

Figure 4-3. *Model of hydraulic conductors on the site scale, Rhén et al. /1997b/.*

greenstone. The two southernmost branches, trending NE and dipping NW, can be described as highly fractured and more or less water-bearing. The northern NW-dipping branch, which is approximately 28 m wide in the tunnel, is the most intense part of NE-1 and highly water-bearing.

The fracture zone EW-3 was very well indicated topographically, and geophysically (magnetic, seismic and electric) and in core boreholes KAS06 and KAS07 during the pre-investigations and estimated to be approximately 10 m wide. In the tunnel, EW-3 is found approximately 14 m wide and consisting of a 2-3 m wide crushed central section connected to a contact between Äspö diorite and fine-grained granite.

According to the prediction fracture zone NE-2, trending NE/ENE, should be regarded as the southern part of the main Äspö Shear zone and was expected to follow a somewhat winding course. The dip of NE-2 was estimated to change from steeply northwards in the NE part to steeply southeast in the SW part of the zone and to be only moderately hydraulically conductive. The south-western part of the zone NE-2 was judged'probable'. In the tunnel NE-2 has been demonstrated to be a 'minor' fracture zone dipping to the SE.

The fracture zone EW-1 was early indicated by the airborne geophysical survey and the lineament interpretation. Ground geophysical investigation confirmed the extent of EW-1 in more detail. In the first drilling campaign a cored borehole (KAS04) - inclined at 60° to the SE crossed the zone. EW-1 is very well indicated topographically (50-100 m wide depression in the ground extending many hundreds of metres), geo-physically (low-magnetic and low-resistivity zone 200-300 m wide), geologically (outcrops in a trench with mylonites and crushed sections) and in boreholes (mylonites and many highly fractured and altered sections in drill cores). Fracture zone EW-1 can be regarded as a part of the about 300 m wide low-magnetic zone (Äspö shear zone), trending NE, which divides Äspö into two main blocks.

Minor fracture zones

Gently dipping (<35°) fracture zones (GDF) on the surface of Äspö were first described by and interpreted as superficial stress-relief to the surface exaggerated by the retreating Quaternary ice sheets. Further studies of the surface geology revealed the presence of three gentle thrusts on Äspö striking E-W and dipping N all of which appeared to be associated with early gently dipping gneiss zones, thrusts and high fault scarps. Interpretations based on seismic reflections suggested the presence of gently dipping fracture zones with a 90-133 m spacing at depth. Two well defined gently dipping minor fracture zones were found in the tunnel. The first one intersects the tunnel at chainage 220m. It consists of anastomosing fractures striking NW and dipping 25°SW with a spacing of less than 10 cm. The width of the zone is 0.5 m. The second and most prominent gently dipping fracture zone appears at chainage 1744 m down to 1850 m. Intense fracturing trending NE and dipping 32°SE, sub-parallel to the tunnel for almost a hundred metres.

A number of minor fracture zones striking approximately NNW to NNE have been mapped on outcrops in Äspö. More or less extensive, they seem to branch out in an en-échelon pattern across the island. Only a few of them are topographically significant but normally too narrow to be geologically unambiguously indicated. All these minor fracture zones were described under the designation 'NNW' in the predictions. The different sub-zones, expected to be 0.1-5 m wide, in the system 'NNW' were predicted to be 'possible-probable' and their predicted position in the tunnel approximate. The mapping underground found several indications of minor fracture zones, generally not wider than 1 m. The water-bearing minor fracture zone NNW-4W is an example of a minor fracture zone which is indicated in the tunnel by three intersections at 2020 m, 2120 and 2914 m, with 5-10 cm wide fractures in this metre-wide section of cataclastic granite filled by grout.

Small scale fractures

Thorough analyses of the small scale fractures in the rock mass at Äspö have been made. The data base consists of more than ten thousand fracture observations. A special study with the main aim of synthesising the structural geology of water-bearing fractures has been made. Most fractures mapped at the Äspö HRL (all fractures >1 m in the tunnel except fractures in 'fracture zones') fall into five clusters. Four are steep and strike NS, NNW, WNW and NE; a fifth cluster is subhorizontal, see *Figure 4-4*. The NE set is less pronounced compared to the other sets.

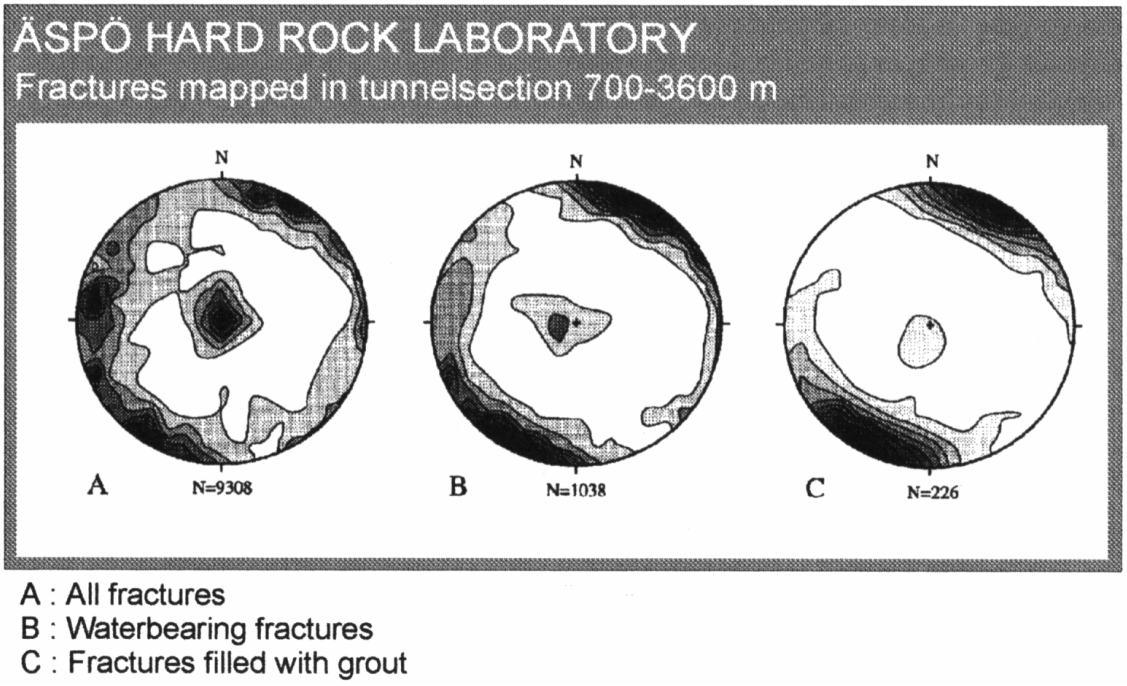

Figure 4-4. *Schmidt nets with lower hemisphere projection of Kamb contoured poles to fracture planes. Contour interval 2.0 sigma. N = sample size. /Hermanson, 1995, Rhén et al. ,1997b/.*

A: All fractures from 705 m to the end of the TBM tunnel, 3600 m. The plot shows five concentrations of fracture orientations, one sub-horizontal set, four steep sets striking N-S, NNW, WNW-NW and a comparatively less pronounced NE set.

B: Water-bearing fractures from the same part of the tunnel as A. The steep set striking WNW-NW is more pronounced compared with the same set in plot A. The other sets are less evident.

C: Fractures with grout from the same part of the tunnel as A. The plot is dominated by steep fractures striking WNW-NW. All other sets mentioned earlier are still visible, though not as pronounced as the WNW-NW set.

The array of fractures coated with the mineral assemblage chlorite-calcite can be represented by the same five sets. Most of the mapped fractures containing water are arranged into a single intense cluster of steep fractures striking WNW. A succession of fracture fillings of decreasing age has been proposed and includes: quartz, epidote, red staining, chlorite, Fe-oxy-hydroxides and calcite. The arrays of mineralised fractures

differ considerably with mineral infilling. Younger arrays are more complex due to the superposition of new fracture sets and reactivation of old sets. Repeated and sequential reactivation of the same faults has been demonstrated by superposition of different mineral coatings. Fractures trace lengths are log-normally distributed in all rock types. Fracture trace lengths do not vary with rock type. Mapped waterbearing fractures generally have coatings enriched in epidote, quartz and Fe-oxides. Fractures with injected grout are steep, strike WNW and generally longer than other fractures.

4.2 Overview of Hydrogeology

4.2.1 Hydraulic conductor domains

The geometry of the hydraulic conductor domains described in In *Rhén et al. /1997b/* are mainly defined by the major fracture zones described above in Section 4.1. The minor fracture zones in the 'NNW-system' are also important conductors and form a few hydraulic domains. A few hydraulic conductor domains were also added to the hydrogeological model in order to explain some of the responses obtained in the interference tests. A simplified model of the hydraulic conductor domains was made by fitting planes to the observations at the surface and in the boreholes. This model is shown in *Figure 4-3*.

The evaluated transmissivities are generally in the range 10^{-6}-10^{-4} m^2/s with a median of about 10^{-5} m^2/s. The greatest transmissivities for these larger features are for the hydraulic conductor domains below the Baltic Sea and for the minor fracture zone NNW-4. The largest transmissivity is approximately $3 \cdot 10^{-4}$ m^2/s for hydraulic conductor domain NE-1.

4.2.2 Hydraulic rock mass domain

The major hydraulic characteristics of the rock outside the hydraulic conductor domains are summarised as below.

An investigation of the structural geology of water-bearing fractures was made in the tunnel. It was found that the entire fracture system consists of five main sets, see *Figure 4-4*. The mapped water-bearing fractures and the fractures filled with grout (from the pre-grouting ahead of the tunnel face) are dominated by a subvertical fracture set striking WNW-NW. The N-S and NNW subvertical sets are also present but these subvertical sets are less pronounced compared to the entire fracture set. The mapped grout-filled fractures should be a good indicator of the water conducting fractures, as the grouting was performed generally 5-15 m ahead of the tunnel face where the rock mass should be fairly undisturbed. This indicates that the hydraulic property of the rock mass is probably anisotropic. Hydraulic tests in probe holes drilled along the tunnel during excavation indicate that subvertical fractures striking approximately WNW and N-S are more transmissive than the others are. It is believed that, on a larger scale, the WNW and N-S fracture sets form the hydraulic conductors called "NNW", see *Figure 4-3*.

4.3 Bore holes drilled at surface

Seven of the core bore holes drilled from the surface are included in this study, KAS02 - KAS08. Below in *Figure 4-5* the positions are plotted. Of the 48 HPF:s observed (based on $T \geq 10^{-5}$ m^2/s) in the surface bore holes 27 can be coupled to a deterministic zone (Generally a major fracture zone with large extent which has been defined to position

and extension), as presented in *Rhén et al. (1997b)* and *Figure 4-3*. The HPF:s are also frequently clustered and some of these clusters can be coupled to deterministic zones. For example, cluster at the bottom of KAS08 is a part of fracture zone NE-1. The positions of the HPF:s are presented in *Appendix 1* and an overview in *Appendix 4.*

Figure 4-5. *Positions of HPF:s in KAS bore holes marked as diamonds. Criterion : T ³ 10^{-5} m^2/s.*

4.4 Bore holes drilled in the Äspö Tunnel

The bore holes drilled, and hydraulic tested, after chainage 1400 m were selected for this study. In *Figure 4-6* the observations of HPF according to the criterion $T \geq 10^{-5}$ m^2/s, and in *Figure 4-7* according to the criterion $Q \geq 100$ l/min, are presented. The positions of the HPF:s are presented in *Appendix 1* and an overview in *Appendix 4*. Of the 31 HPF:s (based on $T \geq 10^{-5}$ m^2/s) observed in the tunnel core bore holes 17 can be coupled to a deterministic zone as presented in *Rhén et al. /1997b/* and *Figure 4-3*. Of the 37 HPF:s in probe holes, 12 can be coupled to a deterministic zone. Including the results from the bore holes drilled from surface, *Section 4.3*, it is found that out of 116 HPF:s 56 can be judged to be in connection with a deterministic zone found in *Figure 4-3*.

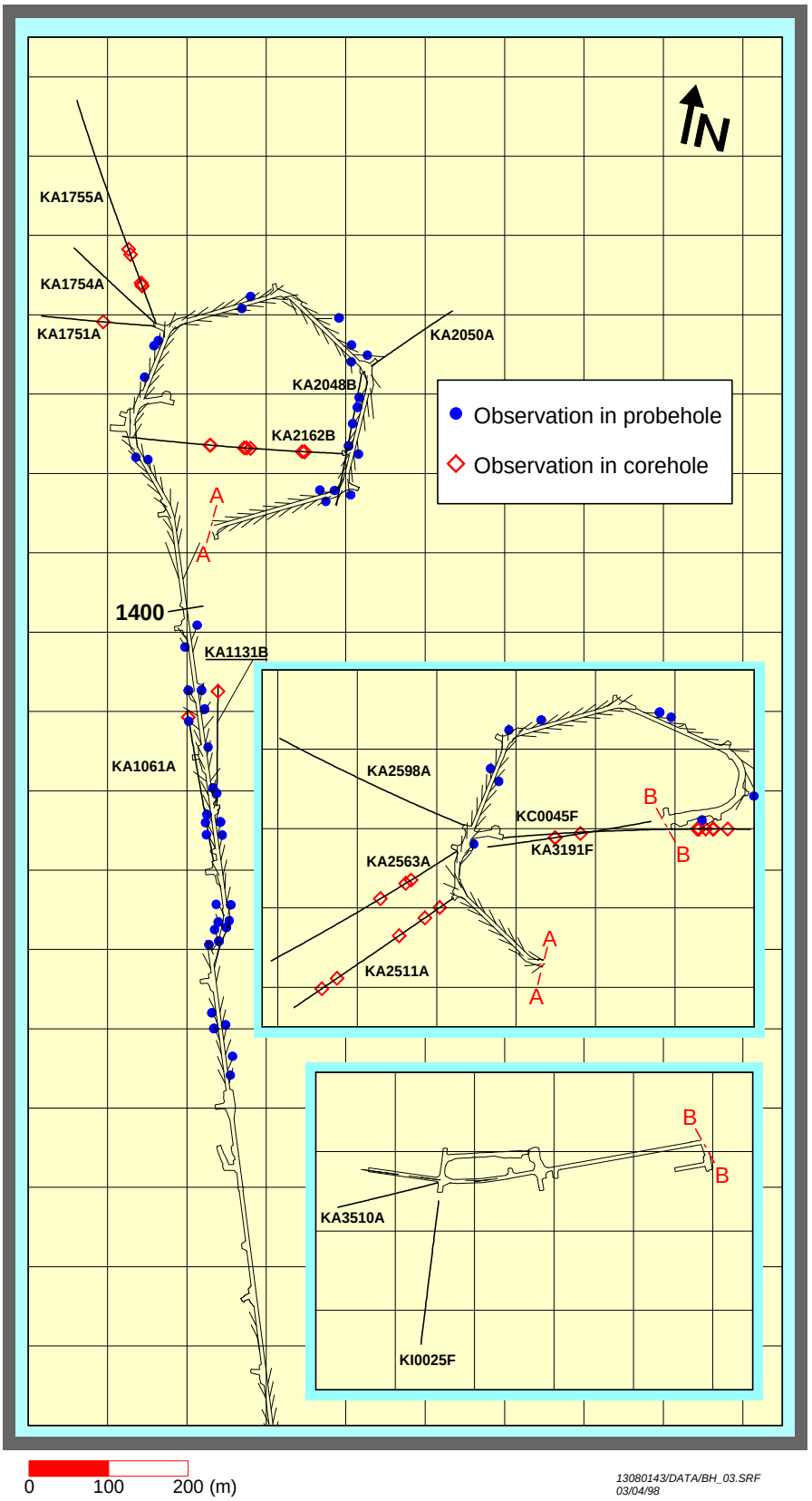

Figure 4-6. *Observations of HPF:s in core holes and probe holes drilled from the tunnel. Criterion:* $T \geq 10^{-5}$ m^2/s.

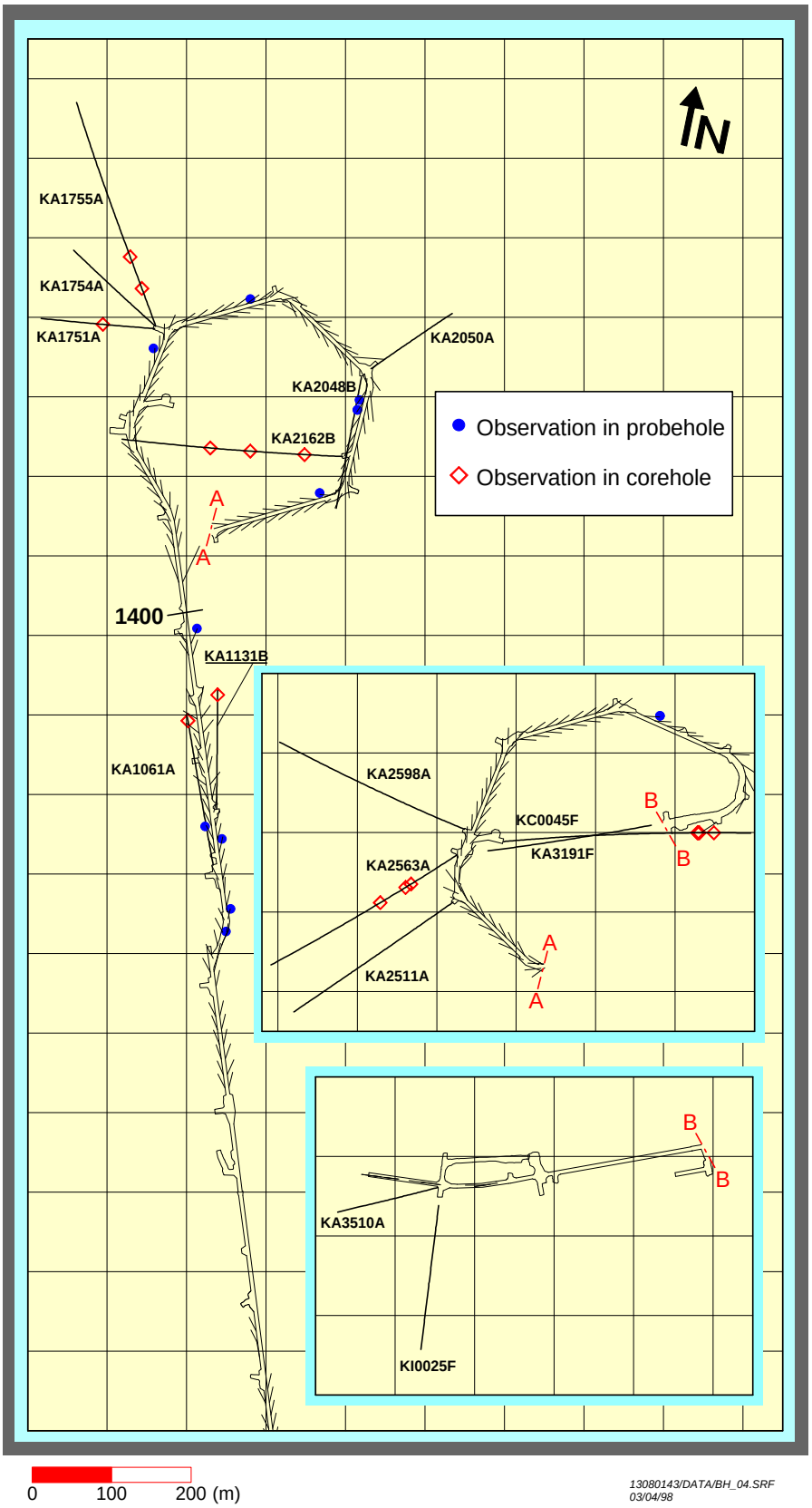

Figure 4-7. *Observations of HPF:s in core holes and bore holes drilled from the tunnel, Criterion : Q ³ 100 l/min.*

4.5 HPF:s Versus Depth

In *Figure 4-8,* the observed HPF:s are plotted versus depth in the rock mass. The features with $T \leq 10^{-4}$ m^2/s in *Figure 4-8* are located more or less over Southern Äspö, see Appendix 1.

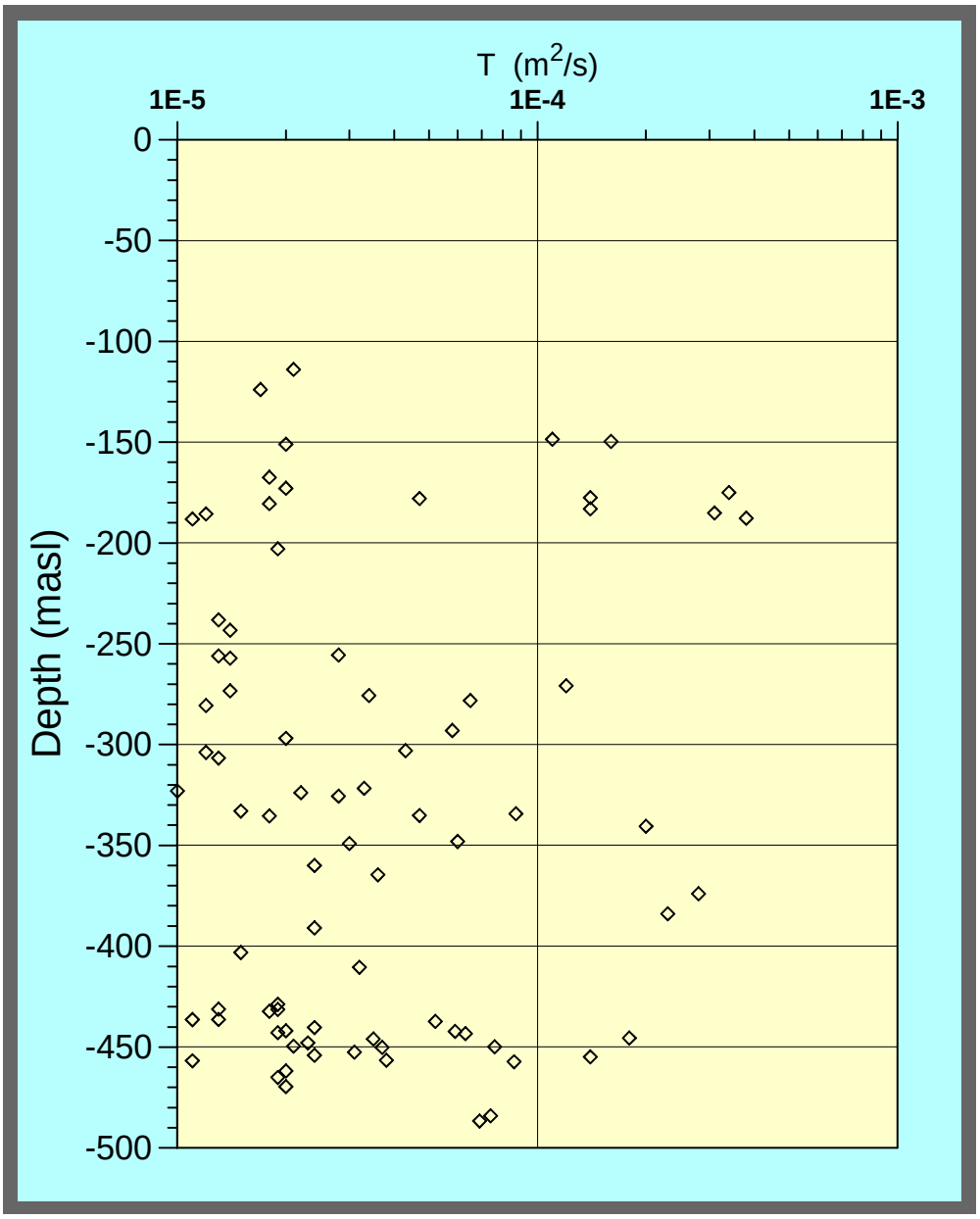

Figure 4-8. *HPF:s, based on T ³ 10^{-5} m^2/s, versus depth*

5 Results

In this Chapter the results from a few different HPF studies are presented. The estimates of the transmissivities are based on the assumption that the dynamic viscosity of the fluid and fluid density is approximately constant within the rock volume tested.

5.1 Distance between HPF:s

In this analysis the distance between different HPF:s were studied. The criterion $T \geq 10^{-5}$ m^2/s to define a HPF was used for all three kinds of bore holes; surface holes, core holes in tunnel and probe holes in tunnel. The criterion $Q \geq 100$ l/min was only used for core holes in tunnel.

The statistical analyses were made using three different methods in estimating the distances between the different HPF:s. In Figure 5-1 the different methods are shown as methods A, B and C.

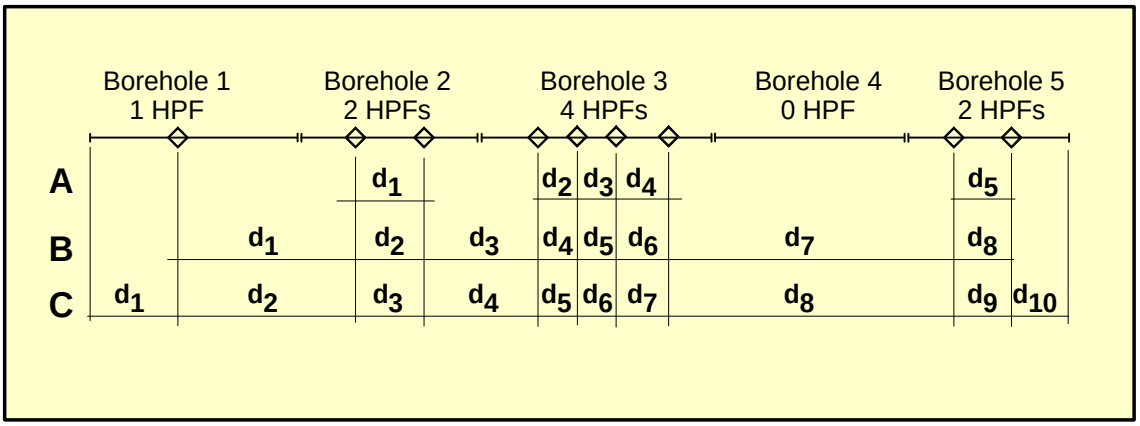

Figure 5-1. *Methods for calculation of distance between HPF:s in several bore holes.*

With method A only the internal distances within a bore hole are accounted for. The beginning and ending of every bore hole will not be included in the statistics, but the true distances are used in the calculations. This way of calculating may lead to an underestimation of the mean distances, at least if there are few observations along each bore hole, see *Figure 5-1*. With method B the available bore holes are combined in a random order to make a ”long bore hole”. Only 4 random arrangements of the bore holes were made for calculation of statistics. The calculated mean values and distribution characteristics based on B should be more reasonable estimates compared to calculations based on A. However, the first and last part of the ”long bore hole” will not be included in the analysis using method B. With method C every bore hole meter is used to estimate the arithmetic distance only between the HPF:s. Surface bore holes drilled on southern Äspö and bore holes drilled in tunnel section 1400 - 3600 were used for the analysis presented in Section 5.1.

5.1.1 Criterion T ³ 10^{-5} m^2/s

The criterion T ≥ 10^{-5} m^2/s was used for both bore holes where injection tests were made (surface bore holes KAS02-08) and bore holes where pressure build-up tests were made (tunnel bore holes).

Bore holes drilled at surface

Of the core bore holes drilled at the surface, five bore holes (KAS02, 05-08) were chosen to be studied for the distance between HPF:s. These are all located on southern Äspö where the tunnel spiral is situated. HPF:s between approximate 200 to 500 metres depth were chosen, see *Rhén et al /1997a/*. Method A is used in the first analysis.

Figure 5-2 shows the cumulative frequency distribution of the distance between HPF:s. *Table 5-1* shows the arithmetic mean distance and the median distance for different transmissivity intervals.

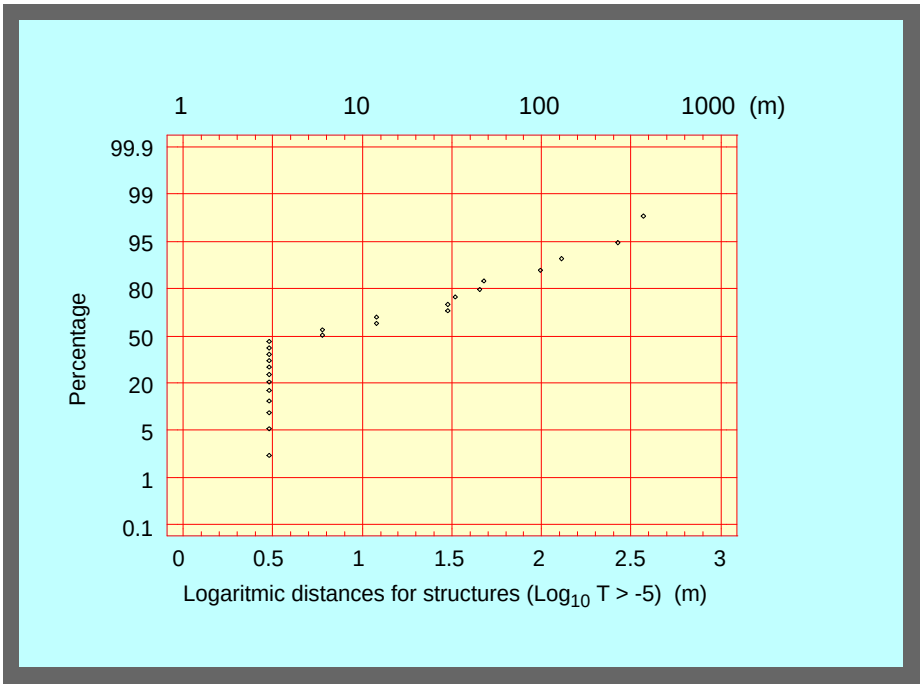

/13080143/DATA/KASDIST1.SRF 12/03/97

Figure 5-2. *The logarithmic distance ($LOG_{10}(D)$) between HPF:s. Criterion : T ³ 10^{-5} m^2/s. Method A.*

Table 5-1. Distance between hydraulic conductors with a transmissivity (T) greater than a specified value of the transmissivity (T_j) or within a range given by the transmissivities T_i and T_j. Data: Injection tests with 3 m packer spacing in cored bore holes KAS02, 05, 06, 07 and 08 for depth 200 to 500 m below sea level. Method A.

Distance between structures when $T \geq T_j$			Distance between structures when $T_i \geq T \geq T_j$			
KAS02, 05-08			KAS02, 05-08			
T_j (m^2/s)	Arithmetic mean distance (m)	Median distance (m)	T_i (m^2/s)	T_j (m^2/s)	Arithmetic mean distance (m)	Median distance (m)
1E-11	3.27	3.00	1E-10	1E-11	9.04	3.00
1E-10	4.11	3.00	1E-09	1E-10	8.35	3.00
1E-09	7.57	3.00	1E-08	1E-09	25.22	10.50
1E-08	9.82	3.00	1E-07	1E-08	26.39	9.00
1E-07	13.79	3.00	1E-06	1E-07	32.17	18.00
1E-06	20.88	9.00	1E-05	1E-06	28.89	12.00
1E-05	44.88	6.00	1E-04	1E-05	59.05	6.00
1E-04	156.00	120.00	1E-03	1E-04	156.00	120.00

The arithmetic mean value gives expected numbers of structures on a longer part of the bore hole

It should be remembered that the statistics are based on tests of relatively short duration. Particularly the lower transmissivities do not necessarily represent fractures that are connected to other fractures. The statistics are to some extent biased because two of the bore holes as well as the dominating numbers of water fractures are sub-vertical. This means that the distance between the conductors should become overestimated to some extent as the bore holes are sub-vertical. However, the bore holes were also targeting major fracture zones which may bias the sample so that the average distances become underestimated if it is the properties of the rock mass inbetween the major fracture zones that is considered.

When using method B the distances increase as can be observed in *Figure 5-3* and *Table 5-2.* The data sets consists of the 5 core bore holes with the following random order:

DATA SET 1	DATA SET 2	DATA SET 3	DATA SET 4
KAS05	KAS05	KAS02	KAS06
KAS06	KAS08	KAS08	KAS02
KAS07	KAS07	KAS07	KAS07
KAS08	KAS02	KAS05	KAS05
KAS02	KAS06	KAS06	KAS08

The total length of the ”long bore hole” is 2535.00 m, which is equal to the bore hole length with all injection tests. The length of the “bore hole” not included in the statistical analysis (beginning and end of bore hole) is for data set 1: 774 m, data set 2: 318 m, data set 3: 246 m and for data set 4: 102 m.

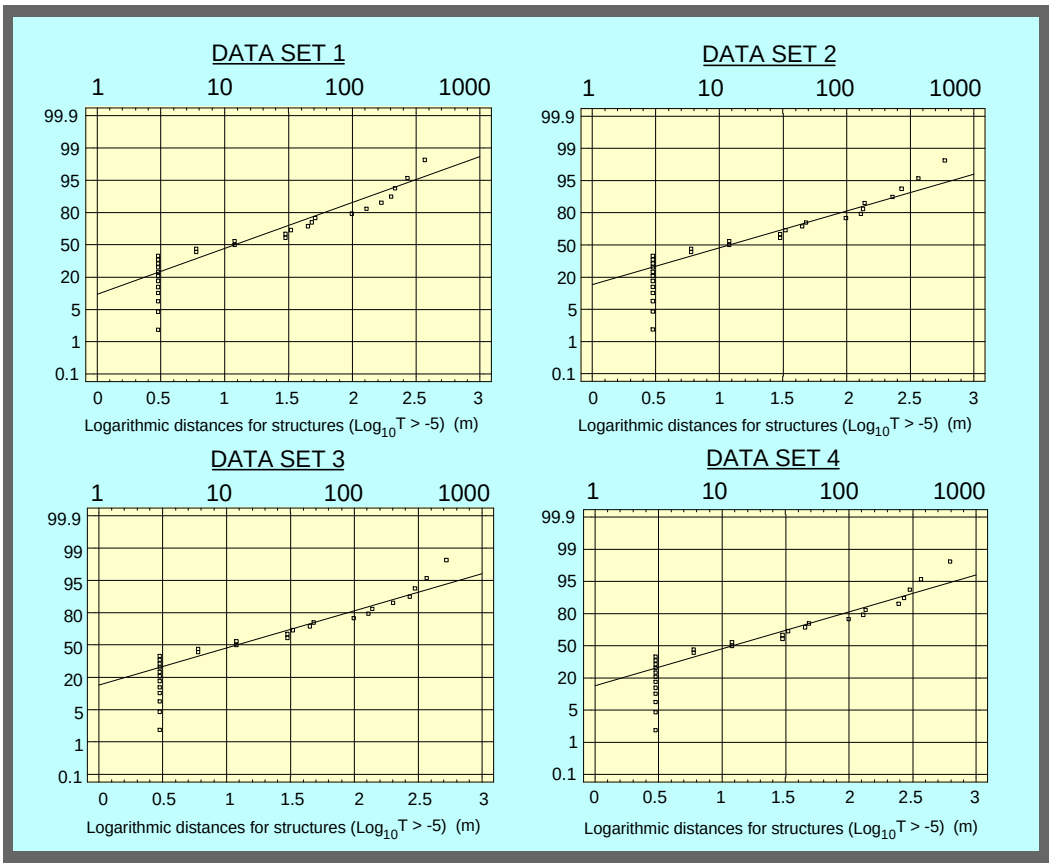

Figure 5-3*. The logarithmic distance (Log_{10} (D)) between HPF:s in core holes from surface. Criterion : T ³ 10^{-5} m^2/s. Method B.*

Table 5-2. Distance between hydraulic conductors with a transmissivity (T) greater than 10^{-5} m^2/s. Data from core bore holes (injection tests) drilled from surface (KAS02, 05-08). The first arithmetic mean distance is for the whole "long bore hole" (2535.00 m) while the second is for the bore hole length calculated according to method B.

Data set	Section in "long bore hole" (m)	Arithmetic Mean distance - I (m) (Method C)	Arithmetic mean distance - II (m) (Method B)	Geometric mean distance (m) (B)	Median distance (m) (B)
1	288.00 - 2049.00	84.50	58.70	16.00	12.00
2	288.00 - 2505.00	84.50	73.90	17.09	12.00
3	216.00 - 2505.00	84.50	76.30	17.42	12.00
4	102.00 - 2535.00	84.50	81.10	17.64	12.00

A total of 30 HPF:s, thus giving 29 distances, were used for the statistical analysis, based on $T \geq 10^{-5}$ m^2/s, in the "long bore hole". All the analysed statistical parameters (Method B) are presented below. The statistics in *Table 5-2* and *Figure 5-3* give probably more realistic statistics of the distances compared to *Table 5-1* and *Figure 5-2*. However, one can notice that there are a large number of HPF:s with short distances. They are located mainly at the bottom of KAS08 and KAS04, representing fracture zones NE-1 and EW-1 respectively. Of these two zones only EW-1 is intersected by the sub-horizontal core holes reported below while the probe holes does not intersect neither one. Therefore, an alternative analysis was made where all the HPF:s, but one, at the bottom of KAS08 was excluded. The data sets are named 1B - 4B and are identical to data sets 1 - 4 apart from the above explained exclusion. This means that five of the 3-meter distances and one of the 6-meter distances are excluded from the alternative data sets.

A total of 24 HPF:s, thus giving 23 distances, were used for the statistical analysis of data sets 1B - 4B, based on $T \geq 10^{-5}$ m^2/s, in the "long bore hole". All the analysed statistical parameters (Method B) are presented below. In the data set, there are still seven short distances (3m) . They are located in KAS04 (two short distances), KAS06 (three short distances), KAS07 (two short distances) and KAS08 (one short distance). One should possibly merge these HPF:s with short distances into single HPF:s. In that way the statistics would better show the large scale behaviour of the HPF:s.

Summary Statistics for Data set 1	Summary Statistics for Data set 2
Count = 29	Count = 29
Average = 1.20422	Average = 1.23282
Median = 1.07918	Median = 1.07918
Mode = 0.477121	Mode = 0.477121
Geometric mean = 0.975386	Geometric mean = 0.988156
Variance = 0.571693	Variance = 0.632978
Standard deviation = 0.756104	Standard deviation = 0.795599
Standard error = 0.140405	Standard error = 0.147739
Minimum = 0.477121	Minimum = 0.477121
Maximum = 2.56703	Maximum = 2.77159
Range = 2.08991	Range = 2.29447
Lower quartile = 0.477121	Lower quartile = 0.477121
Upper quartile = 1.70757	Upper quartile = 1.99564
Interquartile range = 1.23045	Interquartile range = 1.51851
Skewness = 0.450965	Skewness = 0.50251
Stnd. skewness = 0.991439	Stnd. skewness = 1.10476
Kurtosis = -1.37872	Kurtosis = -1.27523
Stnd. kurtosis = -1.51554	Stnd. kurtosis = -1.40179
Coeff. of variation = 62.7877%	Coeff. of variation = 64.5351%
Sum = 34.9225	Sum = 35.7517

Summary Statistics for Data set 3	Summary Statistics for Data set 4
Count = 29	Count = 29
Average = 1.24111	Average = 1.2464
Median = 1.07918	Median = 1.07918
Mode = 0.477121	Mode = 0.477121
Geometric mean = 0.991863	Geometric mean = 0.993921
Variance = 0.649583	Variance = 0.664003
Standard deviation = 0.805967	Standard deviation = 0.814864
Standard error = 0.149664	Standard error = 0.151316
Minimum = 0.477121	Minimum = 0.477121
Maximum = 2.72016	Maximum = 2.79518
Range = 2.24304	Range = 2.31806
Lower quartile = 0.477121	Lower quartile = 0.477121
Upper quartile = 1.99564	Upper quartile = 1.99564
Interquartile range = 1.51851	Interquartile range = 1.51851
Skewness = 0.497992	Skewness = 0.518887
Stnd. skewness = 1.09483	Stnd. skewness = 1.14077
Kurtosis = -1.3262	Kurtosis = -1.27886
Stnd. kurtosis = -1.45781	Stnd. kurtosis = -1.40578
Coeff. of variation = 64.939%	Coeff. of variation = 65.3775%
Sum = 35.9923	Sum = 36.1455

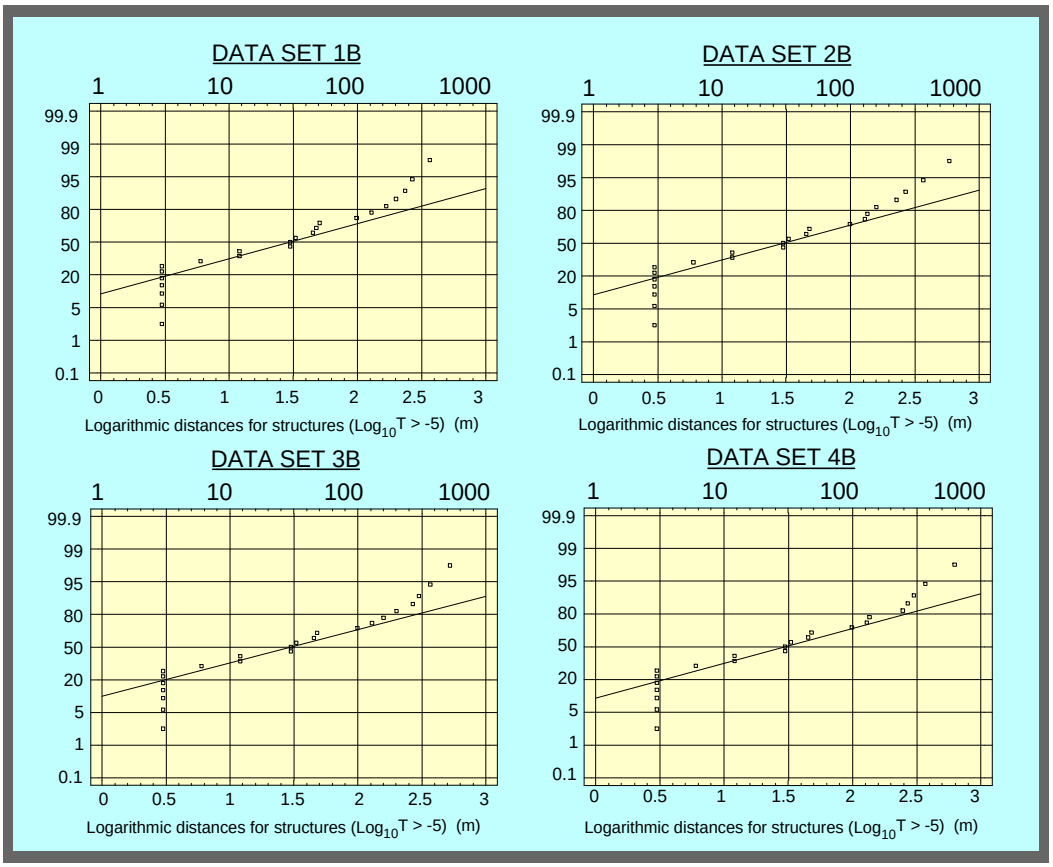

Figure 5-4*. The logarithmic distance (Log_{10} (D)) between HPF:s in core holes from surface. Bottom of KAS 08 not included (six HPF:s). Criterion: T ³ 10^{-5} m^2/s. Method B.*

Table 5-3. Distance between hydraulic conductors with a transmissivity (T) greater than 10^{-5} m^2/s. Bottom of KAS08 is not included except for one HPF (six HPF:s excluded). Data from core bore holes (injection tests) drilled from surface (KAS02, 05-08). The first arithmetic mean distance is for the whole "long bore hole" (2535.00 m) while the second is for the bore hole length calculated according to method B.

Data set	Section in "long bore hole" (m)	Arithmetic mean distance - I (m) (Method C)	Arithmetic mean distance - II (m) (Method B)	Geometric mean distance (m) (B)	Median distance (m) (B)
1	288.00 - 2049.00	105.62	73.38	24.13	30.00
2	288.00 - 2505.00	105.62	92.38	26.27	30.00
3	216.00 - 2505.00	105.62	95.38	26.91	30.00
4	102.00 - 2520.00	105.62	100.75	27.16	30.00

Summary Statistics for Data set 1B	Summary Statistics forData set 2B
Count = 23	Count = 23
Average = 1.38257	Average = 1.41954
Median = 1.47712	Median = 1.47712
Mode = 0.477121	Mode = 0.477121
Geometric mean = 1.15153	Geometric mean = 1.17114
Variance = 0.570166	Variance = 0.635216
Standard deviation = 0.755094	Standard deviation = 0.797004
Standard error = 0.157448	Standard error = 0.166187
Minimum = 0.477121	Minimum = 0.477121
Maximum = 2.56703	Maximum = 2.77159
Range = 2.08991	Range = 2.29447
Lower quartile = 0.477121	Lower quartile = 0.477121
Upper quartile = 2.11059	Upper quartile = 2.13033
Interquartile range = 1.63347	Interquartile range = 1.65321
Skewness = 0.0461852	Skewness = 0.1016
Stnd. skewness = 0.0904256	Stnd. skewness = 0.198921
Kurtosis = -1.49591	Kurtosis = -1.44481
Stnd. kurtosis = -1.46441	Stnd. kurtosis = -1.41439
Coeff. of variation = 54.6154%	Coeff. of variation = 56.1452%
Sum = 31.799	Sum = 32.6494

Summary Statistics for Data set 3B	Summary Statistics for Data set 4B
Count = 23	Count = 23
Average = 1.43	Average = 1.43399
Median = 1.47712	Median = 1.47712
Mode = 0.477121	Mode = 0.477121
Geometric mean = 1.17669	Geometric mean = 1.17831
Variance = 0.652242	Variance = 0.663842
Standard deviation = 0.807615	Standard deviation = 0.814765
Standard error = 0.168399	Standard error = 0.16989
Minimum = 0.477121	Minimum = 0.477121
Maximum = 2.72016	Maximum = 2.79518
Range = 2.24304	Range = 2.31806
Lower quartile = 0.477121	Lower quartile = 0.477121
Upper quartile = 2.2014	Upper quartile = 2.13033
Interquartile range = 1.72428	Interquartile range = 1.65321
Skewness = 0.0943967	Skewness = 0.122139
Stnd. skewness = 0.184818	Stnd. skewness = 0.239134
Kurtosis = -1.50656	Kurtosis = -1.46052
Stnd. kurtosis = -1.47484	Stnd. kurtosis = -1.42977
Coeff. of variation = 56.4765%	Coeff. of variation = 56.818%
Sum = 32.8901	Sum = 32.9818

Tunnel bore holes - core holes

Several core drilled bore holes were drilled from the tunnel during the construction of Äspö HRL. The entire bore holes or at some occasions part of the bore holes were pressure build-up tested and some were also flow logged, using either a UCM probe or a spinner probe.

If transmissivity (T) is evaluated for the entire bore hole, or for a part of it, (T_{tot}) and flow logging has been done, the approximate T distribution along the bore hole is estimated according to *Earlougher /1977/* as $T_i = T_{tot} \cdot dQ_i/Q_{tot}$, where Q_{tot} is the total flow rate for the same bore hole section as T_{tot} and dQ_i is the flow rate change per length i.

The *Figure 5-5* shows the cumulative frequency distribution of the distance between HPF:s when using method A. *Table 5-4* shows the arithmetic mean distance and the median distance when using method A.

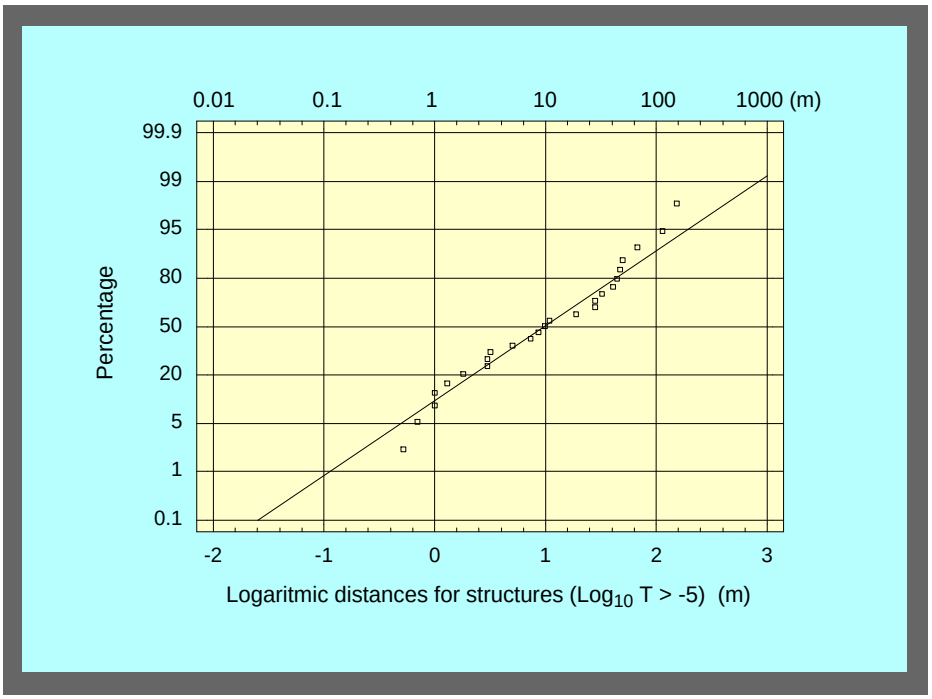

Figure 5-5. *The logarithmic distance (Log_{10} (D)) between HPF:s when using method A. Criterion: T ³ 10^{-5} m^2/s.*

Table 5-4. Distance between hydraulic conductors with a transmissivity (T) greater than a specified value of the transmissivity (T_j) or within a range given by the transmissivities T_i and T_j. Data from core bore holes in Äspö tunnel chainage 1400-3600 m. Method A.

Distance between structures when $T \geq T_j$			**Distance between structures when $T_i \geq T \geq T_j$**			
	Tunnel core holes				**Tunnel core holes**	
T_j (m^2/s)	**Arithmetic mean distance (m)**	**Median distance (m)**	**T_i (m^2/s)**	**T_j (m^2/s)**	**Arithmetic mean distance (m)**	**Median distance (m)**
10^{-8}	(14.18)	(8.80)	10^{-7}	10^{-8}	(22.86)	(25.00)
10^{-7}	(14.15)	(9.05)	10^{-6}	10^{-7}	(38.35)	(28.60)
10^{-6}	14.36	8.00	10^{-5}	10^{-6}	15.15	9.57
10^{-5}	27.21	9.80	10^{-4}	10^{-5}	22.96	9.80

The statistics for $T < 10^{-6}$ are uncertain due to the test methodology (pressure build-up test and flow logging). Due to the cumulative measurement of the flow rate there is a tendency that the low transmissive features are masked by the high transmissive ones.

As an alternative analysis of the distances between the different HPF:s in the tunnel core bore holes, the bore holes were divided in 3 metres sections starting from the beginning of the bore hole, in the same manner as for the KAS bore holes from surface. In doing this we eliminated the shortest distances that are one reason why the statistics for distances in the tunnel core bore holes are shorter than in the surface bore holes. In *Table 5-5* the statistics from this analysis is presented.

Table 5-5. Distance between hydraulic conductors with a transmissivity (T) greater than a specified value of the transmissivity (T_j) or within a range given by the transmissivities T_i and T_j. Data from core bore holes in Äspö tunnel chainage 1400-3600 m. Data modified to 3 metres sections. Method A.

Distance between structures when $T \geq T_j$			Distance between structures when $T_i \geq T \geq T_j$			
Tunnel core holes			Tunnel core holes			
T_j (m^2/s)	Arithmetic mean distance (m)	Median distance (m)	T_i (m^2/s)	T_j (m^2/s)	Arithmetic mean distance (m)	Median distance (m)
10^{-8}	(16.20)	(10.00)	10^{-7}	10^{-8}	(22.86)	(25.00)
10^{-7}	(16.39)	(10.15)	10^{-6}	10^{-7}	(41.93)	(30.00)
10^{-6}	16.86	10.46	10^{-5}	10^{-6}	17.09	12.00
10^{-5}	36.23	27.75	10^{-4}	10^{-5}	38.24	27.88

As in the earlier analysis the statistics for $T < 10^{-6}$ are uncertain due to the test methodology (pressure build-up test and flow logging). Due to the cumulative measurement of the flow rate there is a tendency that the low transmissive features are masked by the high transmissive ones.

When using method B the distances increase as can be observed in *Figure 5-6* and *Table 5-6.* The data sets consists of the 11 core bore holes used in this study in the following order (randomly prepared):

DATA SET 1	DATA SET 2	DATA SET 3	DATA SET 4
KA2162B	KA1754A	KA3510A	KA3191F
KI0025F	KA2598A	KA2563A	KA3510A
KA2511A	KA2162B	KA2598A	KA1755A
KA1754A	KI0025F	KA3191F	KA2598A
KA1755A	KA3510A	KA1755A	KC0045F
KA2563A	KA2563A	KC0045F	KA2511A
KA2598A	KA1751A	KA1754A	KA1751A
KA3191F	KC0045F	KI0025F	KA1754A
KA3510A	KA2511A	KA2162B	KI0025F
KA1751A	KA3191F	KA2511A	KA2162B
KC0045F	KA1755A	KA1751A	KA2563A

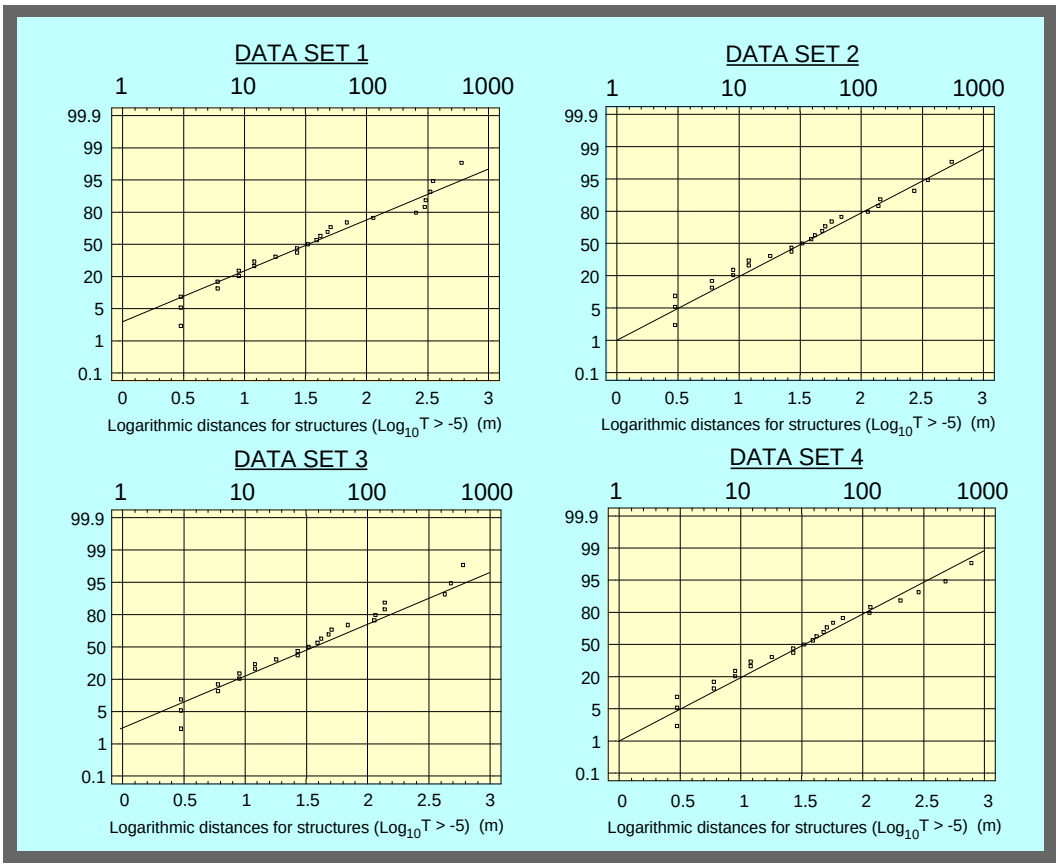

Figure 5-6*. The logarithmic distance (Log_{10} (D)) between HPF:s in core holes. Criterion: T ³ 10^{-5} m^2/s. Method B.*

Table 5-6. Distance between hydraulic conductors with a transmissivity (T) greater than 10^{-5} m^2/s. Data from core bore holes in Äspö tunnel chainage 1400-3600 m. Data modified to 3 metres sections. The first arithmetic mean distance is for the whole ”long bore hole” (2754.58 m) while the second is for the bore hole length calculated according to method B.

Data set	Section in ”long bore hole” (m)	Arithmetic mean distance - I (m) (Method C)	Arithmetic mean distance - II (m) (Method B)	Geometric mean distance (m) (B)	Median distance (m) (B)
1	48.00 - 2721.58	105.94	102.83	34.36	33.00
2	498.00 - 2542.00	105.94	78.62	30.09	33.00
3	240.00 - 2667.58	105.94	93.37	31.98	33.00
4	90.00 - 2548.58	105.94	94.56	31.19	33.00

The total length of the ”long bore hole” is 2754.58 m. The length of “the long bore hole” is not included in statistical analysis (beginning and end of bore hole) is for data set 1: 81 m, data set 2: 710.58 m, data set 3: 327 m and for data set 4: 296 m.

It should be observed that while 31 HPF:s are found, based on $T \geq 10^{-5}$ m^2/s, there are only 26 HPF:s in the ”long bore hole” divided into 3 m sections. This is due to that nearby-lying HPF:s may go into the same 3 meter section. Accordingly, the statistics above is for 25 distances only. All the analysed statistical parameters (Method B) are presented below.

Summary Statistics for Data set 1	Summary Statistics for Data set 2
Count = 25	Count = 25
Average = 1.53609	Average = 1.47842
Median = 1.51851	Median = 1.51851
Mode = 0.477121	Mode = 0.477121
Geometric mean = 1.35576	Geometric mean = 1.32084
Variance = 0.50859	Variance = 0.421677
Standard deviation = 0.713155	Standard deviation = 0.649367
Standard error = 0.142631	Standard error = 0.129873
Minimum = 0.477121	Minimum = 0.477121
Maximum = 2.77743	Maximum = 2.73957
Range = 2.30031	Range = 2.26245
Lower quartile = 0.954243	Lower quartile = 0.954243
Upper quartile = 2.0569	Upper quartile = 1.83885
Interquartile range = 1.10266	Interquartile range = 0.884607
Skewness = 0.172254	Skewness = 0.14151
Stnd. skewness = 0.351611	Stnd. skewness = 0.288857
Kurtosis = -1.06387	Kurtosis = -0.735003
Stnd. kurtosis = -1.08581	Stnd. kurtosis = -0.750159
Coeff. of variation = 46.4268%	Coeff. of variation = 43.9231%
Sum = 38.4022	Sum = 36.9604

Summary Statistics for Data set 3	Summary Statistics for Data set 4
Count = 25	Count = 25
Average = 1.50487	Average = 1.49409
Median = 1.51851	Median = 1.51851
Mode = 0.477121	Mode = 0.477121
Geometric mean = 1.33664	Geometric mean = 1.32876
Variance = 0.465151	Variance = 0.459027
Standard deviation = 0.68202	Standard deviation = 0.677515
Standard error = 0.136404	Standard error = 0.135503
Minimum = 0.477121	Minimum = 0.477121
Maximum = 2.77743	Maximum = 2.89186
Range = 2.30031	Range = 2.41474
Lower quartile = 0.954243	Lower quartile = 0.954243
Upper quartile = 2.0569	Upper quartile = 1.83885
Interquartile range = 1.10266	Interquartile range = 0.884607
Skewness = 0.212603	Skewness = 0.28062
Stnd. skewness = 0.433973	Stnd. skewness = 0.572813
Kurtosis = -0.737367	Kurtosis = -0.542155
Stnd. kurtosis = -0.752572	Stnd. kurtosis = -0.553335
Coeff. of variation = 45.3207%	Coeff. of variation = 45.3462%
Sum = 37.6218	Sum = 37.3524

Tunnel bore holes - probe holes

During the construction of Äspö HRL a pair of 20-meter long probe bore holes were drilled in each wall with an angle of 20° to the wall. The pair was meant to be drilled and pressure build-up tested every fourth round (about every 16 m), but in some cases they were not drilled or not tested.

During the drilling of the probe holes the drill depth at which an increase in the amount of water flowing-in was documented. The flow rate out of the bore hole was also estimated and documented. The number of increasing flow-rate-steps was generally 1-6 (very often just 1), but in a few of the probe holes it was not possible to define any position for the flow rate increase. The transmissivity of each fracture was calculated as:

$$T_f = T_{ij} = T_i \cdot Q_{ij} / Q_i \qquad (5\text{-}1)$$

Q_{ij} is the estimated inflow during drilling from each fracture, Q_i the total inflow to the bore hole and T_i the evaluated transmissivity of the bore hole. The position of each inflow Q_{ij} was projected on the tunnel line, and this position and T_{ij} were then used to estimate the statistics (Method B).

Figure 5-7 and *Table 5-7* show the statistics for pressure build-up tests in the tunnel, which were performed in more or less horizontal bore holes. The sample is clearly biased for low transmissivities.

Firstly, the method used (identifying transmissive structures in probe holes during drilling) leads to underestimation of low-conductivity features, because they are masked by higher flow rates. This probably affects the statistics for low-transmissive features. The statistics is probably not relevant for $T < 10^{-7}$ m^2/s. Secondly it has not been possible to drill every fourth round, which causes a few false ”long” distances.

All the analysed statistical parameters (Method B) are presented below.

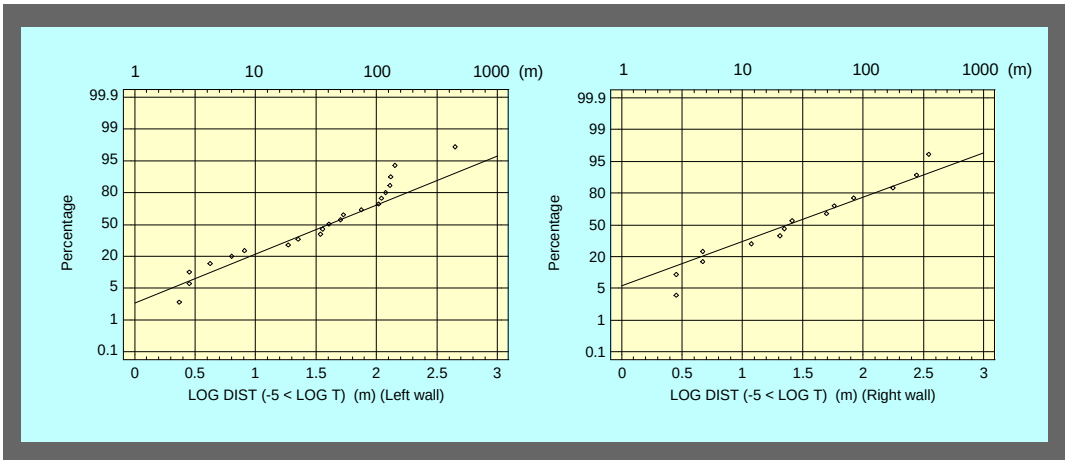

Figure 5-7. *The logarithmic distance (Log_{10} (D)) between HPF:s in probe holes in the Äspö tunnel, chainage 1400 - 3600 metres. Method B.*

Summary Statistics for LOG_GT5 (Left wall)	Summary Statistics for LOG_GT5 (Right wall)
Count = 21	Count = 14
Average = 1.49461	Average = 1.42873
Median = 1.60764	Median = 1.38027
Mode =	Mode = 0.450107
Geometric mean = 1.30519	Geometric mean = 1.23724
Variance = 0.440294	Variance = 0.505174
Standard deviation = 0.663546	Standard deviation = 0.710756
Standard error = 0.144798	Standard error = 0.189957
Minimum = 0.370926	Minimum = 0.450107
Maximum = 2.6491	Maximum = 2.54191
Range = 2.27817	Range = 2.0918
Lower quartile = 0.907031	Lower quartile = 0.674281
Upper quartile = 2.04272	Upper quartile = 1.92282
Interquartile range = 1.13569	Interquartile range = 1.24854
Skewness = -0.383763	Skewness = 0.0900466
Stnd. skewness = -0.717955	Stnd. skewness = 0.137548
Kurtosis = -0.907302	Kurtosis = -1.14699
Stnd. kurtosis = -0.848703	Stnd. kurtosis = -0.87603
Coeff. of variation = 44.396%	Coeff. of variation = 49.7474%
Sum = 31.3868	Sum = 20.0022

Table 5-7. Distance between hydraulic conductors with a transmissivity (T) greater than a specified value of the transmissivity (T_j) or within a range given by the transmissivities T_i and T_j. Data: probe holes in tunnel section 1400-3600 m. Values for $T < 10^{-7}$ m^2/s is uncertain. Method B.

Distance between structures when $T^3 T_j$					
	Left tunnel wall			Right tunnel wall	
T_j (m^2/s)	Arithmetic mean distance (m)	Median distance (m)	T_j (m^2/s)	Arithmetic mean distance (m)	Median distance (m)
(1E-11)	(18.93)	(13.65)	(1E-11)	(20.05)	(13.09)
(1E-10)	(19.86)	(14.14)	(1E-10)	(20.25)	(13.14)
(1E-09)	(20.88)	(13.65)	(1E-09)	(22.01)	(11.73)
(1E-08)	(24.41)	(13.24)	(1E-08)	(24.70)	(11.49)
1E-07	32.51	14.39	1E-07	36.16	12.65
1E-06	36.62	19.19	1E-06	55.22	10.20
1E-05	73.25	40.52	1E-05	77.73	24.08

5.1.2 Criterion Q ≥ 100 l/min

When using the other HPF criterion, Q ³ 100 l/min, only data from the core bore holes in the tunnel was used. The statistics are presented in *Table 5-8* below.

Table 5-8. Distance between HPF:s in tunnel core bore holes, chainage 1400-3600 m. Method A.

Distance between structures when Q ³ Q_j		
Q_j (l/min)	**Arithmetic mean distance (m)**	**Median distance (m)**
100	25.43	18.30

5.1.3 Summary

In *Table 5-9* the results are summarised. No values for geometric mean distance and standard deviation i given for method C. The reason is that for the HPF:s at both ends of the "long bore hole" the distances to the HPF:s outside the "long bore hole" is unknown. It could be handled as the distance between the bore holes, just adding d1 and d10 and use it as a distance in either end of the long bore hole, see *Figure 5-1*. However, this was not done in this study.

The results presented may to some extent be biased due to a few reasons. First the water conducting fractures have been found to be sub-vertical */Rhén et al, 1997b*/ and therefore one could expect to find larger mean distances in the sub-vertical bore holes compared to sub-horizontal ones. This cannot be seen in *Table 5-9*. However, as was commented earlier, some short distances should possibly be excluded. One should possibly merge these HPF:s with short distances into single HPF:s. In that way the statistics would better show the large scale behaviour of the HPF:s, and the distances for the sub-vertical holes would increase.

Secondly the major fracture zones, which were deterministically defined, are all sub-vertical and then drilling sub-vertical bore holes through them may give a long intersection length which possibly can result in a few more HPF:s compared if the bore hole had been horizontal. As several of the sub-vertical bore holes drilled from the surface were targeting these major zones this may be the explanation why there is no clear difference between sub-horizontal and sub-vertical bore holes.

If features having a transmissivity $T \geq 10^{-6}$ m^2/s are studied one can see the expected difference between sub-vertical and sub-horizontal bore holes, see *Tables 5-1* and *5-5*. The reason is that the calculated distances are based on a larger data set that is less affected of the major fracture zones and probably gives better statistical estimates of the rock mass. However, this study has mainly been focusing on features having a transmissivity $T \geq 10^{-5}$ m^2/s.

The statistics inferred is dependent of the scale of observations. It is possibly better to use larger interval than 3 m to describe the spatial distribution of distances between HPF:s on a scale of several hundred meters, at least if simple measures as arithmetic mean is used as a measure for HPF:s between the large deterministic zones.

Despite the difficulties mentioned above, the statistics for the three data sets representing different bore hole groups are surprisingly similar. Recalculations of the data from the subvertical bore holes, according to the reasons mentioned above, may however increase the mean distances somewhat.

Table 5-9. The statistics of the distance between hydraulic conductors with a transmissivity (T) greater than a specified value of the transmissivity (T_j).

Bore holes drilled at surface **T_j (m^2/s)**	**Arithmetic mean distance** **D_a (m)**	**Geometric mean distance D_g (m)**	**Standard deviation of $Log_{10}D$**
$T \geq 10^{-5}$ (Method A)	45	11	0.70
$T \geq 10^{-5}$ (Method B)	60 - 80	16 - 18	0.76 - 0.81
$T \geq 10^{-5}$ (Method B) (bottom of KAS08 excluded)	75 - 100	24 -27	0.76 - 0.81
$T \geq 10^{-5}$ (Method C)	85	-	-
$T \geq 10^{-5}$ (Method C) (bottom of KAS08 excluded)	106	-	-
Core holes in the tunnel **T_j (m^2/s)**			
$T \geq 10^{-5}$ (Method A)	27	9	0.73
$T \geq 10^{-5}$ (3 m section data) (Method A)	36	21	0.47
$T \geq 10^{-5}$ (3 m section data) (Method B)	80 - 100	30 - 34	0.65 - 0.71
$T \geq 10^{-5}$ (3 m section data) (Method C)	106	-	-
Probe holes in the tunnel **T_j (m^2/s)**			
$T \geq 10^{-5}$ (Method B)	73 - 78	27 - 31	0.66 - 0.71

5.2 Correlation Study

It is of interest to make a first attempt at setting the occurrence of HPF:s in a structural geological context. Of special interest in this study is if HPF:s occur in the vicinity of :

- any special rock type
- any special rock contact
- rock veins
- crush zones/natural joints
- areas where RQD is high/low

Rockveins: Part of core mapped as rockvein if length of mapped rock type along the core < 1m.

Crush zones: Part of core mapped as crush zone if the core could not be reconstructed due to gravel–like material and/or core loss. Width of crush zones are generally a few centimetres or larger.

Natural joints: The mapped fractures that are considered open for water flow.

RQD: Rock Quality Designation. Based on core mapping and represents the total length of whole (full-diameter) bits of core, 10 cm or longer, in competent rock, calculated as a percentage of the theoretical length of considered (at least 1 m), including any loss of core. The calculation is based on natural joints.

In *Appendix 4* an overview of all the core bore holes included in this study is presented. These bore holes are:

KAS02-08	KA1751A
KA1754A	KA1755A
KA2162B	KA2511A
KA2563A	KA2598A
KC0045F	KA3191F
KA3510A	

In *Appendix 3*, a table is presented showing the details of this correlation study.

The evaluation of HPF:s for the surface bore holes is based on the injection tests with a packer spacing of three metres and accordingly the geological data for the same packer interval.

The evaluation of HPF:s in the tunnel core holes is based on positions of flows into the bore holes. If these are based on drilling records, it is judged that there exists an uncertainty of +/- 1-meter from the given position. If flow logging is the base of position a HPF, the position is generally judged to be more certain than the drilling records. How-

ever, in this evaluation +/- 1 meter from the observed HPF has been the base for the bore hole section to be used for the evaluation. Due to the above reasons, the length of a "HPF section" or "HPF interval", mentioned in the text below, is 2-3 m long. In *Appendix 3*, the positions for the HPF:s and logging methods are shown in detail.

In the bore holes mentioned above the total number of HPF:s, based on $T \geq 10^{-5}$ m^2/s, are 79, and this correlation study is based on those data.

5.2.1 Rock type

The rocktype(s) within an interval around the HPF of ±1 meter for tunnel bore holes and within the packer-interval (3 m) with a HPF for the surface bore holes was examined. Thus, one or more rock types can be found in the 79 intervals for the HPF:s. Total number of observations of different rock types were 95 within these 79 sections. In *Figure 5-8* below, the results are shown.

Äspö diorite and Småland (Ävrö) granite are the dominating lithological units on Äspö, with an approximately 53-55 % and 24-28 % share respectively (*Stanfors et al /1997/*, tunnel section 1475-2874m). Approximately 14-15% of the rock mass consists of fine-grained granite while the amount of greenstone is 3-8 % and pegmatite and mylonite-hybridized rock about 0 - 1 % each. Considering the above mentioned proportions of the lithological units, the HPF:s are more than twice as frequent in fine-grained granite compared to other lithological units. Småland (Ävrö) granite and Äspö diorite have the same frequency and greenstone somewhat larger frequency compared to Småland (Ävrö) granite and Äspö diorite.

(Observe that veins of a certain rock type within HPF sections is not taken into account in the statistics shown in *Figure 5-8*.)

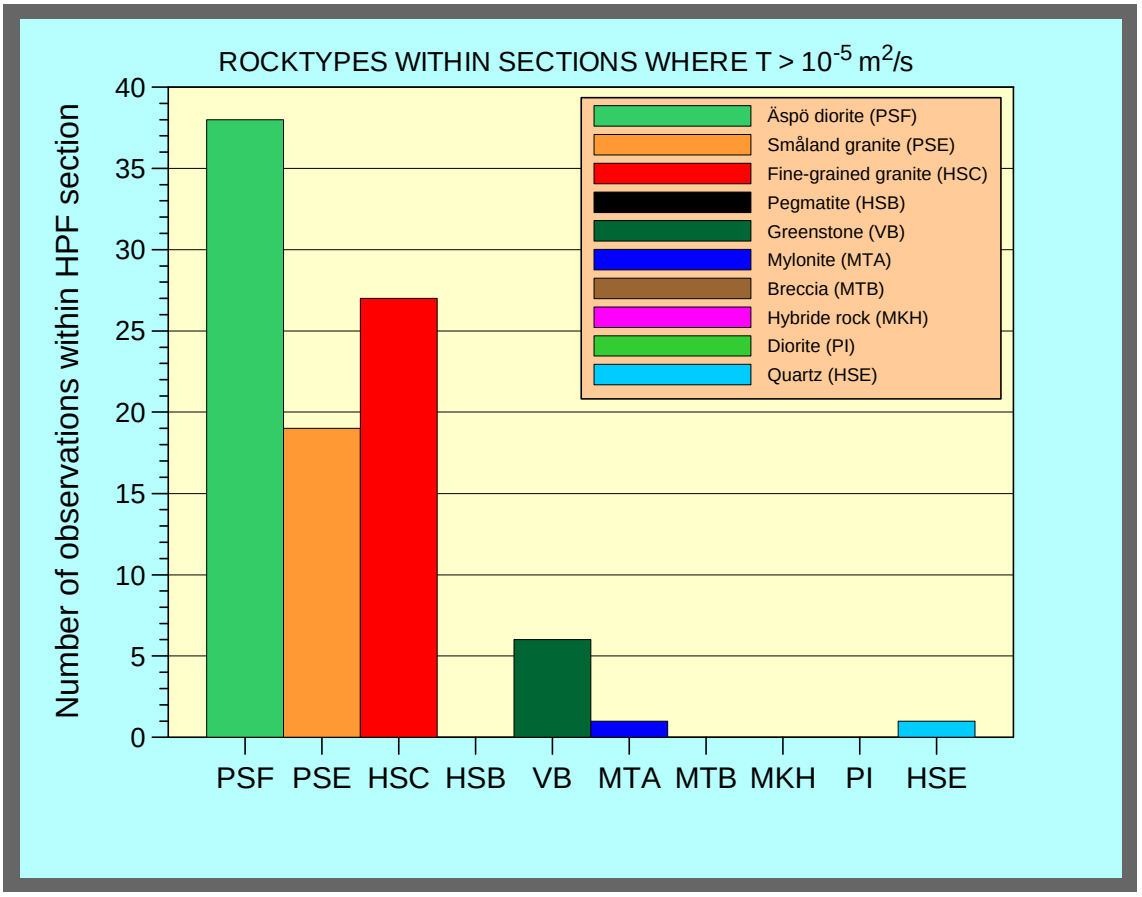

CRITERIA :

TUNNEL BOREHOLES - HPF POSITION +/- 1 meter
SURFACE BOREHOLES - WITHIN PACKER INTERVAL (3 m)

Figure 5-8. *Rock types within the 79 sections with HPF:s. The observations shows the number of different rock types found in within an interval of ±1 meter for tunnel bore holes and within the packer-interval (3 m) with a HPF for the surface bore holes. The total number of rock types is 95 within the 79 sections.*

5.2.2 Rock contacts

The HPF intervals in *Section 5.2.1* with two or more rock types were selected to see if any pattern could be found. Accordingly, for a section with “rock contact(s)”, two or more rock types are present within an interval around the HPF of ±1 meter for tunnel bore holes and within the packer-interval (3 m) with a HPF for the surface bore holes. See *Appendix 3* for details. One should also note that for one contact two rock types are registered. In 15 of the 79 sections, there are “rock contacts” present and the total number of “rock contacts” within these sections is 20. *Figure 5-9* summarises the results. Fine-grained granite is the rock type that occurs most frequently when mapping a contact. In 11 of the 15 sections, Fine-grained granite is one of the rock types. Äspö diorite,

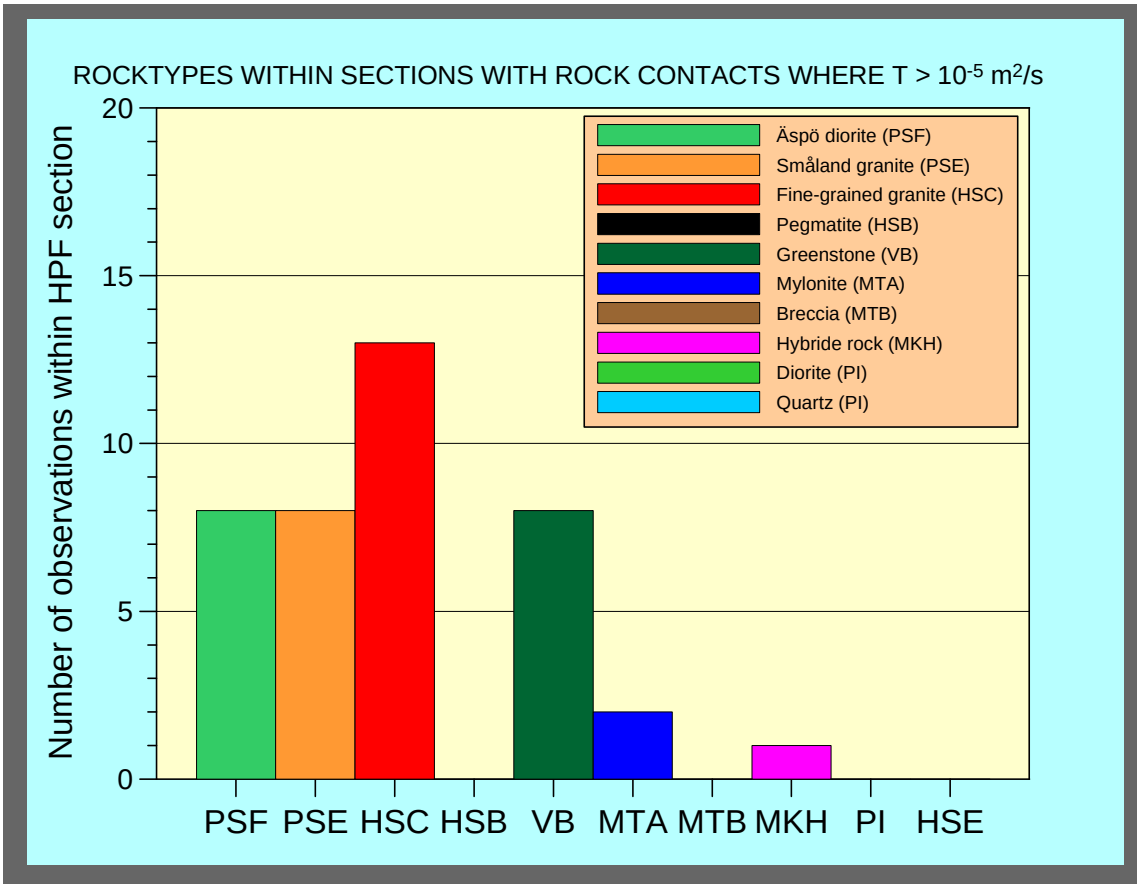

CRITERIA :

TUNNEL BOREHOLES - HPF POSITION +/- 1 meter
SURFACE BOREHOLES - WITHIN PACKER INTERVAL (3 m)

Figure 5-9. *Rock types within the 15 sections with HPF:s and two or more rock types within each section. The observations shows the number of different rock types found in within an interval of ±1 meter for tunnel bore holes and within the packer-interval (3 m) with a HPF for the surface bore holes.*

Småland (Ävrö) granite and greenstone are each of them found in 6 of the 15 sections and mylonite in one section.

Based on the subvertical bore holes, 9-12 rock contacts/ 100 m were predicted in the pre-investigations of the Äspö HRL. The result from the tunnelmapping showed 8-12 rock contacts/ 100 m */Stanfors et al, 1997/*. If the rock contacts are randomly distributed one could expect to find a rock contact within about 25 % of the HPF sections (2-3 m long). The actual number is about 20% (not including veins) and therefor it cannot be

concluded that rock contacts are important for the locations of the HPF:s. However, a difficulty is the classification of a rock contact in the data base. It is the contact between larger bodies that is found in the data base, excluding the contact between the veins and the surrounding rock. See Section 5.1.6 for further discussion.

5.2.3 Rock veins

The HPF intervals in *Section 5.2.1* with one or more rock veins were selected to see if any pattern could be found. In the core mapping a rock type was mapped as a "vein", and not "rock", if the width of the rock type was less than about 100 cm. Accordingly, for a section with one or more rock veins are present within an interval around the HPF of ±1 meter for tunnel bore holes and within the packer-interval (3 m) with a HPF for the surface bore holes. The result is presented in detail in the table in *Appendix 3* and in *Figure 5-10*. In 27 of the 79 sections, there are "rock veins" present and the total number of "rock veins" within these sections is 35. Fine-grained granite is the rock type that occurs most frequently when mapping a vein. The frequency of fine-grained granite, pegmatite and greenstone are about same in the HPF sections. In most sections with pegmatite present, fine-grained granite is present as a "vein" or "rock". In 12 sections with mapped "rock type" Äspö diorite or Småland (Ävrö) granite there are also veins of pegmatite and/or fine-grained granite. This may indicate even stronger correlation between HPF:s and fine-grained granite than shown in Section 5.2.1.

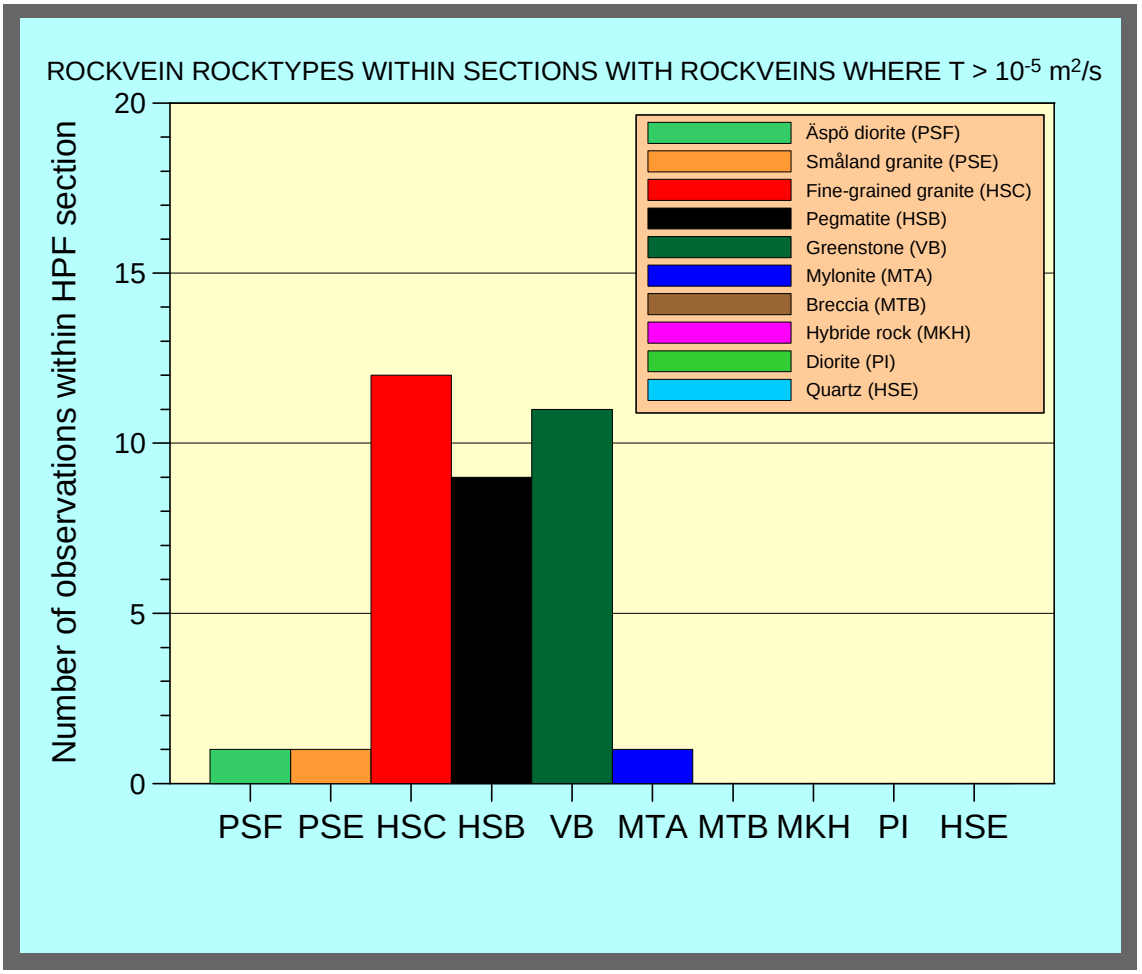

CRITERIA :

TUNNEL BOREHOLES - HPF POSITION +/- 1 meter
SURFACE BOREHOLES - WITHIN PACKER INTERVAL (3 m)

Figure 5-10. *Number of existing rock veins within the 27 sections with HPF:s (one or more veins within each section). The observations shows the number of different rock types found in within an interval of ±1 meter for tunnel bore holes and within the packer-interval (3 m) with a HPF for the surface bore holes.*

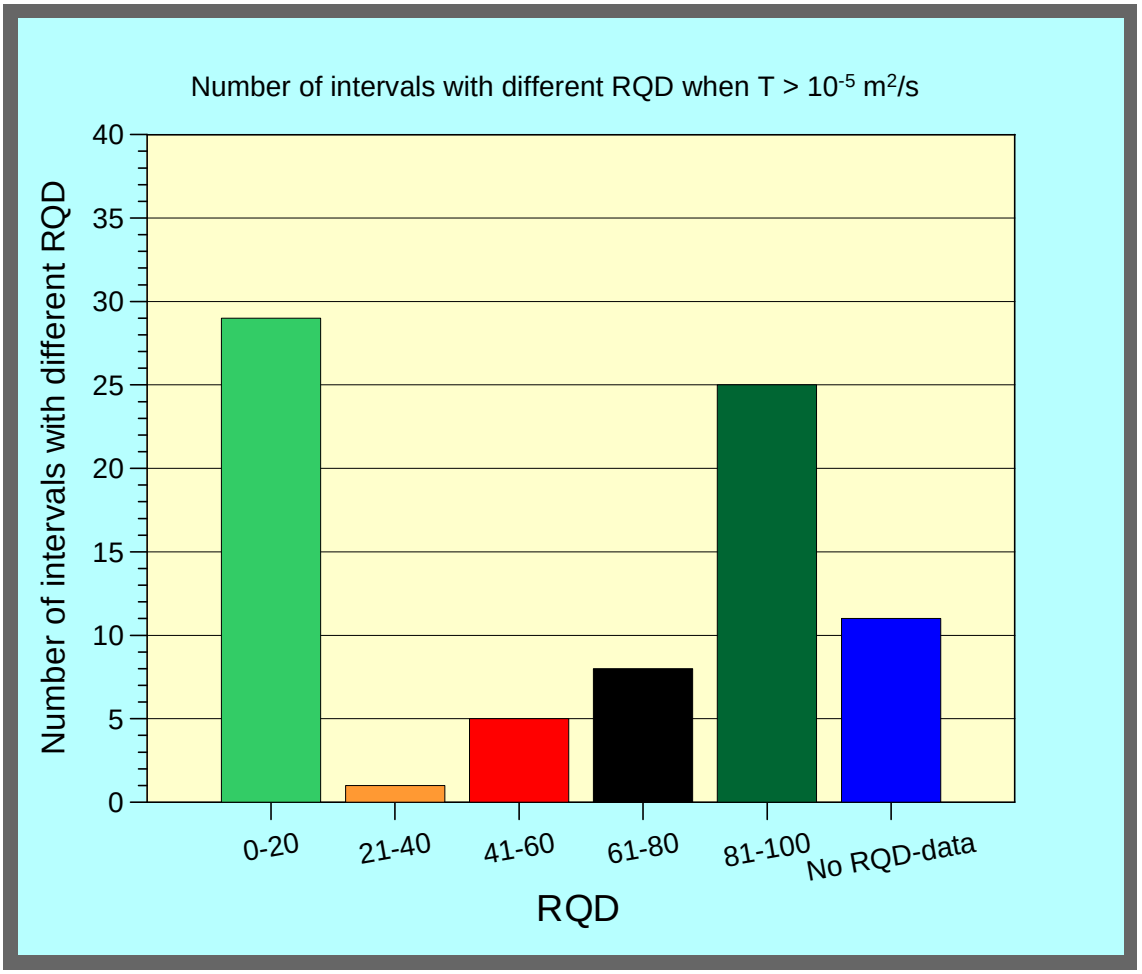

CRITERIA :

TUNNEL BOREHOLES - HPF POSITION +/- 1 meter
SURFACE BOREHOLES - WITHIN PACKER INTERVAL (3 m)
LOWEST RQD WITHIN INTERVAL CHOSEN

Figure 5-11. *Frequency of RQD for the intervals where HPF:s were found.*

5.2.4 RQD

RQD has generally been calculated for 1-m sections. In the study concerning RQD and HPF:s the lowest RQD value for a bore hole section of 2 or 3 m were used (within the same intervals described in *Section 5.2.1*) as the relevant RQD value for the actual HPF. For some bore holes no RQD-data were available. In the table in *Appendix 3* all details are presented. In *Figure 5-11* the distribution of RQD-values are presented. As can be

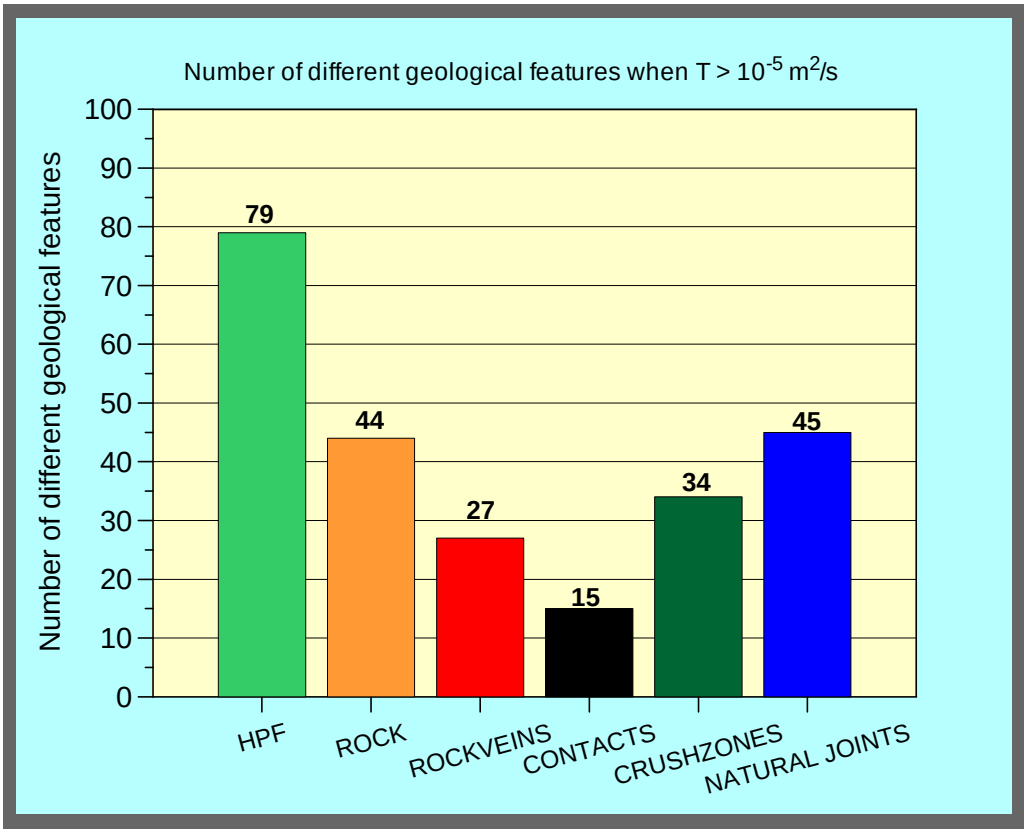

Figure 5-12. *The total number of HPF:s and the number of different geological features within an interval associated to the HPF.*

noticed, the lowest RQD interval, 0-20, is the most frequent but the RQD interval 81-100 has also a high frequency. This shows that HPF:s are also found in sparsely fractured rock and not only in highly fractured rock.

5.2.5 Crush zones/natural joints

79 HPF:s were identified in the bore holes studied. In those cases where a HPF occurs there must be a crush zone or a natural joint. Of these 79 cases 34 were related to a crush zone while in 45 cases there was one or several natural joints in the section defined for the HPF, see *Figure 5-12*. The detailed result is presented in the table in *Appendix 3*.

5.2.6 Summary

As was shown in Section 5.2.1 there are normally just one rock (not taking into account the veins) within the interval for the HPF:s. Rock veins are found in 27 sections and rock contacts are found in 15 sections, and among these, rock veins and rock contacts

are both found in 7 sections. If sections having veins or rock contacts are excluded, still 44 sections of 79 have just one rock type, see *Figure 5-12*. In 15 of these 44 sections, the rock type is fine-grained granite and the majority of the 15 sections are located in the lower parts of the bore holes KAS04, KAS08 and in the middle part of KA2162B. Some of these sections are in direct contact (nearby sections) with each other within a bore hole. In 27 of the sections, fine-grained granite is present with width thicker than 1 m, alone or together with other rock types. In 37 of the 79 sections, fine-grained granite is present, if sections with veins of fine-grained granite are also included. Fine-grained granite dominates the HPF:s, if the proportions of each lithological unit in the Äspö rock mass is taken into consideration. There are slightly more intervals where only natural joints have been mapped compared to crush zones. It is obvious that there are highly transmissive features that cannot be connected to highly fractured zones. In *Appendix 3,* the details can be studied.

Conclusion can be made that the frequence of HPF:s is higher in larger bodies of fine-grained granite compared to other rock types and that HPF:s can be connected to fracture zones as well to one or a few fractures.

Further can be concluded that rock contacts and veins are not dominating sections with HPF:s. However, in the sections with HPF:s and veins and/or rock contacts, the resolution of the data has not permitted to see if HPF:s are located close to a rock contact or within or close to a vein. It may be the case that for example veins of fine-grained granite increase the probability of getting a HPF.

5.3 Grouting bore holes

During the construction of Äspö HRL, records were kept of all grouting bore holes, the flow into each bore hole etc. From these data a transmissivity were calculated for each bore hole. Using the two HPF criterion's produces a number of tunnel faces where these criterion's are met, see *Figure 5-13, Figure 5-14.* In *Appendix 2* tables of the data are shown. Only data after chainage 1400 meter are presented.

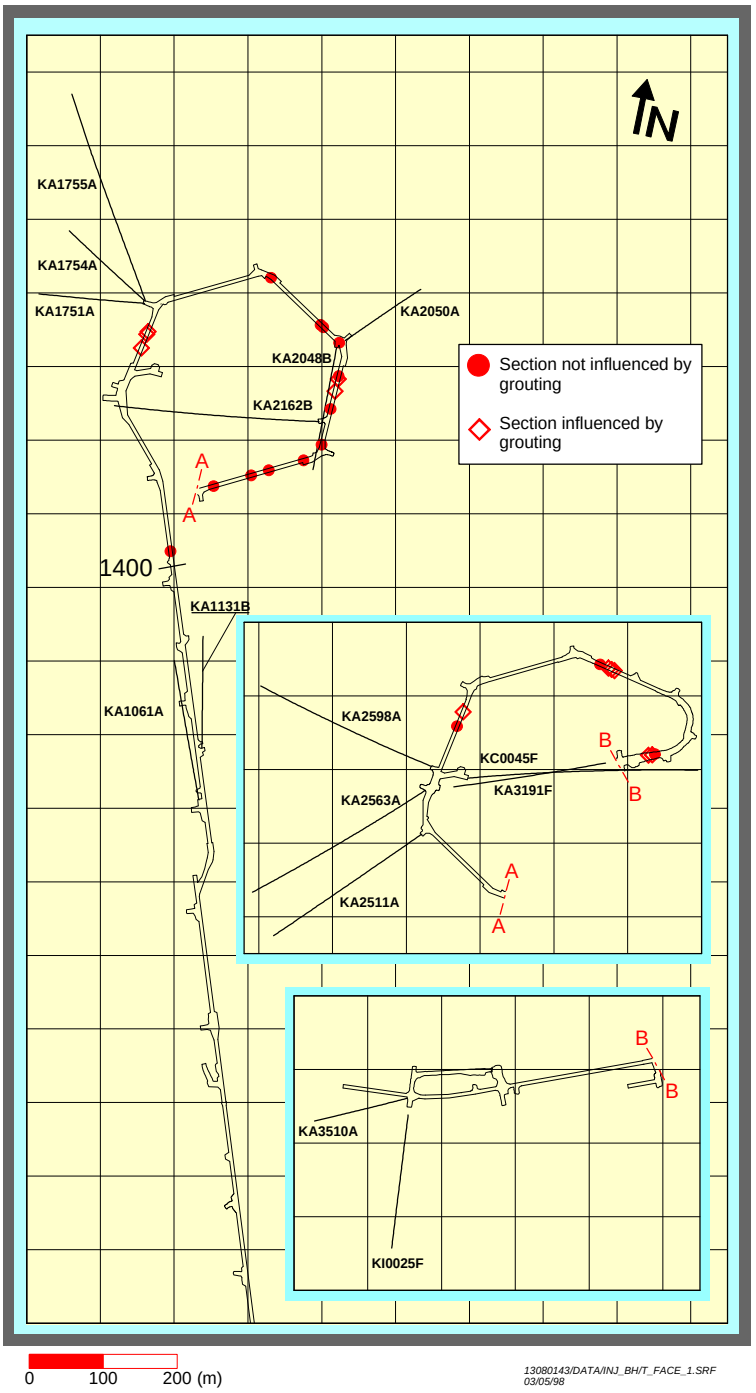

Figure 5-13. *Observations of T ³ 1·10^{-5} m^2/s at tunnel faces between tunnel section 1400 and 3600 metres. (Results from tunnel section 0 - 1400 metres are not shown).*

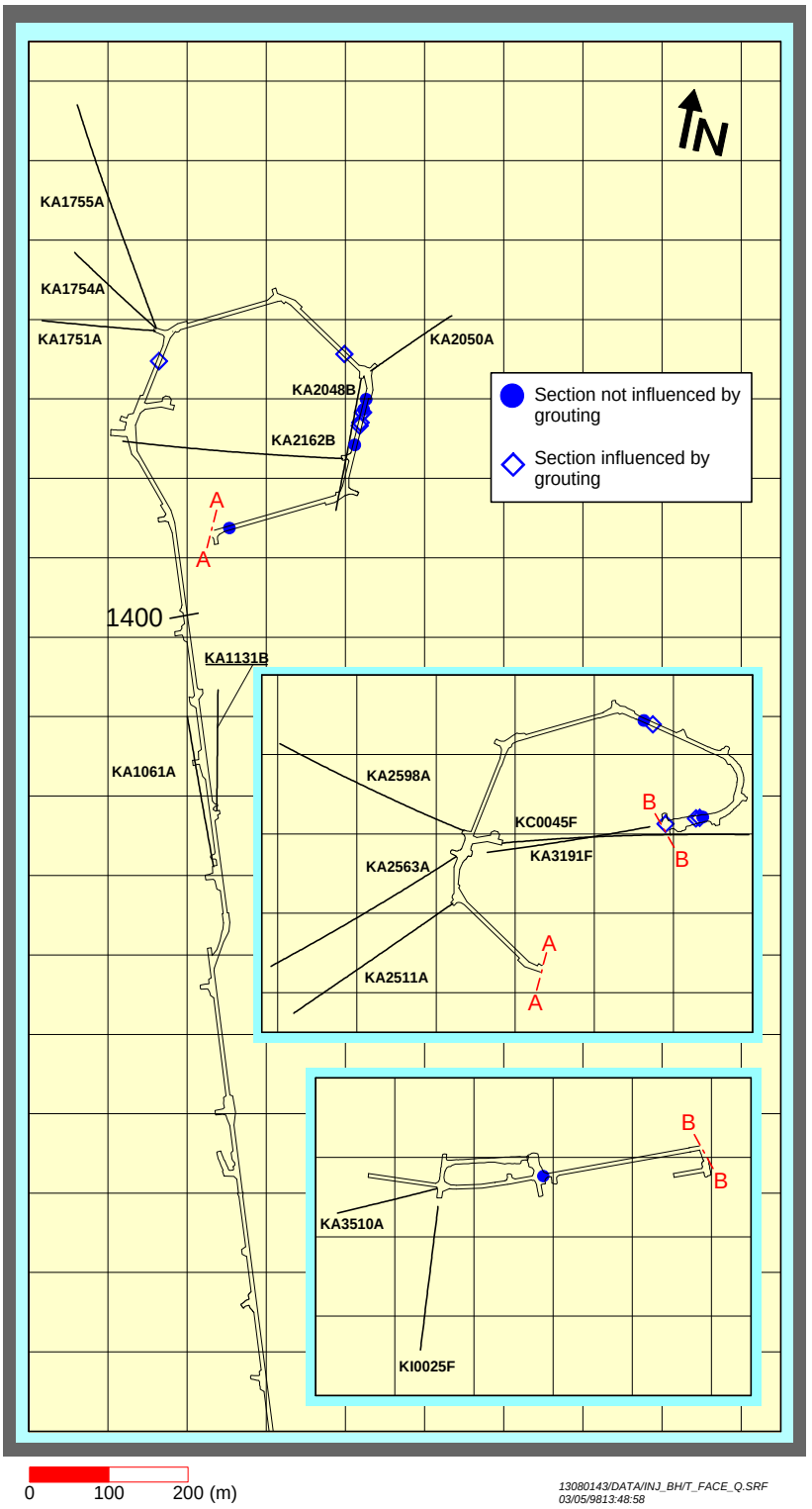

Figure 5-14. *Observations of Q ³ 100 l/min at tunnel faces between tunnel section 1400 and 3600 metres (Results from tunnel section 0 - 1400 metres are not shown).*

Since grouting was made during the construction, some tunnel faces were already influenced by earlier pre-grouting operations. The chainages presented in *Table A2-1* and *Table A2-2* are the chainages where the tunnel faces were which are estimated not to be influenced by grouting. A total of 50 tunnel face positions were grouted in the tunnel between the chainage 1400 - 3600 metres. Of these positions, 25 are estimated not to be influenced by previous grouting. *Table A2-1* and *Table A2-2* present the HPF:s found at those chainages. A total of 52 HPF:s were found according to the criterion $T \geq 10^{-5}$ m^2/s and 23 HPF:s according to the criterion $Q \geq 100$ l/min, in these 25 tunnel faces not influenced by earlier grouting.

Due to the exclusion of some tunnel face positions (positions assumed to be influenced by previous grouting) the data sets presented in *Table A2-1* and *Table A2-2* is biased to some extent. The *Figures 5-13* and *5-14*, however show the position of the grouted tunnel face positions where HPF:s. were found. These figures show a more representative picture of the frequency of HPF:s along the tunnel and the tables *Table A2-1* and *Table A2-2* show how frequent HPF:s may be when drilling a number of bore holes from the tunnel face into a rock volume of around $10 \times 10 \times 10$ m^3 (or less sometimes). Several HPF: s found at one tunnel face may of course represent one or several features.

Several of the HPF sections are located where fracture zone NNW-4 is interpreted to intersect the tunnel. A few are located approximately where fracture swarms NNW-1, NNW-2 and NNW-7 are interpreted to intersect the tunnel, see *Figure 4-3*.

5.4 Size of HPF

It is not possible to define the actual size(s) of the HPF:s but a possible range can be given. Assuming a transmissivity of 10^{-5} m^2/s, a storage coefficient of 10^{-6}-10^{-5} according to *Rhén et al /1997b/,* radial flow and test time of 10 minutes (test times for most of the transient injection tests performed) gives a radius of influence of 30-100 m.

6 Conclusions

The definition of the HPF:s (High-Permeability Features) as having a transmissivity $T \geq 10^{-5}$ m^2/s or a flow rate $Q \geq 100$ l/min into a bore hole with pressure close to atmospheric was more or less arbitrarily chosen for this study. However, it was known from the previous studies at Äspö HRL that features, with properties around these values mentioned above, were not uncommon and not all of them could be explained by fracture zones with large extent defined deterministically using geological, geophysical, hydrogeological and hydrochemistry data. This study has shown this in a more clear way and the main conclusions are presented below.

HPF:s and large deterministically defined fracture zones:

- About 50 % of the HPF:s can be connected to the deterministically defined fracture zones with a large extent, which were based on evaluation of geological, geophysical hydrogeological and hydrochemistry data. The rest of the HPF should be modelled as fairly large features in-between the deterministic zones. The radius of these features may be around 30-100m.

- The implication of the size of the HPF:s is that there should be a correlation model for the assigning of the hydraulic properties to the hydraulic rock domains taking the size into account. The present SKB model over Äspö from 1997 does not consider this. The hydraulic conductor domains in the present model are not affected of the results.

Distances between HPF:s:

- The distances between HPF:s have a lognormal distribution.

- The arithmetic mean distance between HPF:s, defined as features having a transmissivity $T \geq 10^{-5}$ m^2/s, is for the sub-vertical bore holes drilled from surface 75−106 m. The arithmetic mean distance between HPF:s, is for the sub-horizontal bore holes drilled from the tunnel spiral 73-106 m. The corresponding geometric mean values are 24-27 m and 27 - 34 m respectively. Possibly, the distances estimated from the sub-vertical bore holes should be somewhat larger than the figures given above.

- The statistics of the distances is dependent of the scale of observations. It is possibly better to use larger interval than 3 m to describe the spatial distribution of distances between HPF:s on a scale of several hundred meters, at least if simple measures as arithmetic mean is used as a measure for HPF:s between the large deterministic zones.

The coupling between HPF and lithology and fracturing:

- Somewhat less than half of the HPF:s can be explained by what was classified as crush zones during the mapping of the cores and the rest by one or a few natural joints. It clearly shows that high permeability features exist in the sparsely frac-

tured rock mass. The evaluation of the RQD for the intervals having a HPF shows the same thing, both very low and very high RQD value are found in the bore hole intervals having a HPF.

- HPF:s are most frequent in fine-grained granite, taking into account the amount of different rock types at Äspö HRL. Äspö diorite and Småland (Ävrö) granite, which are the dominating lithological units, have approximately the same frequency of HPF:s and is about half of the frequency in fine-grained granite. The frequency of HPF:s in greenstone is somewhat greater than in Äspö diorite and Småland (Ävrö) granite. In pegmatite and mylonite-hybridized rock the frequency is about the same as in greenstone, but the conclusion is very uncertain due to the small sample size

- Only about 20 % of the HPF:s are found near rock contacts. Fine-grained granite is the dominating rock type found in these rock contacts.

- About 35 % of the HPF:s are found in intervals containing rock veins. Fine-grained granite, pegmatite and greenstone are the dominating rock types found in intervals having a HPF and rock veins.

- Further can be concluded that rock contacts and veins are not dominating sections with HPF:s. Most sections with a HPF has just one rock type and no rock contacts or veins.

- In the sections with HPF:s and veins and/or rock contacts, the resolution of the data has not permitted to see if HPF:s are located close to a rock contact, within, or close to a vein. It may be the case that for example veins of fine-grained granite increase the probability of getting a HPF. In nearly 50 % of the sections with HPF fine-grained granite was present as the rock type or as a vein.

- Mapping of groutfilled fractures in the tunnel and analyses of the transmissvities from the probe holes drilled along the tunnel has shown that subvertical fractures with strike WNW-NW and around N-S are important hydraulic conductors. If there are any differences of the frequency of the HPF:s in the horizontal plane has not been investigated but is likely, due to the above mentioned investigations.

- Most of the investigated rock volume is between large fracture zones (EW-1 and NE-1). This rock volume may have been sheared, creating the existing hydraulically important subvertical fractures, which seems to be in an en-échelon pattern, with strikes WNW-NW and around N-S. These fracture sets also seems to form larger subvertical hydraulic features striking NNW, which hydraulic interference tests seem to conform. However, in most bore holes it is not possible to examine the direction of individual fractures, as it is not documented in the data base. It is therefor difficult to conform that the HPF:s are a part of the subvertical fractures with strike WNW-NW and around N-S.

- The ductile deformations giving foliation and gneissic zones trending NE-ENE, dipping to the NNW does not seem to have any major impact on the dominant hydraulic features, consisting of subvertical fractures with strike WNW-NW and around N-S.

- Some of the larger bodies of fine-grained granite occur as dikes but it is not very clear because of strong deformation. These bodies, at least near the surface, are elongated in the ENE-NE direction. Considering the hydraulic interference tests, the direction of the fine-grained bodies does not seem to have a large impact of the direction of the larger hydraulic features, as the NNW features. One exception is possible one or several fine-granite body(ies) that is believed to be at a depth of about 300 m within the tunnel spiral .

- The brittle deformation has caused a much denser fracture pattern in the fin-grained granite compared to the other rock types. Fine-grained granite may in an effective way interconnect fracture systems even if the amount of fine-grained granite is fairly small. If fine-grained granite is distributed within the rock mass as a large number of veins, as can be seen in the Äspö tunnel, possibly the fine-grained granite can be parts of larger fracture planes or system of larger fracture planes forming HPF:s. However, in the tunnel there are also many examples of small and winding veins of fine-grained granite that are not fractured.

HPF; $T \geq 10^{-5}$ m^2/s or $Q \geq 100$ l/min:

- The number of the HPF:s defined as features having a transmissivity $T \geq 10^{-5}$ m^2/s are greater than if HPF are defined as features having a flow rate $Q \geq 100$ l/min into a bore hole with pressure close to atmospheric. However, the flow rate Q is dependent of the depth below surface and the transmissivity of the feature(s) intersecting the bore hole. Q is therefor not a good measure of a HPF.

Further studies should be based on the following:

- Distances should be bases on a modified version of method C, where distance d_1 and d_{10} are added and used it as a distance in either end of the synthetic “long bore hole”, see *Figure 5-1*.

- Statistics should be made for several length scales, preferably 3, 6 and possibly 9 m as a large number of tests are based on 3 m packer interval.

- Distances between features with lower transmissivities than 10^{-5} m^2/s should be studied.

7 References

Earlougher R C, 1977. Advances in well test analysis. SPE monograph Volume 5 of Henry L. Doherty Series

Rhén I, Bäckblom G, Gustafson G, Stanfors R, Wikberg P, 1997a. Äspö HRL - Geoscientific evaluation 1997/2. Results from pre-investigations and detailed site characterisation. Summary report. SKB TR 97-03.

Rhén I, Gustafson G, Stanfors R, Wikberg P, 1997b. Äspö HRL - Geoscientific evaluation 1997/5. Models based on site characterisation 1986-1995. SKB TR 97-06.

Rhén I, Gustafson G, Wikberg P, 1997c. Äspö HRL - Geoscientific evaluation 1997/4. Results from pre-investigations and detailed site characterisation. Comparison of predictions and observations. Hydrogeology, groundwater chemistry and transport of solutes. SKB TR 97-05

Stanfors R, Olsson P, Stille H, 1997. Äspö HRL - Geoscientific evaluation 1997/3. Results from pre-investigations and detailed site characterisation. Comparison of predictions and observations. Geology and mechanical stability. SKB TR 97-04

Svensson U, 1997. A site scale analysis of groundwater flow and salinity distribution in the Äspö area. SKB Technical Report TR 97-17.

APPENDIX 1. HPF Positions in bore holes

Bore hole	=	Bore hole name
Tot_bh_len	=	Total length of bore hole
Secup	=	Upper (outermost) section
Seclow	=	Lower (innermost) section
T	=	Transmissivity (m^2/s)
Q	=	Flow rate out of test section (l/min)
Testtype	=	Type of test methodology
		3 = pressure build-up test
		5 = injection test
		T_Qdh = transmissivity estimated from
		specific capacity according to *Rhén et al /1997b/.*
Det.zone	=	Deterministic zone name

Coreboreholes KAS tests in 3 metres scale. Tunnel coreboreholes.

Borehole	Tot_bh_len	Meas. sect. of bh		T > 1E-5 m²/s		T	Q	Testype	Det. zone
		Secup	Seclow	Secup	Seclow				
(-)	(m)	(m)	(m)	(m)	(m)	(m²/s)	(l/min)		
KAS02	924.04	102	801	314	317	1.30E-05	1.3	5	
KAS03	1002.06	103	550	358	361	6.00E-05	1.79	5	NNW-8
KAS03	1002.06	103	550	370	373	2.40E-05	1.97	5	NNW-8
KAS03	1002.06	103	550	448	451	5.20E-05	1.72	5	
KAS03	1002.06	103	550	451	454	2.40E-05	1.54	5	
KAS04	481	133	457	187	190	1.60E-04	1.68	5	
KAS04	481	133	457	208	211	1.80E-05	1.42	5	
KAS04	481	133	457	217	220	3.40E-04	2.13	5	
KAS04	481	133	457	220	223	1.40E-04	1.96	5	
KAS04	481	133	457	229	232	3.10E-04	1.97	5	
KAS04	481	133	457	232	235	3.80E-04	1.54	5	
KAS04	481	133	457	292	295	1.30E-05	1.75	5	
KAS04	481	133	457	337	340	3.40E-05	2.04	5	EW-1S
KAS04	481	133	457	340	343	6.50E-05	2.1	5	EW-1S
KAS04	481	133	457	343	346	1.20E-05	1.53	5	EW-1S
KAS04	481	133	457	358	361	5.80E-05	1.81	5	EW-1S
KAS04	481	133	457	397	400	2.80E-05	1.47	5	
KAS04	481	133	457	406	409	1.50E-05	1.38	5	
KAS04	481	133	457	415	418	2.00E-04	1.37	5	
KAS05	549	157	541	442	445	1.80E-05	0.906	5	
KAS06	602.17	105	591	207	210	2.00E-05	1.04	5	NNW-1
KAS06	602.17	105	591	213	216	4.70E-05	0.662	5	NNW-1
KAS06	602.17	105	591	216	219	1.80E-05	2.03	5	NNW-1
KAS06	602.17	105	591	219	222	1.40E-04	2.01	5	NNW-1
KAS06	602.17	105	591	222	225	1.20E-05	1.08	5	NNW-1
KAS06	602.17	105	591	225	228	1.10E-05	1.85	5	NNW-1
KAS06	602.17	105	591	354	357	2.00E-05	1.34	5	
KAS06	602.17	105	591	399	402	8.70E-05	1.67	5	NNW-2
KAS06	602.17	105	591	447	450	2.80E-04	1.6	5	NNW-2
KAS06	602.17	105	591	459	462	2.30E-04	0.039	5	
KAS06	602.17	105	591	558	561	1.90E-05	1.36	5	
KAS07	604	106	592	241	244	1.90E-05	4.693	5	NNW-7
KAS07	604	106	592	508	511	1.90E-05	1.117	5	NE-1
KAS07	604	106	592	511	514	1.30E-05	0.764	5	NE-1
KAS07	604	106	592	541	544	3.80E-05	7.473	5	NE-1
KAS07	604	106	592	574	577	7.40E-05	7.599	5	NE-1
KAS07	604	106	592	577	580	6.90E-05	0.357	5	NE-1
KAS08	601	106	580	142	145	2.10E-05	1.43	5	
KAS08	601	106	580	154	157	1.70E-05	1.51	5	
KAS08	601	106	580	184	187	1.10E-04	1.38	5	
KAS08	601	106	580	187	190	2.00E-05	0.501	5	
KAS08	601	106	580	556	559	1.80E-04	1.63	5	NE-1
KAS08	601	106	580	559	562	2.30E-05	1.56	5	NE-1
KAS08	601	106	580	562	565	3.70E-05	1.28	5	NE-1
KAS08	601	106	580	565	568	3.10E-05	1.59	5	NE-1
KAS08	601	106	580	568	571	1.40E-04	2.26	5	NE-1
KAS08	601	106	580	571	574	8.60E-05	1.47	5	NE-1
KAS08	601	106	580	577	580	2.00E-05	0.877	5	NE-1
KA1751A	149.9	0	149.9	65	66	1.40E-05	104	3	
KA1755A	320.58	0	320.58	52.6	52.6	2.80E-05	140	3	
KA1755A	320.6	0	320.58	53.9	53.9	1.30E-05	63	3	
KA1755A	320.6	0	320.58	57.1	57.1	1.40E-05	72	3	
KA1755A	320.6	0	320.58	97.7	97.7	1.20E-04	582	T_Qdh	EW-1S
KA1755A	320.6	0	320.58	105	105	1.40E-05	72	3	EW-1S
KA2162B	288.1	0	288.1	50	50	4.30E-05	279	3	NNW-2
KA2162B	288.1	0	288.1	53	53	1.20E-05	75	3	NNW-2
KA2162B	288.1	0	288.1	121	121	3.30E-05	222	3	NNW-1
KA2162B	288.1	0	288.1	126	126	1.00E-05	42	3	NNW-1
KA2162B	288.1	0	288.1	129	129	2.20E-05	90	3	NNW-1
KA2162B	288.1	0	288.1	173	173	4.70E-05	197	3	NNW-7
KA2162B	288.1	0	288.1	174	174	1.80E-05	75	3	NNW-7
KA2511A	293	0	293	25	25	3.00E-05	30	3	
KA2511A	293	0	293	52.75	52.75	3.60E-05	36	3	NNW-5
KA2511A	293	0	293	100.1	100.1	2.40E-05	24	3	
KA2511A	293	0	293	214	214	2.40E-05	24	3	
KA2511A	293	0	293	242	242	2.00E-05	20	3	
KC0045F	336.7	0	336.7	264.2	264.2	2.00E-05	215	3	NNW-4
KC0045F	336.7	0	336.7	264.9	264.9	5.90E-05	625	3	NNW-4
KC0045F	336.7	0	336.7	266.7	266.7	1.90E-05	200	3	NNW-4
KC0045F	336.7	0	336.7	275.4	275.4	3.50E-05	50	3	NNW-4
KC0045F	336.7	0	336.7	285.2	285.2	2.10E-05	30	3	NNW-4
KC0045F	336.7	0	336.7	286.2	286.2	7.60E-05	108	3	NNW-4
KC0045F	336.7	0	336.7	305.2	305.2	1.10E-05	16	3	
KA3191F	210.4	0	210.4	91	91	1.90E-05	89	T_Qdh	NNW-2
KA3191F	210.4	0	210.4	123.58	123.58	1.30E-05	60	T_Qdh	
KA3191F	210.4	0	210.4	124.1	124.1	1.10E-05	50	T_Qdh	
KA2563A	362	0	362	90.35	94.85	1.50E-05	120	3	
KA2563A	362	0	362	102.03	105.01	3.20E-05	714	3	
KA2563A	362	0	362	152.98	153.41	6.30E-05	114	3	

APPENDIX 2. HPF:s in grouted tunnel sections

Table A2-1. Tunnel face positions where T_{TOT} 3 $1 \cdot 10^{-5}$ m^2/s for non-grouted tunnel face positions.
Protocol No : The number of the grouting protocol.
Tunnel_pos : Chainage for the tunnel face.
Bh_no : Number of the bore hole in the grouting protocol.
Bh_len : Length of the grouting bore hole.
QF : Free flow out from the drilled grouting bore hole.
T_TOT : Evaluated transmissivity for the grout hole.

Protocol No.	Tunnel_pos (m)	Bh_no	Bh_len (m)	QF (l/min)	T_TOT (m^2/s)
103	1402	1	9	20	4.8E-05
103	1402	4	9	45	3.2E-05
103	1402	6	9	65	3.2E-05
103	1402	7	9	65	3.2E-05
103	1402	8	9	70	3.2E-05
103	1402	9	9	60	3.2E-05
103	1402	10	9	65	3.2E-05
103	1402	11	9	55	3.2E-05
103	1402	12	9	55	3.2E-05
103	1402	13	9	35	3.2E-05
103	1402	14	9	20	3.2E-05
103	1402	15	9	30	3.2E-05
103	1402	16	9	35	3.2E-05
103	1402	18	9	15	1.6E-05
103	1402	19	9	35	1.6E-05
103	1402	20	9	30	1.6E-05
114	1920	4	9	25	9.5E-04
114	1920	6	9	24	9.5E-04
114	1920	7	9	21	9.5E-04
115	2013	1	9	30	8.2E-05
115	2013	2	9	26	8.0E-05
118	2018	10	9	55	2.4E-05
119	2048	5	9	45	4.8E-04
119	2048	6	9	40	4.8E-04
119	2048	7	9	50	4.0E-04
121	2096	5	12	350	9.5E-05
121	2096	6	16	300	9.5E-05
126	2142	4	9	120	4.8E-04
128	2192	6	9	90	1.2E-05
131	2227	1	9	75	1.2E-04
131	2227	8	9	90	1.2E-04
131	2227	10	9	60	1.2E-04
133	2276	7	12	27	3.2E-05
133	2276	8	15	58	3.2E-05
133	2276	9	12	57	3.2E-05
133	2276	10	12	59	3.2E-05
134	2301	7	9	42	1.2E-05
134	2301	8	9	45	1.2E-05
134	2301	9	9	39	9.9E-06
134	2301	10	9	28	1.2E-05
135	2354	6	9	100	3.2E-05
135	2354	7	9	125	3.2E-05
135	2354	8	9	175	3.2E-05
135	2354	9	9	0	3.2E-05
135	2354	10	9	100	3.2E-05
135	2354	11	9	120	3.2E-05
202	2661	2	15	41.5	1.9E-05
208	2900	2	15	500	8.4E-05
212	3123	1	15	300	8.6E-05
212	3123	2	6	300	8.6E-05
212	3123	9	15	400	8.6E-05
212	3123	11	15	400	8.6E-05

Table A2-2. Tunnel face positions where Q_F ³ 100 l/min for non-grouted tunnel face positions.
Protocol No : The number of the grouting protocol.
Tunnel_pos : Chainage for the tunnel face.
Bh_no : Number of the bore hole in the grouting protocol.
Bh_len : Length of the grouting bore hole.
QF : Free flow out from the drilled grouting bore hole.
T_TOT : Evaluated transmissivity for the grout hole.

Protocol No.	Tunnel_pos (m)	Bh_no	Bh_len (m)	QF (l/min)	T_TOT (m^2/s)
120	2083	10	9	100	6.1E-06
120	2083	11	9	100	6.1E-06
120	2083	12	12	100	6.1E-06
120	2083	13	12	100	6.1E-06
120	2083	14	12	100	6.1E-06
120	2083	15	12	100	6.1E-06
120	2083	16	9	100	6.1E-06
120	2083	17	9	100	6.1E-06
120	2083	18	9	100	6.1E-06
121	2096	5	12	350	9.5E-05
121	2096	6	16	300	9.5E-05
126	2142	4	9	120	4.8E-04
135	2354	6	9	100	3.2E-05
135	2354	7	9	125	3.2E-05
135	2354	8	9	175	3.2E-05
135	2354	10	9	100	3.2E-05
135	2354	11	9	120	3.2E-05
208	2900	2	15	500	8.4E-05
212	3123	1	15	300	8.6E-05
212	3123	2	6	300	8.6E-05
212	3123	9	15	400	8.6E-05
212	3123	11	15	400	8.6E-05
230	3376	5	31.5	115	4.8E-06

APPENDIX 3. Correlation study

Bore hole	=	Bore hole name
Secup	=	Upper (outermost) section
Seclow	=	Lower (innermost) section
RQD	=	RQD index of section
Natural joints	=	No joints (0)
		Joints (1)
Crush zone	=	No crush zone(0)
		Crush zone (1)
Rockvein	=	No veins (0)
		Existence of vein in section
		(Geological name)
Veintype_no	=	Geological name index
Contact	=	No contact (0)
		Contact (Combination of rock types)
Contact_no	=	Index of contact combination
Rocktype	=	Geological name of rock type
Rocktype_no	=	Index of rock type
T (m^2/s)	=	Transmissivity (m^2/s)

P:\13080143\DATA\GEOLOGI\[Corr_T.xls]Blad1

Correlation T > $1 \cdot 10^{-5}$ m^2/s

Total number :				45	34		35		20		95	79
Borehole	Secup	Seclow	RQD	Natural joints	Crush zone	Rockvein	Veintype_no	Contact	Contact_no	Rocktype	Rocktype_no	T (m^2/s)
KA1751A	65	66	-	1	0	VB	5	0	-	PSE	2	1.4E-05
KA1755A	52.6	52.6	100	1	0	HSC	3	0	-	PSF	1	2.8E-05
	53.9	53.9	100	1	0	0	-	0	-	PSF	1	1.3E-05
	57.1	57.1	100	1	0	MTA	6	0	-	PSF	1	1.4E-05
	97.7	97.7	0	0	1	0	-	PSF-HSC	13	HSC	3	1.2E-04
										PSF	1	
	105	105	0	0	1	0	-	0	-	HSC	3	1.4E-05
KA2162B	50	50	-	1	0	0	-	0	-	PSE	2	4.3E-05
	53	53	-	1	0	0	-	0	-	PSE	2	1.2E-05
	121	121	-	1	0	HSC	3	0	-	PSE	2	3.3E-05
	126	126	-	0	1	0	-	0	-	HSC	3	1.0E-05
	129	129	-	0	1	0	-	0	-	HSC	3	2.2E-05
	173	173	-	0	1	0	-	0	-	HSC	3	4.7E-05
	174	174	-	0	1	0	-	0	-	HSC	3	1.8E-05
KA2511A	25	25	93	1	0	0	-	0	-	PSF	1	3.0E-05
	52.75	52.75	92	1	0	HSC	3	0	-	PSF	1	3.6E-05
	100.1	100.1	98	1	0	0	-	0	-	PSF	1	2.4E-05
	214	214	75	1	0	0	-	PSF-HSC	13	PSF	1	2.4E-05
										HSC	3	
	242	242	0	0	1	0	-	0	-	PSF	1	2.0E-05

\

P:\13080143\DATA\GEOLOGI\[Corr_T.xls]Blad1

Correlation T > $1 \cdot 10^{-5}$ m^2/s

Total number :			45	34		35		20		95	79
Borehole	Secup	Seclow	RQD	Natural joints	Crush zone	Rockvein	Veintype_no	Contact	Contact_no	Rocktype	Rocktype_no	T (m^2/s)
KA2563A	90.35	94.85	-	0	1	VB	5	VB-HSC	35	HSC	3	1.5E-05
						PSF	1			VB	5	
						HSC	3					
						HSB	4					
	102.03	105.01	-	1	0	HSC	3	0	-	PSF	1	3.2E-05
						HSB	4					
	152.98	153.41	-	0	1	0	-	0	-	PSF	1	6.3E-05
KC0045F	264.2	264.2	0	0	1	0	-	0	-	PSF	1	2.0E-05
	264.9	264.9	0	0	1	0	-	0	-	PSF	1	5.9E-05
	266.7	266.7	100	1	0	0	-	0	-	PSF	1	1.9E-05
	275.4	275.4	71	1	0	0	-	0	-	PSF	1	3.5E-05
	285.2	285.2	0	0	1	0	-	0	-	PSF	1	2.1E-05
	286.2	286.2	0	0	1	0	-	0	-	PSF	1	7.6E-05
	305.2	305.2	0	0	1	VB	5	PSE-VB	15	PSF	1	1.1E-05
										VB	5	
KA3191F	91	91	84	1	0	0	-	0	-	PSF	1	1.9E-05
	123.58	123.58	0	0	1	0	-	0	-	PSF	1	1.3E-05
	124.1	124.1	0	0	1	0	-	0	-	PSF	1	1.1E-05

P:\13080143\DATA\GEOLOGI\[Corr_T.xls]Blad1

Correlation T > $1 \cdot 10^{-5}$ m^2/s

Total number :			45	34		35		20		95	79
Borehole	Secup	Seclow	RQD	Natural joints	Crush zone	Rockvein	Veintype_no	Contact	Contact_no	Rocktype	Rocktype_no	T (m^2/s)
KAS02	314	317	0	0	1	0	-	HSC-VB	35	HSC	3	1.3E-05
										VB	5	
KAS03	358	361	69	1	0	0	-	0	-	PSE	2	6.0E-05
	370	373	0	0	1	0	-	0	-	PSE	2	2.4E-05
	448	451	84	1	0	HSB	4	HSC-PSE	23	HSC	3	5.2E-05
										PSE	2	
	451	454	90	1	0	0	-	0	-	PSE	2	2.4E-05

P:\13080143\DATA\GEOLOGI\[Corr_T.xls]Blad1

Correlation T > $1 \cdot 10^{-5}$ m^2/s

Total number :			45	34		35		20		95	79
Borehole	Secup	Seclow	RQD	Natural joints	Crush zone	Rockvein	Veintype_no	Contact	Contact_no	Rocktype	Rocktype_no	T (m^2/s)
KAS04	187	190	70	1	0	0	-	0	-	PSE	2	1.6E-04
	208	211	82	1	0	0	-	0	-	PSE	2	1.8E-05
	217	220	46	1	0	0	-	PSE-MTA	26	MTA	6	3.4E-04
										VB	5	
										PSE	2	
								MTA-VB	56			
								VB-PSE	25			
	220	223	74	1	0	0	-	0	-	PSE	2	1.4E-04
	229	232	58	0	1	HSB	4	HSC-PSE	23	HSC	3	3.1E-04
										PSE	2	
	232	235	94	1	0	HSC	3	0	-	PSE	2	3.8E-04
	292	295	56	1	0	0	-	HSC-PSE	23	HSC	3	1.3E-05
								HSC-PSE	23	PSE	2	
								HSC-PSE	23			
	337	340	0	0	1	HSC	3	HSE-HSC	38	HSE	8	3.4E-05
										HSC	3	
	340	343	22	1	0	0	-	0	-	HSC	3	6.5E-05
	343	346	20	1	0	0	-	0	-	HSC	3	1.2E-05
	358	361	0	0	1	0	-	0	-	HSC	3	5.8E-05
	397	400	0	0	1	0	-	0	-	HSC	3	2.8E-05
	406	409	69	1	0	0	-	0	-	HSC	3	1.5E-05
	415	418	0	0	1	0	-	0	-	HSC	3	2.0E-04

P:\13080143\DATA\GEOLOGI\[Corr_T.xls]Blad1

Correlation T > $1 \cdot 10^{-5}$ m^2/s

Total number :				45	34		35		20		95	79
Borehole	Secup	Seclow	RQD	Natural joints	Crush zone	Rockvein	Veintype_no	Contact	Contact_no	Rocktype	Rocktype_no	T (m^2/s)
KAS05	442	445	56	1	0	VB	5	0	-	PSF	1	1.8E-05
						HSC	3					
						HSB	4					
KAS06	207	210	86	1	0	VB	5	0	-	PSF	1	2.0E-05
	213	216	72	1	0	HSC	3	VB-PSF	15	PSF	1	4.7E-05
						VB	5	PSF-VB	15	VB	5	
	216	219	0	0	1	0	-	0	-	PSF	1	1.8E-05
	219	222	86	1	0	0	-	0	-	PSF	1	1.4E-04
	222	225	100	1	0	HSB	4	0	-	PSF	1	1.2E-05
	225	228	92	1	0	0	-	PSF-VB	15	PSF	1	1.1E-05
										VB	5	
	354	357	91	1	0	HSC	3	0	-	PSF	1	2.0E-05
	399	402	89	1	0	0	-	0	-	PSF	1	8.7E-05
	447	450	0	0	1	0	-	0	-	PSE	2	2.8E-04
	459	462	0	0	1	0	-	PSE-HSC	23	PSE	2	2.3E-04
										HSC	3	
	558	561	100	1	0	0	-	0	-	PSF	1	1.9E-05

P:\13080143\DATA\GEOLOGI\[Corr_T.xls]Blad1

Correlation T > $1 \cdot 10^{-5}$ m^2/s

Total number :			45	34		35		20		95	79
Borehole	Secup	Seclow	RQD	Natural joints	Crush zone	Rockvein	Veintype_no	Contact	Contact_no	Rocktype	Rocktype_no	T (m^2/s)
KAS07	241	244	0	1	0	VB	5	PSF-HSC	13	PSF	1	1.9E-05
										HSC	3	
	508	511	87	1	0	VB	5	0	-	PSF	1	1.9E-05
	511	514	65	1	0	VB	5	0	-	PSF	1	1.3E-05
	541	544	0	0	1	PSE	2	0	-	VB	5	3.8E-05
						HSB	4					
	574	577	89	1	0	HSC	3	0	-	PSE	2	7.4E-05
	577	580	0	0	1	0	-	0	-	PSE	2	6.9E-05
KAS08	142	145	100	1	0	VB	5	0	-	PSF	1	2.1E-05
	154	157	100	1	0	0	-	0	-	PSF	1	1.7E-05
	184	187	93	1	0	HSC	3	0	-	PSF	1	1.1E-04
	187	190	100	1	0	HSB	4	0	-	PSF	1	2.0E-05
	556	559	48	1	0	HSB	4	0	-	HSC	3	1.8E-04
	559	562	0	0	1	0	-	0	-	HSC	3	2.3E-05
	562	565	0	0	1	0	-	0	-	HSC	3	3.7E-05
	565	568	0	0	1	0	-	0	-	HSC	3	3.1E-05
	568	571	0	0	1	0	-	0	-	HSC	3	1.4E-04
	571	574	0	0	1	VB	5	0	-	HSC	3	8.6E-05
	577	580	0	0	1	0	-	HSC-PSF	13	HSC	3	2.0E-05
										PSF	1	

APPENDIX 4. Characterisation of core holes

\

KAS02

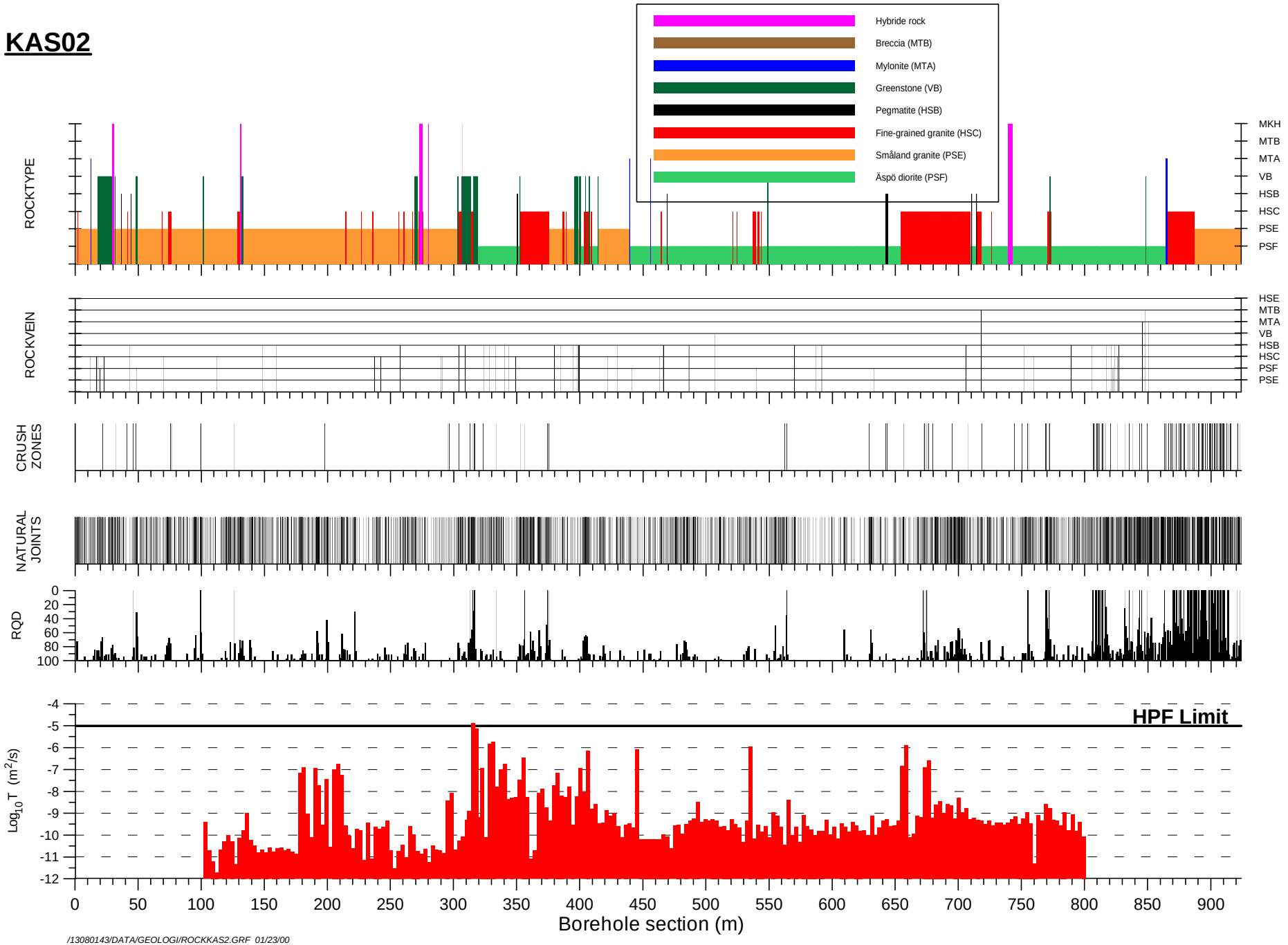
Hybride rock
Breccia (MTB)
Mylonite (MTA)
Greenstone (VB)
Pegmatite (HSB)
Fine-grained granite (HSC)
Småland granite (PSE)
Äspö diorite (PSF)
ROCKTYPE
MKH
MTB
MTA
VB
HSB
HSC
PSE
PSF
ROCKVEIN
HSE
MTB
MTA
VB
HSB
HSC
PSF
PSE
CRUSH ZONES
NATURAL JOINTS
RQD
0
20
40
60
80
100
HPF Limit
Log10 T (m2/s)
-4
-5
-6
-7
-8
-9
-10
-11
-12
0
50
100
150
200
250
300
350
400
450
500
550
600
650
700
750
800
850
900
Borehole section (m)
/13080143/DATA/GEOLOGI/ROCKKAS2.GRF 01/23/00

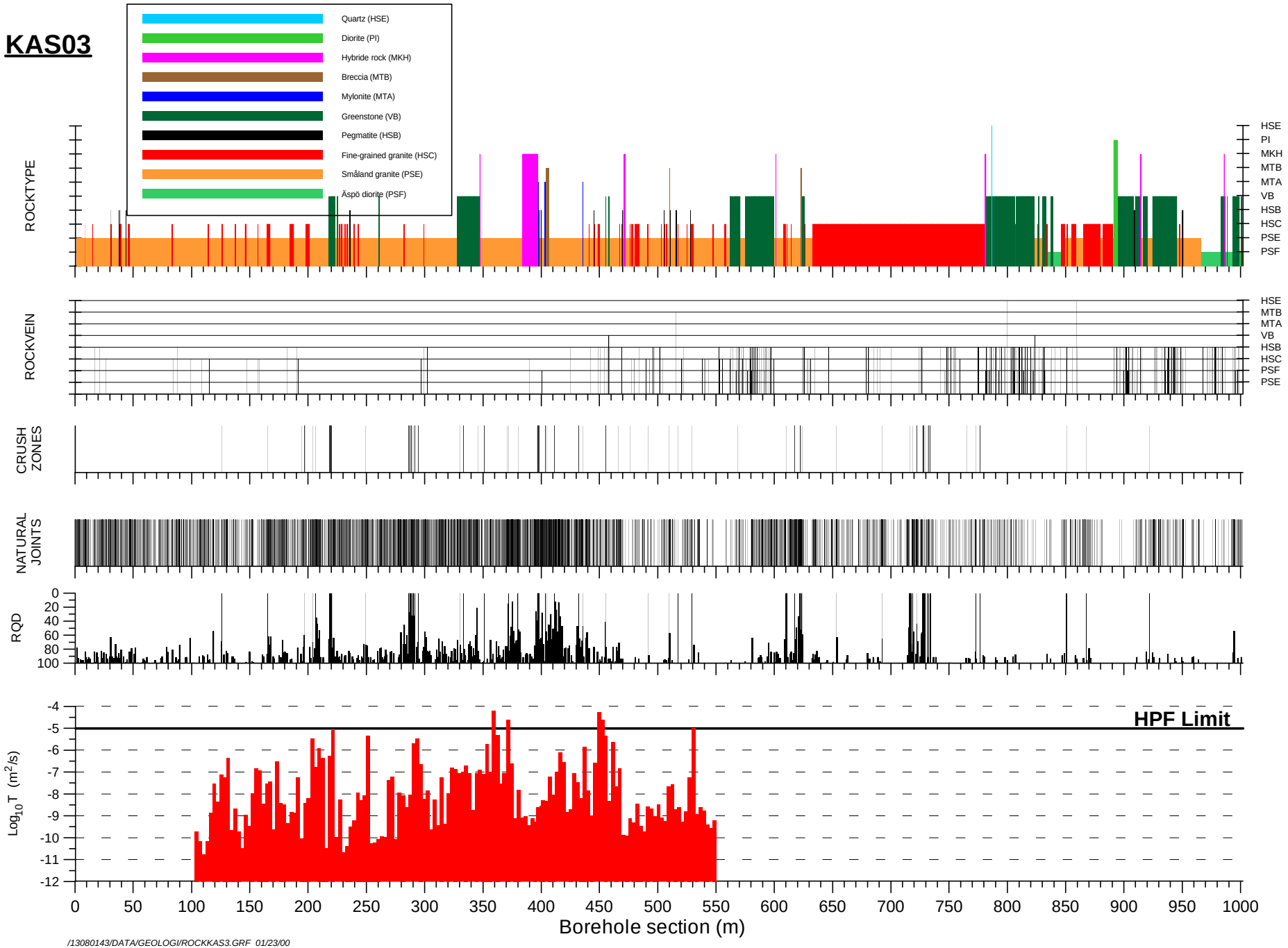
KAS03
Quartz (HSE)
Diorite (PI)
Hybride rock (MKH)
Breccia (MTB)
Mylonite (MTA)
Greenstone (VB)
Pegmatite (HSB)
Fine-grained granite (HSC)
Småland granite (PSE)
Äspö diorite (PSF)
ROCKTYPE
HSE
PI
MKH
MTB
MTA
VB
HSB
HSC
PSE
PSF
ROCKVEIN
HSE
MTB
MTA
VB
HSB
HSC
PSF
PSE
CRUSH ZONES
NATURAL JOINTS
RQD
0
20
40
60
80
100
HPF Limit
Log10 T (m2/s)
-4
-5
-6
-7
-8
-9
-10
-11
-12
0
50
100
150
200
250
300
350
400
450
500
550
600
650
700
750
800
850
900
950
1000
Borehole section (m)
/13080143/DATA/GEOLOGI/ROCKKAS3.GRF 01/23/00

KAS04

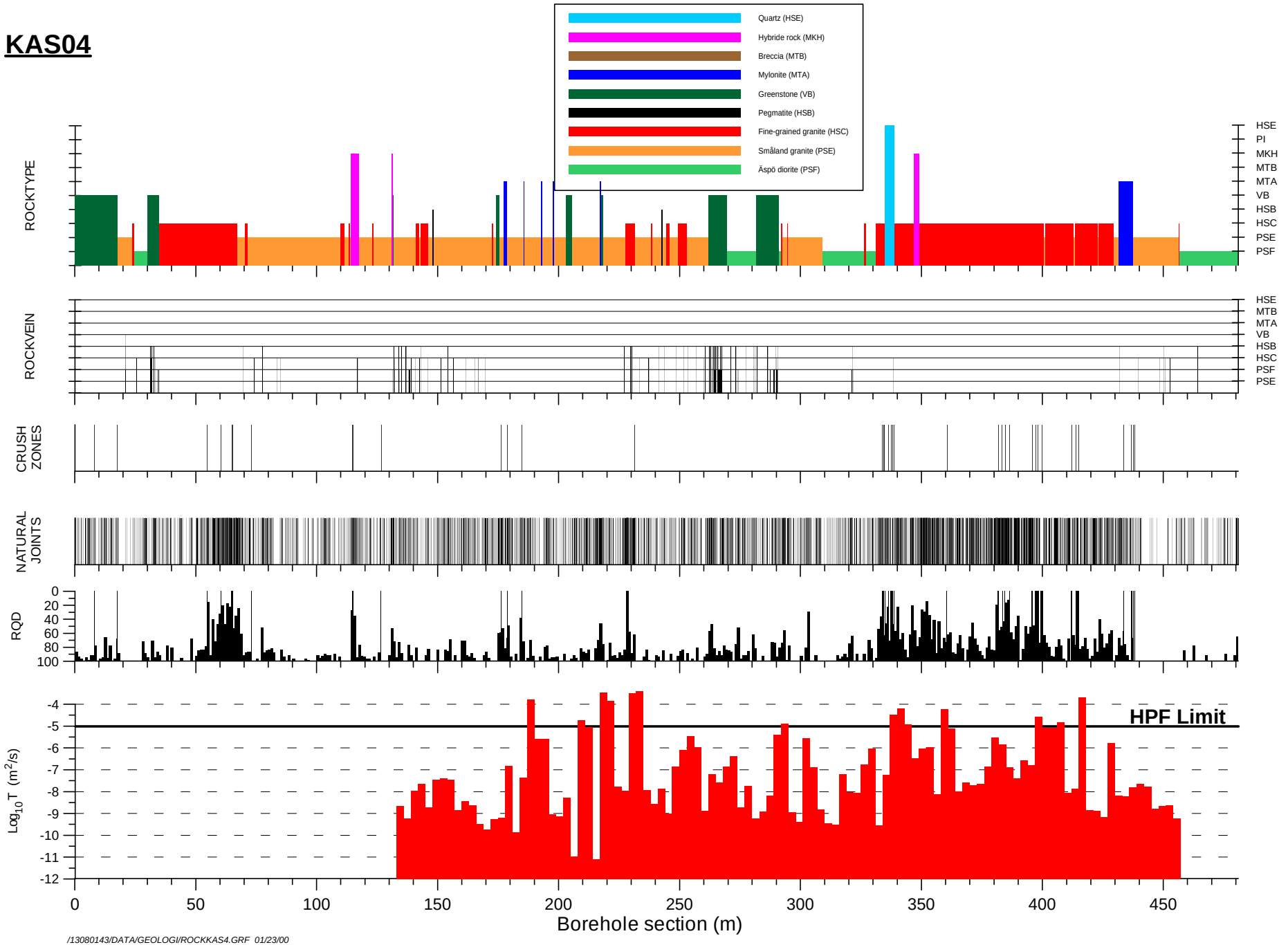

/13080143/DATA/GEOLOGI/ROCKKAS4.GRF 01/23/00

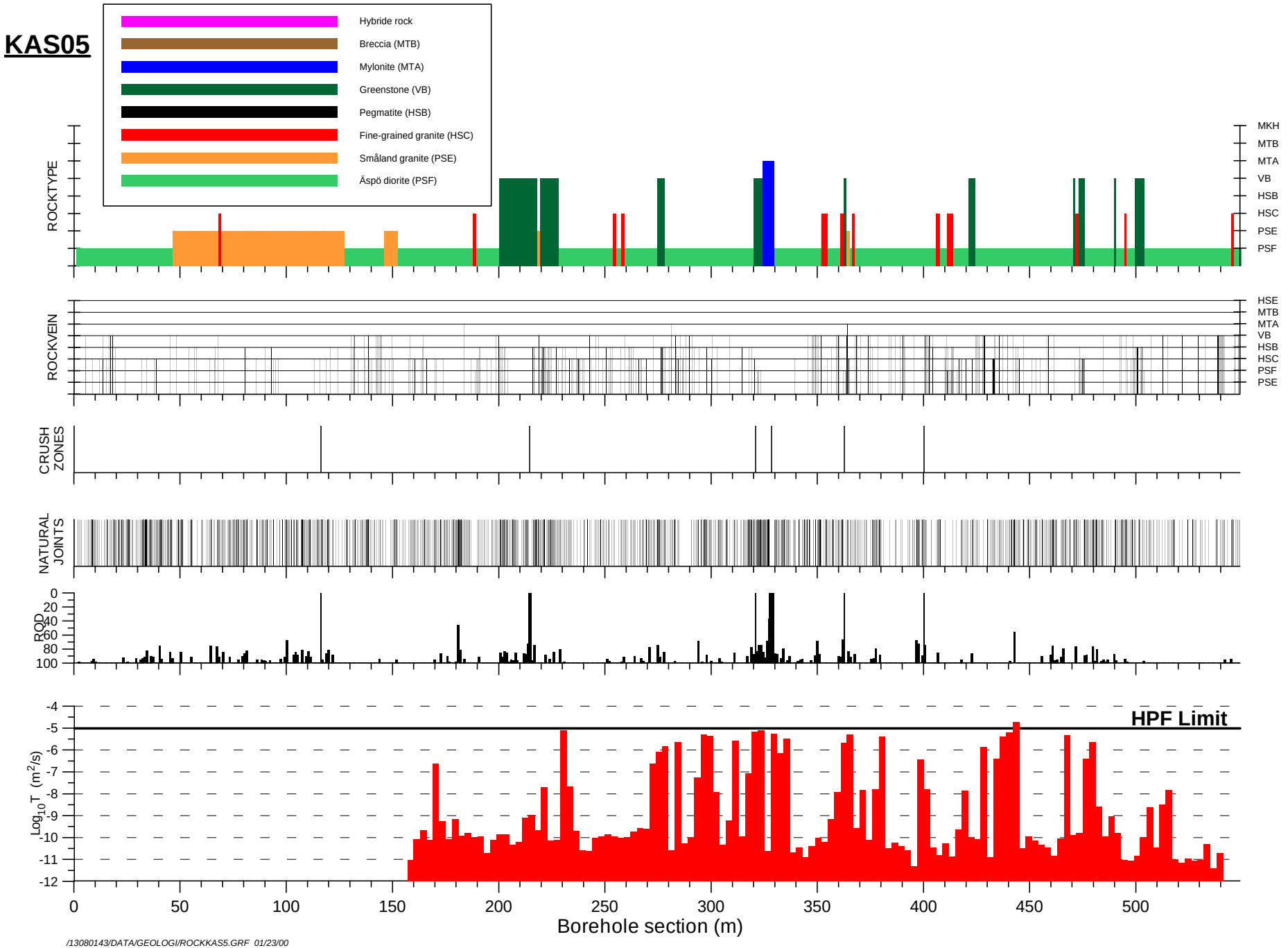
KAS05
Hybride rock
Breccia (MTB)
Mylonite (MTA)
Greenstone (VB)
Pegmatite (HSB)
Fine-grained granite (HSC)
Småland granite (PSE)
Äspö diorite (PSF)
ROCKTYPE
MKH
MTB
MTA
VB
HSB
HSC
PSE
PSF
ROCKVEIN
HSE
MTB
MTA
VB
HSB
HSC
PSF
PSE
CRUSH ZONES
NATURAL JOINTS
RQD
0
20
40
60
80
100
HPF Limit
Log10 T (m2/s)
-4
-5
-6
-7
-8
-9
-10
-11
-12
0
50
100
150
200
250
300
350
400
450
500
Borehole section (m)
/13080143/DATA/GEOLOGI/ROCKKAS5.GRF 01/23/00

KAS06

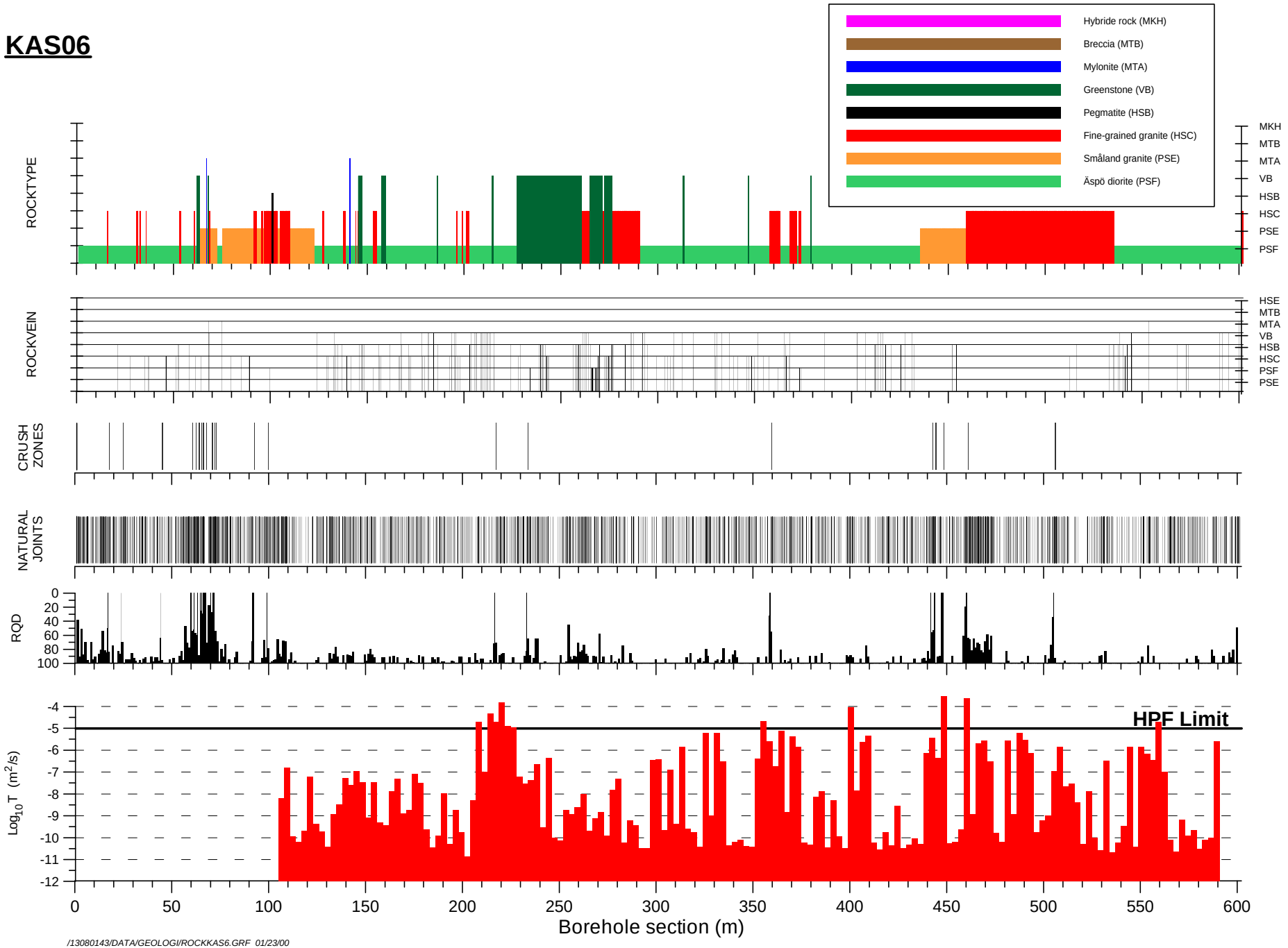
Hybride rock (MKH)
Breccia (MTB)
Mylonite (MTA)
Greenstone (VB)
Pegmatite (HSB)
Fine-grained granite (HSC)
Småland granite (PSE)
Äspö diorite (PSF)
ROCKTYPE
MKH
MTB
MTA
VB
HSB
HSC
PSE
PSF
ROCKVEIN
HSE
MTB
MTA
VB
HSB
HSC
PSF
PSE
CRUSH ZONES
NATURAL JOINTS
RQD
0
20
40
60
80
100
HPF Limit
Log10 T (m2/s)
-4
-5
-6
-7
-8
-9
-10
-11
-12
0
50
100
150
200
250
300
350
400
450
500
550
600
Borehole section (m)
/13080143/DATA/GEOLOGI/ROCKKAS6.GRF 01/23/00

KAS07

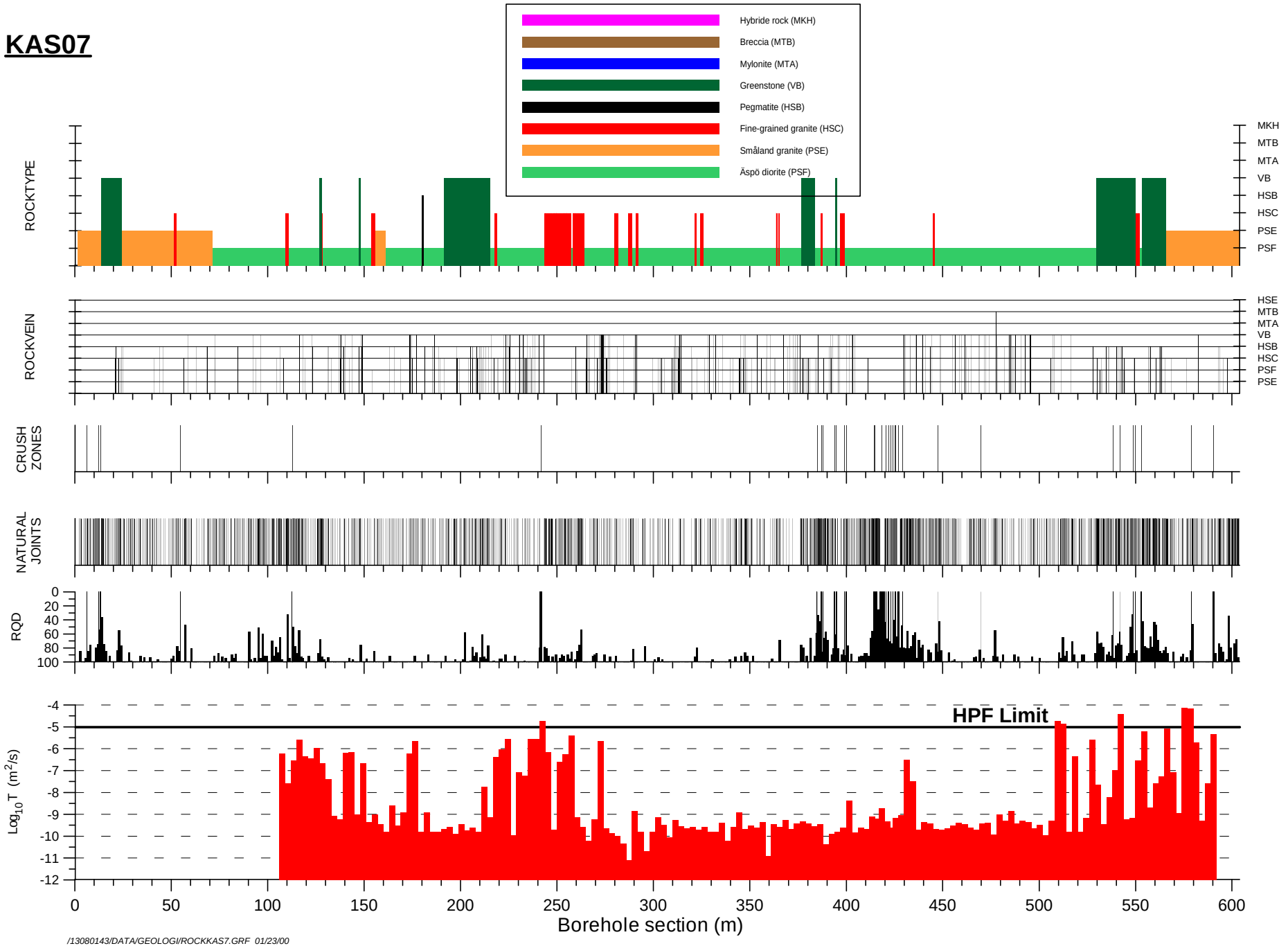

/13080143/DATA/GEOLOGI/ROCKKAS7.GRF 01/23/00

KAS08

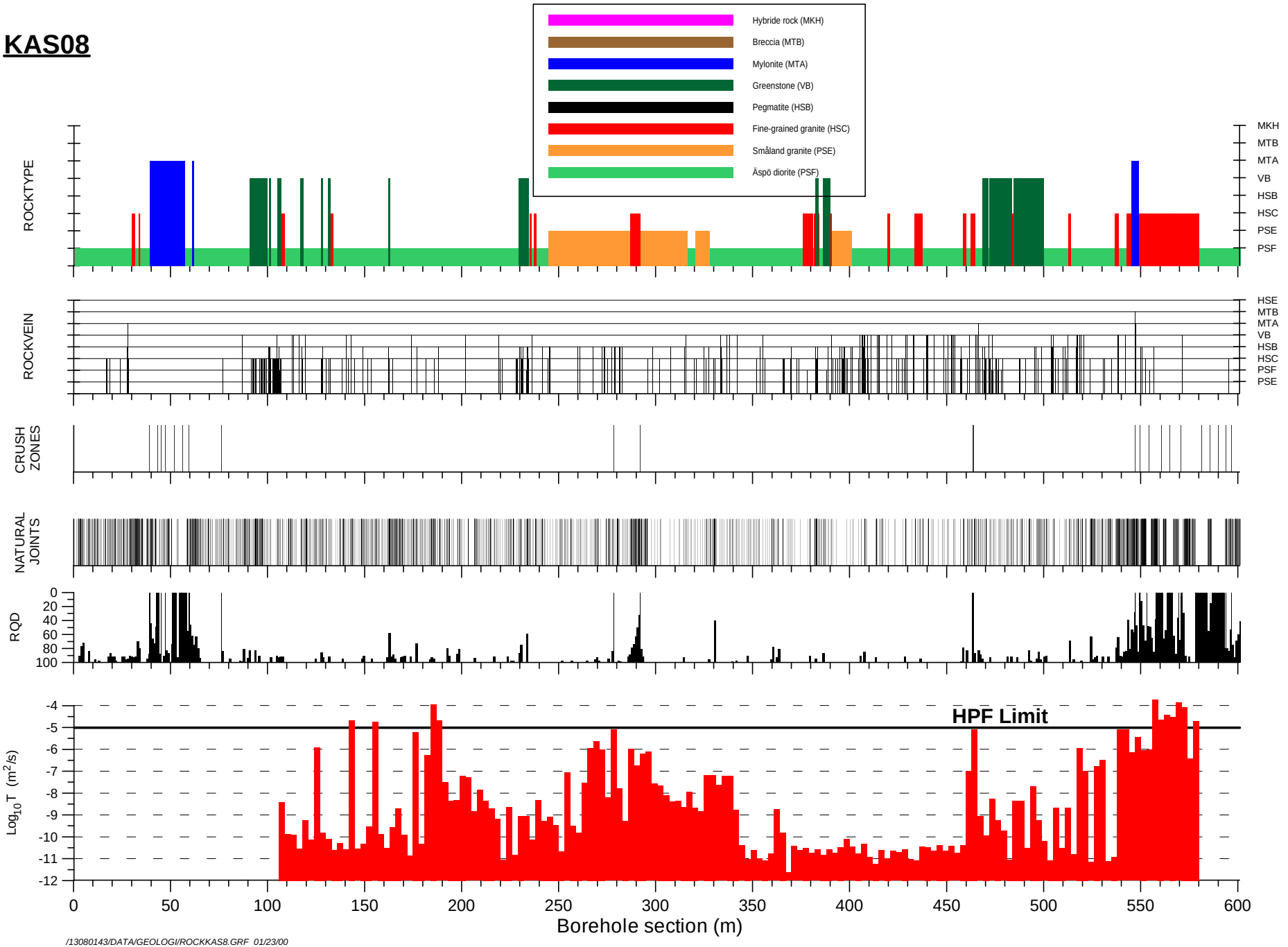

/13080143/DATA/GEOLOGI/ROCKKAS8.GRF 01/23/00

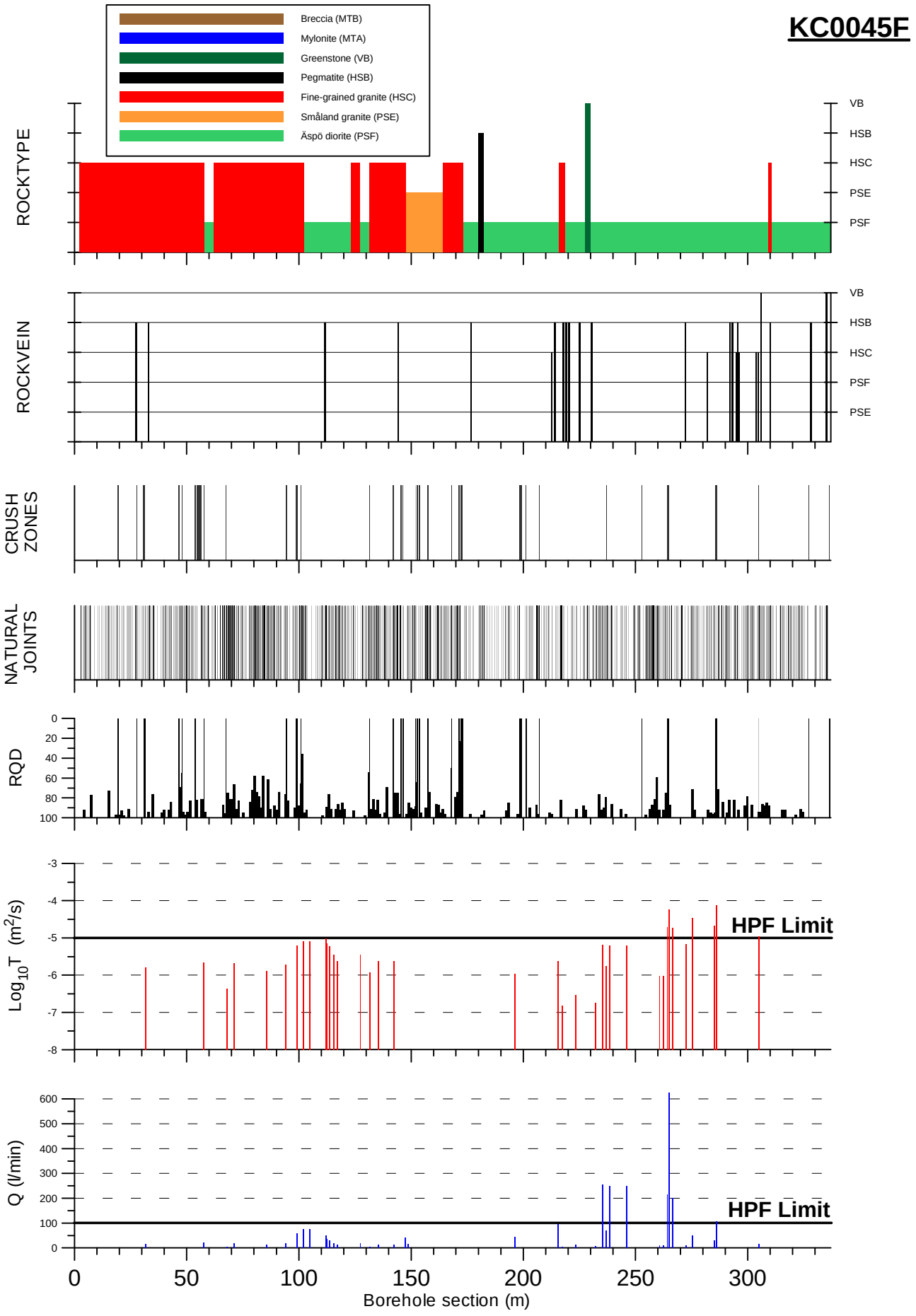

/13080143/DATA/GEOLOGI/ROCK0045.GRF 01/23/00

\

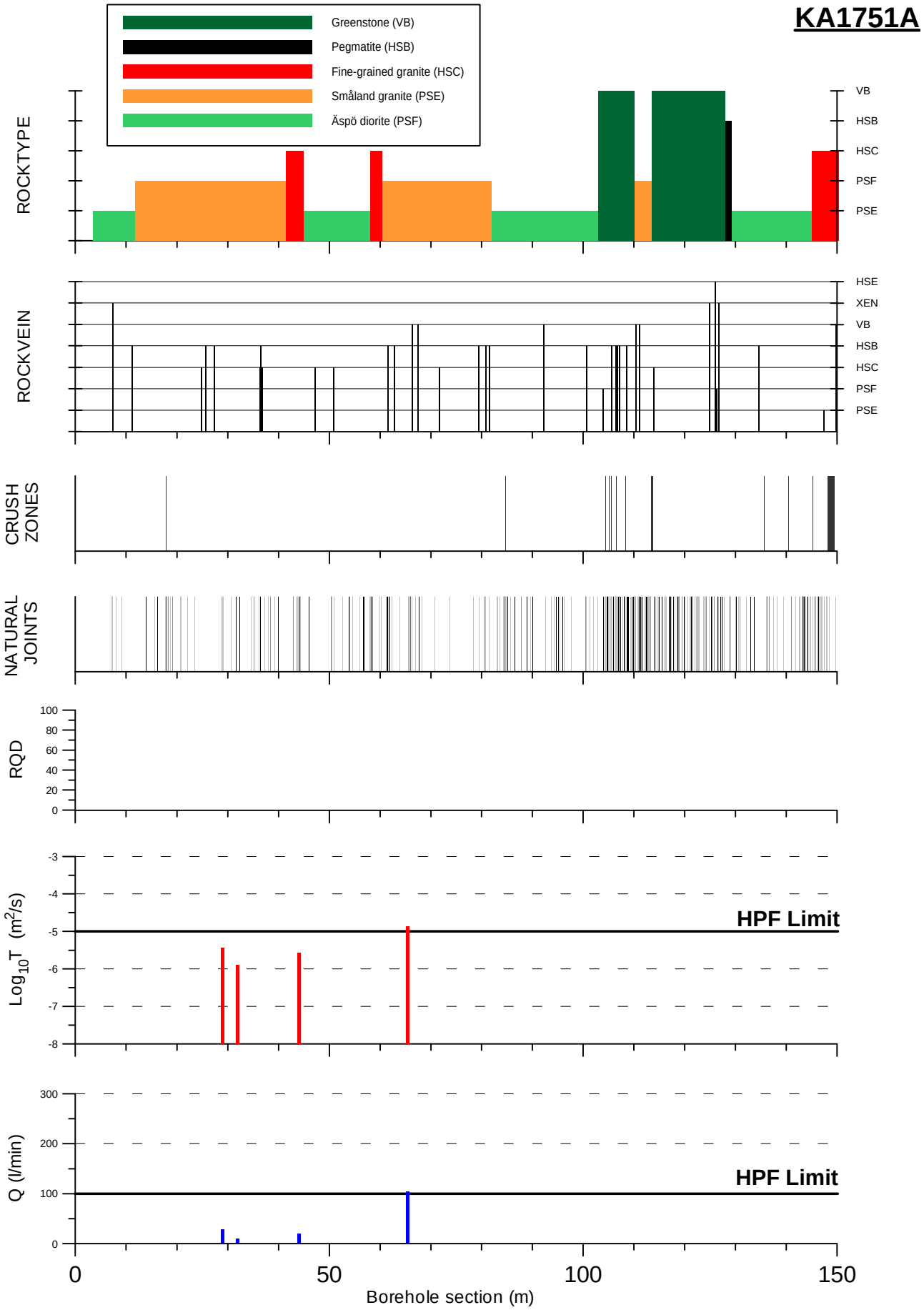

/13080143/DATA/GEOLOGI/ROCK1751.GRF 01/23/00

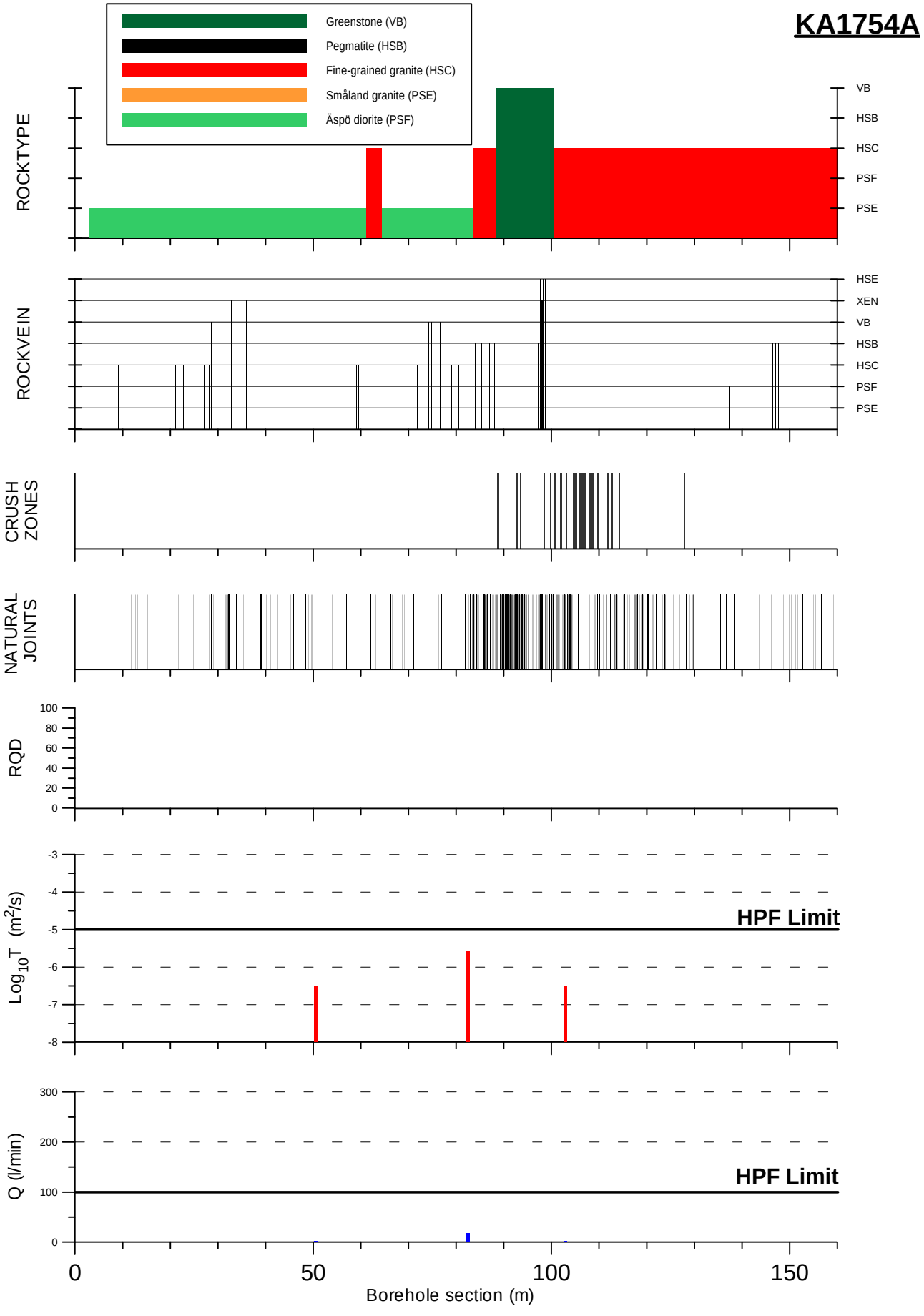

/13080143/DATA/GEOLOGI/ROCK1754.GRF 01/23/00

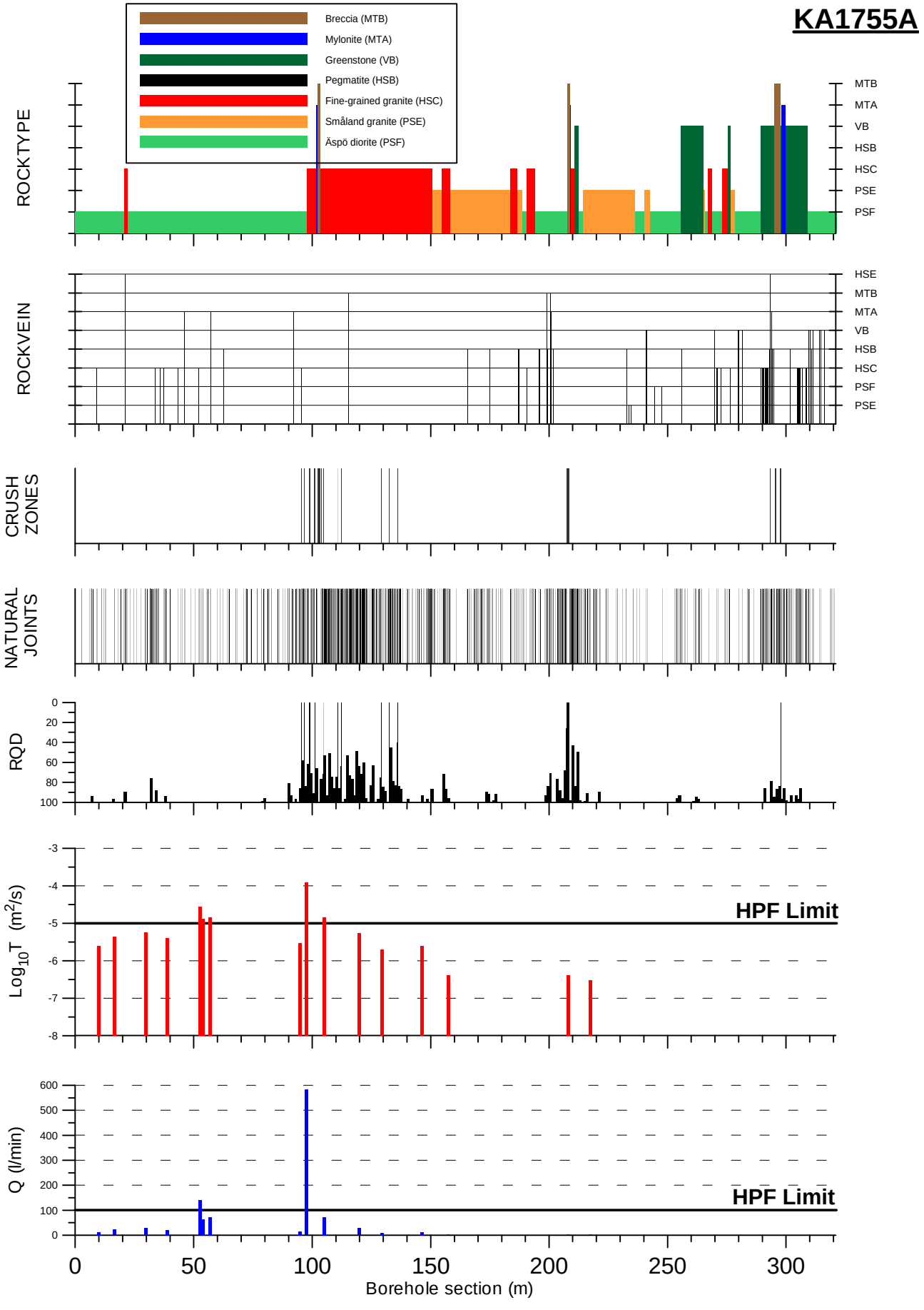

/13080143/DATA/GEOLOGI/ROCK1755.GRF 01/23/00

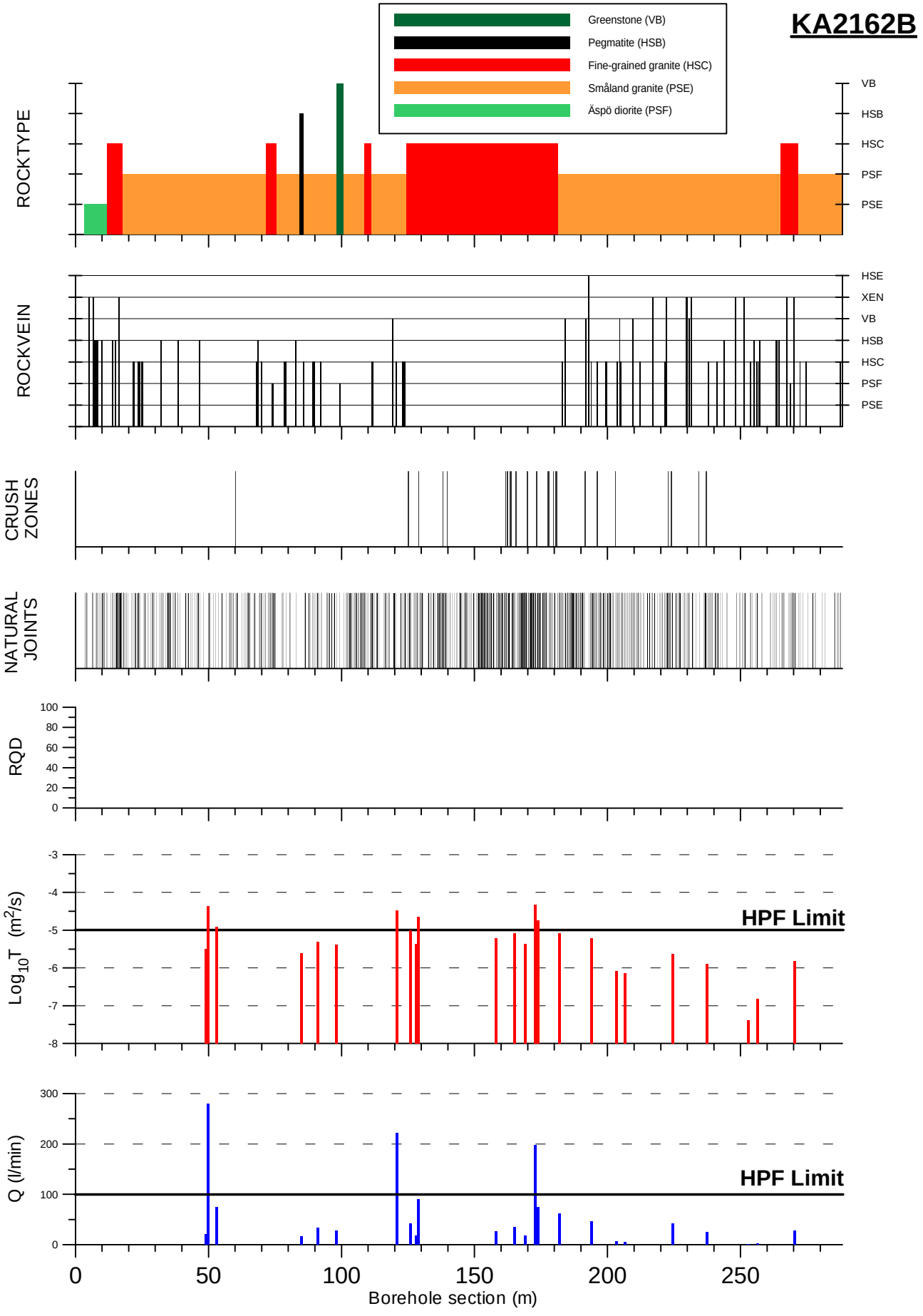

/13080143/DATA/GEOLOGI/ROCK2162.GRF 01/23/00

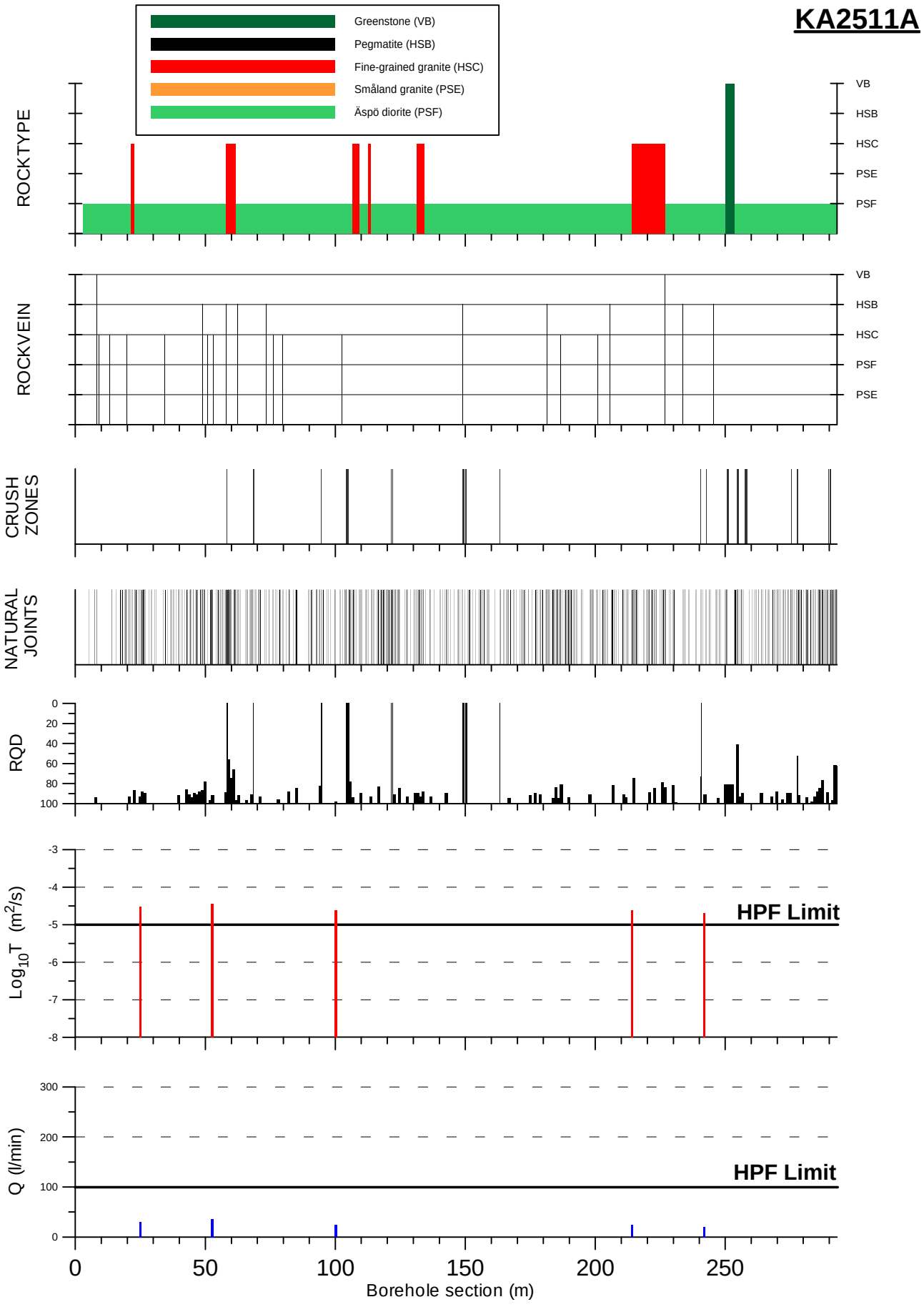

/13080143/DATA/GEOLOGI/ROCK2511.GRF 01/23/00

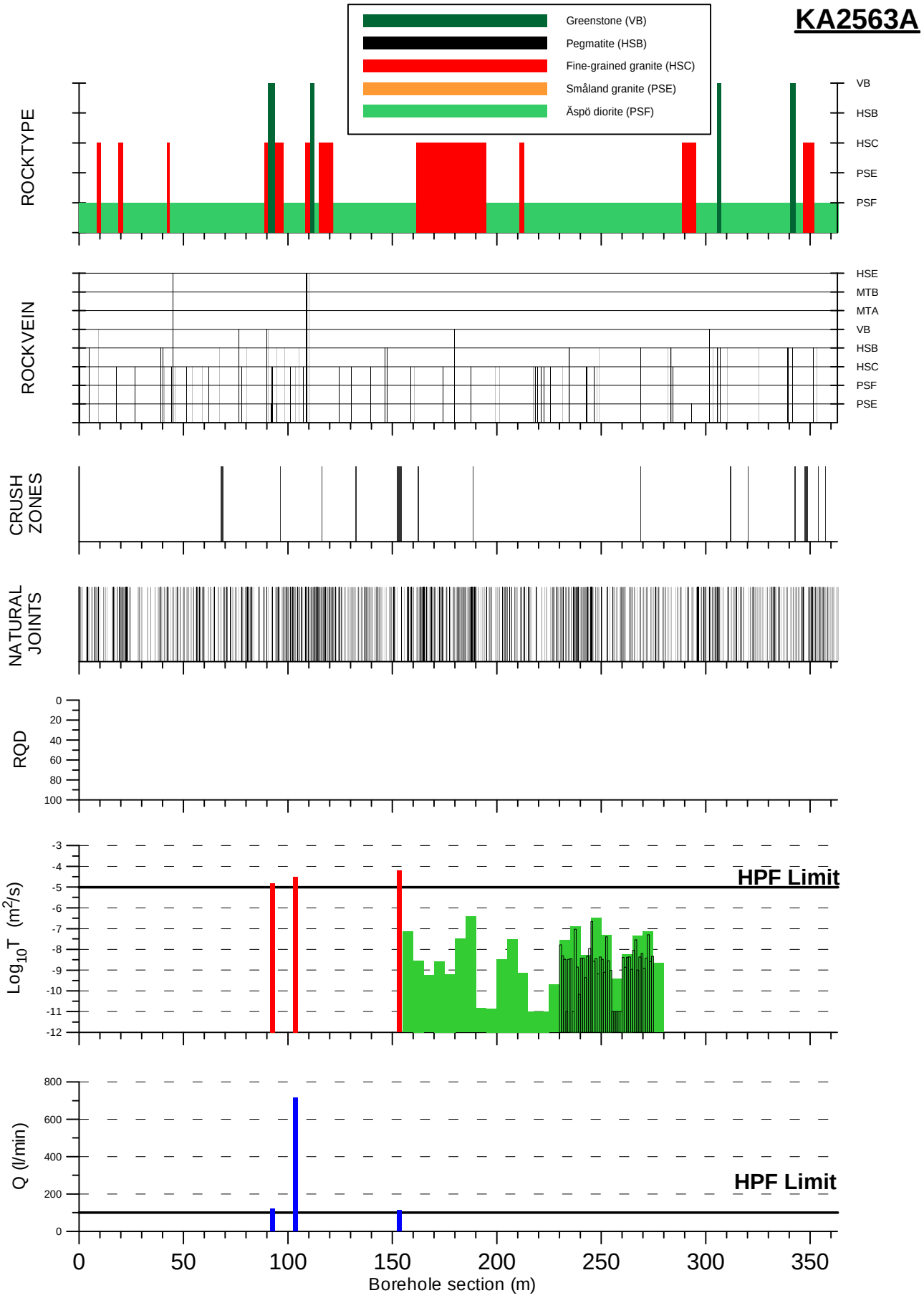

/13080143/DATA/GEOLOGI/ROCK2563.GRF 01/23/00

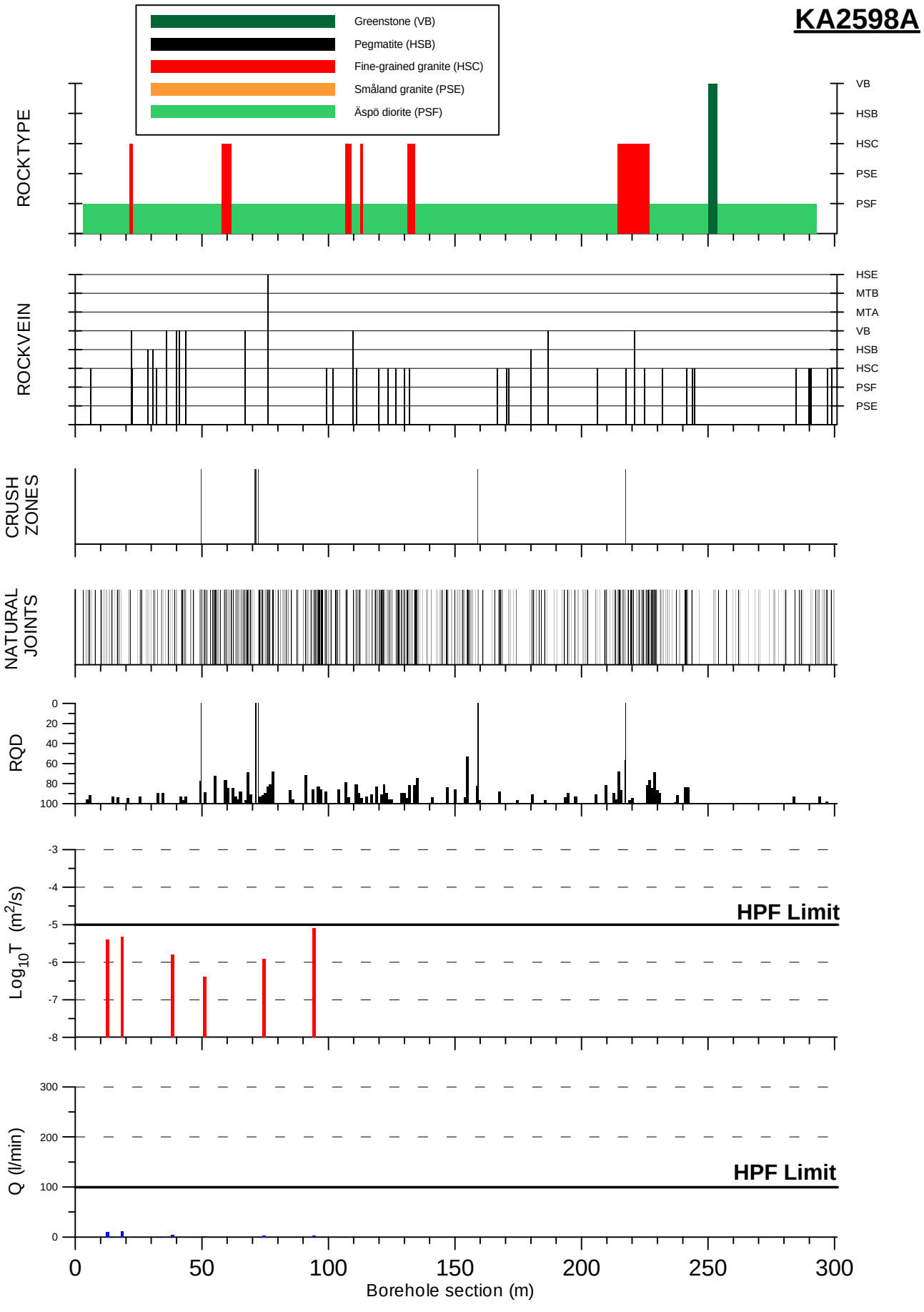

/13080143/DATA/GEOLOGI/ROCK2598.GRF 01/23/00

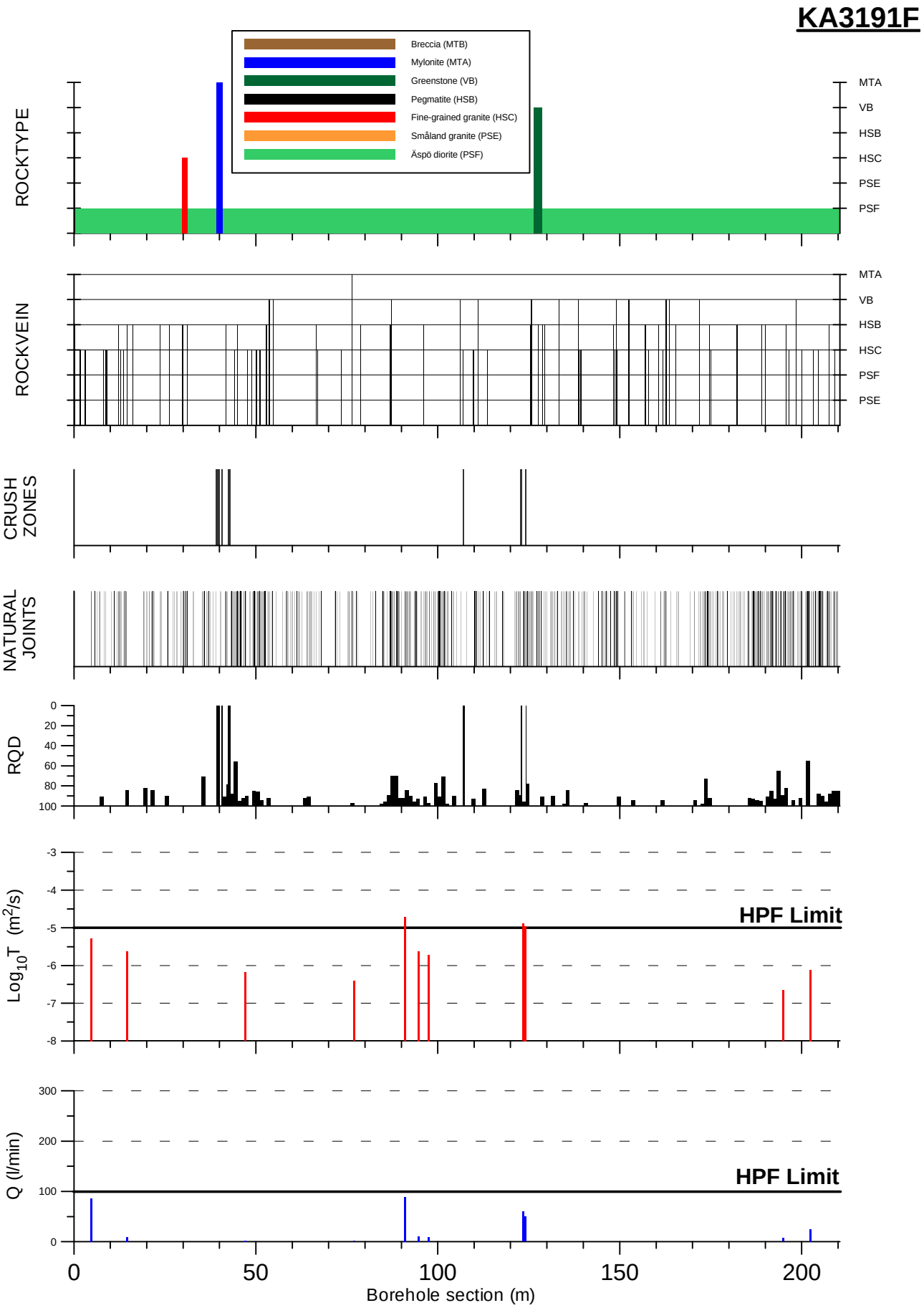

/13080143/DATA/GEOLOGI/ROCK3191.GRF 01/23/00

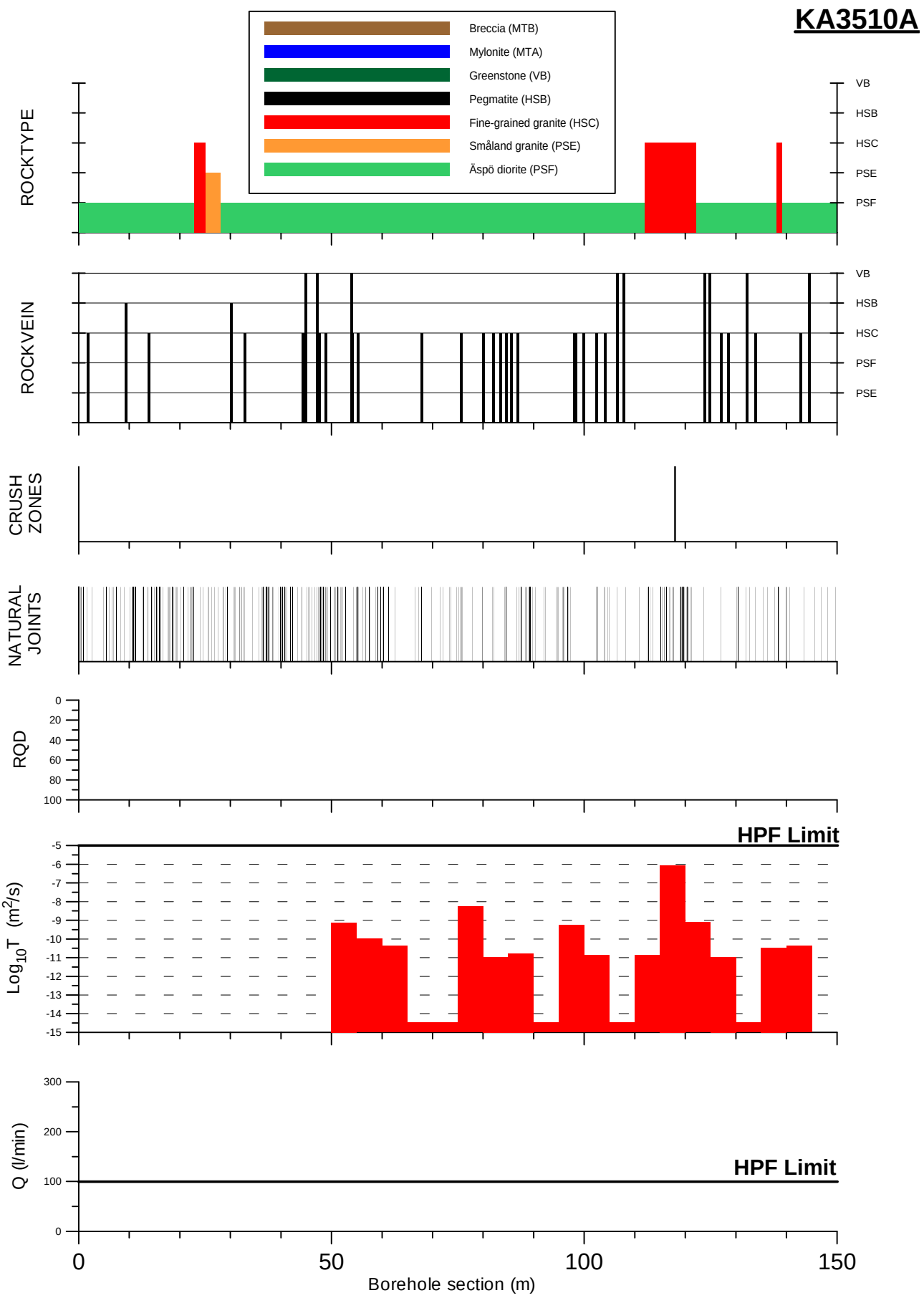

/13080143/DATA/GEOLOGI/ROCK3510.GRF 01/23/00